

# **VERIFICATION OF GRAVIMETRIC GEOIDAL MODELS BY A COMBINATION OF GPS AND ORTHOMETRIC HEIGHTS**

**G. L. ROBINSON**

**May 1991**



**TECHNICAL REPORT  
NO. 152**

## PREFACE

In order to make our extensive series of technical reports more readily available, we have scanned the old master copies and produced electronic versions in Portable Document Format. The quality of the images varies depending on the quality of the originals. The images have not been converted to searchable text.

# **VERIFICATION OF GRAVIMETRIC GEOIDAL MODELS BY A COMBINATION OF GPS AND ORTHOMETRIC HEIGHTS**

G.L. Robinson

Department of Geodesy and Geomatics Engineering  
University of New Brunswick  
P.O. Box 4400  
Fredericton, N.B.  
Canada  
E3B 5A3

May 1991  
Latest Reprinting February 1996

© Gregory L. Robinson, 1991

## PREFACE

This technical report is a reproduction of a thesis submitted in partial fulfillment of the requirements for the degree of Master of Science in Engineering in the Department of Surveying Engineering, October 1990. The research was supervised by Dr. Petr Vaníček and funding was provided partially by the Natural Sciences and Engineering Research Council of Canada.

As with any copyrighted material, permission to reprint or quote extensively from this report must be received from the author. The citation to this work should appear as follows:

Robinson, Gregory L. *Verification of Gravimetric Geoidal Models by a Combination of GPS and Orthometric Heights*. M.Sc.E. thesis, Department of Surveying Engineering Technical Report No. 152, University of New Brunswick, Fredericton, New Brunswick, Canada, 179 pp.

# Abstract

Gravimetric geoidal models such as “UNB Dec. ’86” and “UNB ’90” may be verified by a combination of GPS and orthometric heights. Ideally, the following relationship should equal zero:  $h - H - N$ , where  $h$  is the height above a reference ellipsoid obtained from GPS,  $H$  is its orthometric height, and  $N$  is the geoidal undulation obtained from the gravimetric model. In many cases users are interested in relative positioning and the equation becomes:  $\Delta(h - H - N)$ .

This study looks at each aspect of these equations. The geometric height (or height difference) is defined and the principal sources of error that are encountered in GPS levelling such as tropospheric delay, orbit biases etc. are examined.

The orthometric height (or height difference) is discussed by looking at various systems of height determination and deciding under which system the Canadian vertical network may be categorized, as well as what errors, and of what magnitude, are likely to be encountered. Orthometric heights are measured from the geoid, which in practice is difficult to determine. The surface, not in general coincident with the geoid, from which these measurements are actually made, is investigated.

The three campaigns discussed in this study – North West Territories, Manitoba, and Ontario – are in areas where levelled heights are referenced to the Canadian Geodetic Datum of 1928 in the case of the former two and the International Great Lakes Datum in the case of the latter. These two reference surfaces are discussed in some detail.

The geoidal solutions – “UNB Dec. ’86” and “UNB ’90” are described. The models are fairly similar as both use the same modified version of Stokes’s function so as to limit the area of the earth’s surface over which integration has to take place in order to determine the undulation at a point. “UNB ’90” makes use of an updated gravity data collection. Both solutions make use of terrestrial data for the high frequency

contribution and a satellite reference field for the low frequency contribution. “UNB Dec. ’86” uses Goddard Earth Model, GEM9, whereas “UNB ’90” uses GEM-T1. The implications of changes in reference field are discussed.

All measurements are prone to error and thus each campaign has associated with it a series of stations characterized by a misclosure obtained from  $h - H - N$ . These misclosures may be ordered according to any argument –latitude,  $\phi$ , longitude,  $\lambda$ , orthometric height,  $H$ , etc., in order to search for a statistical dependency between the misclosure and its argument, or in other words, a systematic effect.

The autocorrelation function will detect the presence of systematic “error” and least squares spectral analysis will give more information on the nature of this dependency. Both these tools are described and their validity is demonstrated on a number of simulated data series.

The field data collected during the three campaigns is analysed. The geometric and orthometric heights are combined with geoidal undulations from “UNB Dec. ’86” and then from “UNB ’90” using the misclosure  $h - H - N$ . The resulting data series are ordered according to various arguments and examined for presence of systematic effect by means of the autocorrelation function and spectral analysis. Similar tests are carried out on the data series yielded by  $\Delta(h - H - N)$  ordered according to azimuth and baseline length.

Clear evidence of statistical dependency is detected. Reasons for these dependencies are discussed.

# Contents

<b>Abstract</b>	<b>ii</b>
<b>List of Tables</b>	<b>viii</b>
<b>List of Figures</b>	<b>x</b>
<b>Acknowledgements</b>	<b>xv</b>
<b>1 Introduction</b>	<b>1</b>
<b>2 Height systems</b>	<b>4</b>
2.1 Introduction . . . . .	4
2.2 Geometric heights . . . . .	6
2.3 Heights from levelling. . . . .	6
2.4 Orthometric height correction . . . . .	12
2.5 System used in the Canadian vertical network . . . . .	12
2.5.1 Errors due to neglecting gravity . . . . .	13
2.5.2 Other sources of error . . . . .	14
2.6 Trans-Canada levelling lines . . . . .	15
<b>3 The Canadian vertical datum</b>	<b>18</b>
3.1 Introduction . . . . .	18
3.2 The Canadian datum . . . . .	20

3.2.1	The Canadian Geodetic Datum of 1928 . . . . .	20
3.2.2	The International Great Lakes Datum of 1955 . . . . .	23
<b>4</b>	<b>Determination of the Canadian geoid</b>	<b>25</b>
4.1	The evaluation of the geoid using Stokes's formula . . . . .	25
4.1.1	Introduction . . . . .	25
4.1.2	Stokes's formula . . . . .	26
4.1.3	Evaluation of Stokes's formula . . . . .	27
4.2	Global geopotential models . . . . .	29
4.3	The UNB Dec. '86 Geoid . . . . .	32
4.3.1	Introduction . . . . .	32
4.3.2	Computational strategy for the high frequency contribution . . . . .	32
4.3.3	Sources of gravity data . . . . .	36
4.3.4	Modification of Stokes's function . . . . .	36
4.3.5	Corrections to be applied . . . . .	39
4.3.6	The low frequency contribution . . . . .	43
4.4	Changing of the reference field from one geopotential model to another . . . . .	45
4.5	The UNB '90 geoid . . . . .	46
4.5.1	Introduction . . . . .	46
4.5.2	Computational strategy for the high frequency contribution . . . . .	48
4.5.3	Sources of gravity data . . . . .	48
4.5.4	Modification of Stokes's function . . . . .	48
4.5.5	Corrections to be applied . . . . .	50
4.5.6	The low frequency contribution . . . . .	50
4.6	Comparison between geoidal models . . . . .	52
<b>5</b>	<b>Biases and errors in GPS height differences</b>	<b>56</b>
5.1	The Global Positioning System . . . . .	56
5.2	Carrier phase observations . . . . .	57



5.3	The GPS Networks . . . . .	58
5.3.1	The North West Territories network . . . . .	59
5.3.2	The Ontario network . . . . .	60
5.3.3	The Manitoba network . . . . .	60
5.4	Sources of errors in GPS relative height determination. . . . .	63
5.4.1	The geometry of the satellite configuration . . . . .	63
5.4.2	Orbit biases . . . . .	63
5.4.3	Atmospheric refraction . . . . .	65
5.4.4	Antenna phase centre variations . . . . .	72
5.4.5	Multipath and antenna imaging . . . . .	72
5.4.6	Bias due to errors in station co-ordinates . . . . .	73
5.4.7	Ambiguity resolution and clock biases . . . . .	73
<b>6</b>	<b>Analysis of sample data</b>	<b>75</b>
6.1	Introduction . . . . .	75
6.2	The autocorrelation function . . . . .	76
6.3	Least squares spectral analysis . . . . .	79
6.4	Analyses of simulated data series . . . . .	80
6.4.1	Random data series . . . . .	81
6.4.2	Random data series with trend . . . . .	81
<b>7</b>	<b>Analysis of field data</b>	<b>88</b>
7.1	Introduction . . . . .	88
7.2	Evaluation of data sources . . . . .	88
7.2.1	Levelled heights . . . . .	88
7.2.2	GPS geometric heights . . . . .	91
7.2.3	The regional geoidal models “UNB Dec. ’86” and “UNB ’90” . . . . .	92
7.3	Analysis of point data . . . . .	94
7.4	Analysis of baseline data . . . . .	100

7.5	Profiles of the North West Territories network . . . . .	106
7.6	Analysis of the UNB Dec. '86 geoid . . . . .	111
7.6.1	The North West Territories Network . . . . .	111
7.6.2	The Ontario Network . . . . .	122
7.6.3	The Manitoba network . . . . .	126
7.7	Analysis of the UNB '90 geoid . . . . .	131
7.7.1	The North West Territories Network . . . . .	131
7.7.2	The Ontario and Manitoba networks . . . . .	138
<b>8</b>	<b>Conclusion</b>	<b>142</b>
	<b>Bibliography</b>	<b>145</b>
	<b>Appendices</b>	
<b>I</b>	<b>The Molodenskij truncation coefficients</b>	<b>152</b>
<b>II</b>	<b>The jackknife</b>	<b>154</b>
<b>III</b>	<b>“UNB '90” data series</b>	<b>156</b>

# List of Tables

2.1	Correction for magnetic error (Gareau, 1986). . . . .	15
4.1	Computational strategy for “UNB Dec. ’86”. . . . .	34
4.2	Gravity data used in “UNB Dec. ’86”. . . . .	37
4.3	The total terrestrial contribution for points in the North West Territories Network. . . . .	42
4.4	Gravity data used in “UNB ’90”. . . . .	49
5.1	Effect of orbit uncertainty on baseline height difference. . . . .	65
7.1	Sources of error when using GPS and orthometric heights to verify a gravimetric geoid. . . . .	89
7.2	Estimates of the precision of baseline height differences from differential GPS observations. . . . .	92
7.3	Analysis of the misclosures obtained from UNB86 and GPS/ orthometric levelling. . . . .	94
7.4	Analysis of the misclosures obtained from UNB90 and GPS/ orthometric levelling. . . . .	94
7.5	Goodness of fit test for NWT data series (“UNB Dec. ’86”). . . . .	99
7.6	Summary of the results of the statistical tests carried out on the point data series. . . . .	100
7.7	Summary of the results of the statistical tests carried out on the baseline data series. . . . .	104

7.8	Summary of the analyses of the North West Territories network using “UNB Dec. ’86”.	121
7.9	Summary of the analyses of the Ontario network using “UNB Dec. ’86”.	130
7.10	Summary of the analyses of the Manitoba network using “UNB Dec. ’86”.	137
7.11	Summary of the analyses of the North West Territories network using “UNB ’90”.	139
7.12	Summary of the analyses of the Ontario and Manitoba networks using “UNB ’90”.	141
I.1	The Molodenskij truncation coefficients.	153

# List of Figures

2.1	Heights of points A and B above the ellipsoid and above the geoid. . . . .	5
2.2	Unequal spacing of the equipotential surfaces. . . . .	7
2.3	The orthometric height of A. . . . .	9
2.4	The normal height of A. . . . .	11
2.5	Two levelling lines across Canada (after Lachapelle and Whalen, 1979). . . . .	16
3.1	Sea level as the local reference surface (after Vaníček et al., 1980). . . . .	19
3.2	The 1928 levelling network (Gareau, 1986). . . . .	22
3.3	The International Great Lakes Datum levelling network (after Lippincott, 1985). . . . .	24
4.1	Surface area subdivided into (a) sectors and (b) blocks. . . . .	28
4.2	Results of test on $\Delta N$ taken to various $n_{max}$ with OSU89A. . . . .	31
4.3	“UNB Dec. ’86” gravimetric geoidal undulations (in metres) for the Great Slave Lake Area, NWT. . . . .	33
4.4	The approximate spherical cap used in the UNB Dec. ’86 geoid (after Vaníček et al., 1986). . . . .	35
4.5	Behaviour of Stokes’s function in the original version ( $S(\psi)$ ), unmodified higher order version ( $S_{21}(\psi)$ ) and modified higher order version ( $S_{21}^m(\psi)$ ). . . . .	38
4.6	Calculation of the topographic and indirect effects (after Vaníček and Kleusberg, 1987). . . . .	40
4.7	Accuracy of the GEM9 and GEM-T1 potential coefficients. . . . .	44

4.8	<i>DN</i> (in metres) to be applied to “UNB Dec. ’86” to convert from reference field GEM9 to GEM-T1 for the Great Slave Lake area. . . . .	47
4.9	The application of Kaula’s rule (after Marsh et al.,1988). . . . .	51
4.10	Difference (in metres) between UNB90 and UNB86 for the Great Slave Lake Area. . . . .	53
4.11	Difference (in metres) between UNB86 and OSU86F for the Great Slave Lake Area. . . . .	54
4.12	Difference (in metres) between UNB90 and OSU86F for the Great Slave Lake Area. . . . .	55
5.1	The North West Territories network. . . . .	59
5.2	The Ontario network. . . . .	61
5.3	The Manitoba network . . . . .	62
5.4	The effect of orbit uncertainty on a baseline. . . . .	64
5.5	The effect of modelling errors of wet tropospheric refraction on GPS height differences (after Delikaraoglou, 1989). . . . .	67
5.6	Typical diurnal variations in the Total Electron Content (TEC) (Hol-loway, 1988). . . . .	69
5.7	Sunspot activity. . . . .	70
6.1	The direct interval estimation method (after Craymer, 1984). . . . .	78
6.2	Analysis of the purely random data series. . . . .	82
6.3	Analysis of data series with period 1.5 units. . . . .	83
6.4	Analysis of data series with period 4.5 units. . . . .	85
6.5	Data series with quadratic trend. . . . .	86
6.6	Analysis of the data series with residual quadratic trend. . . . .	87
7.1	The estimated magnitude of errors (in parts per million) of GPS base-lines height differences. . . . .	93
7.2	Histogram for the North West Territories network. . . . .	95
7.3	Histogram for the Ontario network. . . . .	96

7.4	Histogram for the Manitoba network. . . . .	97
7.5	The data distributions for the North West Territories network. . . . .	98
7.6	The normalised data series of baseline misclosures for the North West Territories network (ordered according to length of baseline). . . . .	102
7.7	The normalised data series of baseline misclosures for the Ontario network ordered (according to length of baseline). . . . .	103
7.8	The normalised data series of baseline misclosures for the Manitoba network (ordered according to length of baseline). . . . .	105
7.9	Profile of orthometric heights from Yellowknife to Fort Smith (after Mainville and Veronneau, 1989). . . . .	106
7.10	Profile of geoidal undulations from Yellowknife to Fort Smith -“UNB Dec. ’86”, “UNB Dec. ’86” with reference field changed from GEM9 to GEM-T1 and OSU86F (after Mainville and Veronneau, 1989). . . . .	107
7.11	Profile of the difference between the GPS/ orthometric derived profile and that obtained from “UNB Dec. ’86” with envelope showing limits of GPS heighting accuracy (after Mainville and Veronneau, 1989). . . . .	108
7.12	Profile of geoidal undulations from Yellowknife to Fort Smith -“UNB ’90” and OSU86F. . . . .	109
7.13	Profile of the difference between the GPS/ orthometric derived profile and that obtained from UNB90. . . . .	110
7.14	Analysis of the North West Territories UNB86 data series (ordered according to latitude). . . . .	112
7.15	The North West Territories UNB86 data series (ordered according to longitude). . . . .	113
7.16	Analysis of the North West Territories UNB86 data series ordered according to longitude). . . . .	115
7.17	Analysis of the North West Territories UNB86 data series (ordered according to orthometric height). . . . .	116

7.18	Analysis of the North West Territories UNB86 data series (ordered according to absolute change in orthometric height). . . . .	118
7.19	Analysis of the North West Territories UNB86 data series (ordered according to length of baseline). . . . .	119
7.20	Analysis of the North West Territories UNB86 data series (ordered according to azimuth of the baseline). . . . .	120
7.21	Analysis of the Ontario network UNB86 data series (ordered according to latitude). . . . .	123
7.22	The Ontario network UNB86 data series (ordered according to longitude).124	
7.23	Analysis of the Ontario network UNB86 data series (ordered according to longitude). . . . .	125
7.24	Analysis of the Ontario network UNB86 data series (ordered according to orthometric height). . . . .	127
7.25	Analysis of the Ontario UNB86 data series (ordered according to baseline length). . . . .	128
7.26	Analysis of the Ontario UNB86 data series (ordered according to azimuth). . . . .	129
7.27	Analysis of the Manitoba UNB86 data series (ordered according to latitude). . . . .	132
7.28	Analysis of the Manitoba UNB86 data series (ordered according to longitude). . . . .	133
7.29	Analysis of the Manitoba UNB86 data series (ordered according to orthometric height). . . . .	134
7.30	Analysis of the Manitoba UNB86 data series (ordered according to baseline length). . . . .	135
7.31	Analysis of the Manitoba UNB86 data series (ordered according to azimuth). . . . .	136



III.1 Analysis of the North West Territories network UNB90 data series (ordered according to latitude). . . . .	157
III.2 The North West Territories network UNB90 data series (ordered ac- cording to longitude). . . . .	158
III.3 Analysis of the NWT network UNB90 data series (ordered according to longitude). . . . .	159
III.4 Analysis of the Ontario network UNB90 data series (ordered according to latitude). . . . .	160
III.5 The Ontario network UNB90 data series (ordered according to longitude).	161
III.6 Analysis of the Ontario network UNB90 data series (ordered according to longitude). . . . .	162
III.7 Analysis of the Manitoba network UNB90 data series (ordered accord- ing to latitude). . . . .	163
III.8 Analysis of the Manitoba network UNB90 data series (ordered accord- ing to longitude). . . . .	164

# Acknowledgements

I would like to express my appreciation to Dr. Petr Vaníček for his useful suggestions and guidance during this undertaking. I would also like to thank Dr. Alfred Kleusberg for his review of this thesis.

Discussions with Mr. Mike Craymer helped to clarify many points. Mr. Peng Ong provided the “UNB ’90” undulation values and proved an interesting and illuminating colleague. Mr. Bob Penney of Canada Centre for Surveying patiently ensured that all my requests for information and data were met.

Thanks go to the Department of Surveying Engineering, University of New Brunswick, and the National Research Council of Canada for financial assistance over the past two years.

A heartfelt word of thanks goes to my wife, Jenny, whose special optimism encouraged me when my own faltered.

# Chapter 1

## Introduction

The advent of the Global Positioning System (GPS) is revolutionizing surveying. Levelling, in particular, has traditionally been a time consuming, and, therefore, expensive operation. GPS offers a more economical and efficient alternative, but suffers from the drawback that it yields height differences (and heights) above a reference ellipsoid. These geometric height differences must be converted to orthometric height differences if they are to be useful for most surveying applications. This requires a knowledge of the separation of the geoid and reference ellipsoid or the geoidal undulation. A number of regional geoidal models have become available. The “UNB Dec. ’86” (Vaníček et al., 1986) and “UNB ’90” (Vaníček et al., 1990) gravimetric geoidal models were computed by the the University of New Brunswick under contract to Canada Centre for Surveying, Geodetic Survey of Canada.

These two solutions use the latest available satellite derived geopotential reference models and the most complete gravity data available in advanced computational procedures. A byproduct of the geoidal computation is an assessment of the internal accuracy of the model. However, it is difficult to obtain an independent assessment of the quality of the solution. Some indication is given by comparison with Doppler and orthometric levelling derived undulations (Vaníček et al., 1986, Rapp and Wichiencharoen, 1984 etc.). The calculated geoid is, however, clearly more accurate than

the values with which it is being compared. Seasat altimetry is a useful tool for comparison but its coverage is obviously limited.

GPS provides a very useful standard. It offers geometric height differences to a few parts per million and, when combined with orthometric heights from levelling, geoidal height differences to a few centimetres.

This study makes use of three GPS campaigns undertaken by the Canada Centre for Surveying between 1983 and 1986. The first campaign consists of 93 stations observed with GPS for which first order orthometric heights are available (Mainville and Veronneau, 1989). The second GPS campaign was in southern Ontario and consists of 23 stations for which the orthometric heights are known. The third campaign was observed in central Manitoba and consists of 11 points for which orthometric heights are available. The latter two campaigns are described in Mainville (1987) and Kearsley (1988b).

Before comparisons can be made between the modelled and GPS/ orthometric levelling values it is necessary to have a thorough understanding of the quality of each component – existing vertical networks, GPS derived geometric height differences and the computed geoid. Surveyors are generally interested in relative heights, but absolute values may be of some concern. For example, an orthometric height measured from a datum not coincident with the geoid may be combined with a known geoidal undulation as the  $Z$  coordinate of the station held fixed in a GPS baseline reduction. If the error is large enough the calculated GPS height differences will be seriously affected (Chrzanowski et al., 1988).

Chapter 2 investigates various height systems and their relationships with each other. The levelling height system used in Canada is described as well as errors in the levelling network.

Chapter 3 describes levelling datums and gives reasons why these are not generally coincident with the geoid. A brief description of the two datums relevant to the areas of study is given.

Chapter 4 gives an account of the two UNB regional gravimetric geoid solutions, the sources of the data used and the computational procedures adopted. The geoidal models are compared with each other and with an independently computed solution.

Chapter 5 investigates the various sources of error in GPS and describes how these propagate into the computed geometric height differences. The GPS networks used in this study are described.

Chapter 6 describes mathematical tools that may be used to detect the presence of systematic errors in a data series.

Chapter 7 brings together the material covered in the discussions in the previous chapters. The geoidal undulations obtained from GPS and orthometric levelling are compared with the UNB gravimetric values. The study then moves to the detection of trends, as well as systematic errors in the data.

In Chapter 8 a number of conclusions are drawn and some recommendations are made.

Over time it has become clear that the quality of the gravimetric geoid computed at UNB is very good. With the availability of GPS/ orthometric height derived geoidal undulations this can be confirmed.

# Chapter 2

## Height systems

### 2.1 Introduction

An extraterrestrial positioning system such as GPS will provide the co-ordinates of a receiver in a Cartesian co-ordinate system whose origin, orientation and scale are defined by the adopted positions of the tracking stations that collect the data used for the satellite orbit computations. Since January 1987 the Conventional Terrestrial System, World Geodetic System 1984 (WGS84), has been used as this co-ordinate system. The receivers co-ordinates may then be transformed by well known relationships into geodetic co-ordinates and geometric height with respect to a reference ellipsoid. The reference figure used is the Geodetic Reference Spheroid 1980 (GRS80) (Moritz, 1980).

The system in use prior to WGS84 was WGS72. All the surveys described in this study were undertaken before the adoption of WGS84 but conversion was carried out using a shift of 4.5 metres along the  $Z$  axis, a rotation of 0.554 sec around the  $Z$  axis and a scale of .229 parts per million (Mainville, 1987; Mainville and Veronneau, 1989).

Surveyors are usually interested in the orthometric height,  $H$ , of a point as measured above the geoid and along the plumbline. The departure of the irregular geoid

from the smooth reference ellipsoid is the geoidal undulation,  $N$ , measured along the plumbline. These three elements are related as in Figure 2.1.

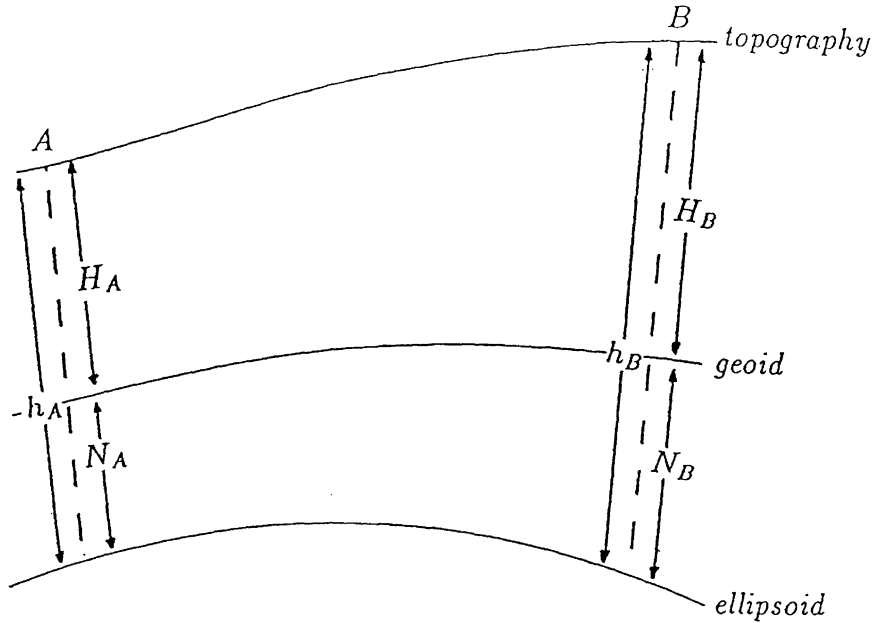


Figure 2.1: Heights of points A and B above the ellipsoid and above the geoid.

Clearly if  $N_A$  and  $h_A$  are known it is a simple matter to obtain  $H_A$ . Conversely, if both the geometric height and the orthometric height are known, it is possible to verify an independently derived geoidal undulation at that point. In the relative approach  $\Delta h_{AB}$ ,  $\Delta N_{AB}$  and  $\Delta H_{AB}$  are usually much more precise because of the tendency of systematic errors to cancel:

$$\Delta N_{AB} = \Delta h_{AB} - \Delta H_{AB}. \quad (2.1)$$

Generally the relative accuracy of a geoidal model such as “UNB Dec. ’86” (Vaníček et al., 1986) or “UNB ’90” (Vaníček et al., 1990) is of concern when used in combination with GPS derived geometric height differences to transfer the known orthometric height of a point, A, to point of unknown orthometric height, B.

Note that for the sake of simplicity  $H$  and  $h$  are shown to be along the same vertical. In fact,  $H$  is along the plumbline and  $h$  is normal to the ellipsoid – the difference between the two is termed the deflection of the vertical. The error induced by this assumption of common geometry is considered insignificant when compared with the uncertainties in the geoid height difference estimates and the orthometric height differences (Zilkoski and Hothem, 1989).

## 2.2 Geometric heights

The geometric height of a point is the distance of that point from a reference ellipsoid measured along the normal to the ellipsoid. All geometric heights in this study have been referred to GRS80.

Consequently, the difference in height between the ends of a baseline,  $\Delta h_{AB}$ , are also referred to the GRS80. However, in practice some uncertainty will be introduced due to the errors in the co-ordinates of the satellite tracking stations and due to errors in the absolute height adopted for the the GPS stations (Holloway, 1988).

## 2.3 Heights from levelling.

Levelling is the process of measuring incremental height differences,  $\delta H$ , between points A and B. Often the height of one point, say A, above the geoid is known and by summing the small differences in height it is hoped that the height of B above the geoid will be obtained. Generally, this will not be so because, as can be seen from the Figure 2.2, levelling accumulates the separation between all equipotential surfaces through which the level passes (Merry, 1985). If the level surfaces were parallel this would not present a problem, but the surfaces converge toward the poles and are perturbed by local variations in the density in the earth and by topographic irregularities. Therefore, unless corrections are applied, levelling is path dependent



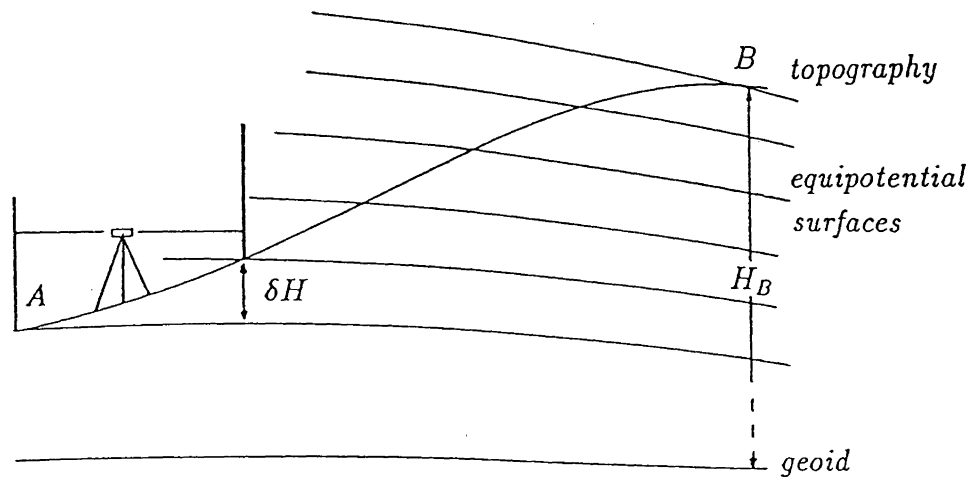


Figure 2.2: Unequal spacing of the equipotential surfaces.

and, in general, levelling in a loop will not yield a final height difference of zero.

However, only one equipotential surface passes through a point, and this can be used to uniquely define the height of a point above the geoid. In this system, which makes use of geopotential numbers, the height of A is given by:

$$C = \int_G^A g dh, \quad (2.2)$$

where  $C$  is the geopotential number that gives the difference between the potential at the geoid and the potential at A ( $W_G - W_A$  is path independent). The drawback of this natural system is that it does not have dimensions of length, but uses instead kilogal metres (acceleration times length).

In order to give the geopotential numbers units of length it is possible to take into account the mean gravity along the plumbline from A to the geoid,  $\bar{g}$ :

$$H = \frac{C}{\bar{g}}. \quad (2.3)$$

This is the orthometric height of A and its units are metres (cf. Figure 2.3). Obviously, it is fairly difficult to determine  $\bar{g}$  as it is necessary to know the variations in gravity between the earth's surface and the geoid.

It is possible to evaluate  $\bar{g}$  in a number of ways. The method ascribed to Helmert regards the crust as having constant density. According to this model,  $\bar{g}$  may be evaluated from the formula:

$$\bar{g} = g + 0.0424 H, \quad (2.4)$$

where  $g$  is measured on the surface of the earth and  $H$  is the approximate orthometric height of the station above the geoid. This equation has been shown to be accurate by using borehole gravimetry, although there may be substantial errors in areas of large density contrast (Merry, 1985).

A number of approximations for  $\bar{g}$  have been proposed and each of these leads to slightly different types of height.

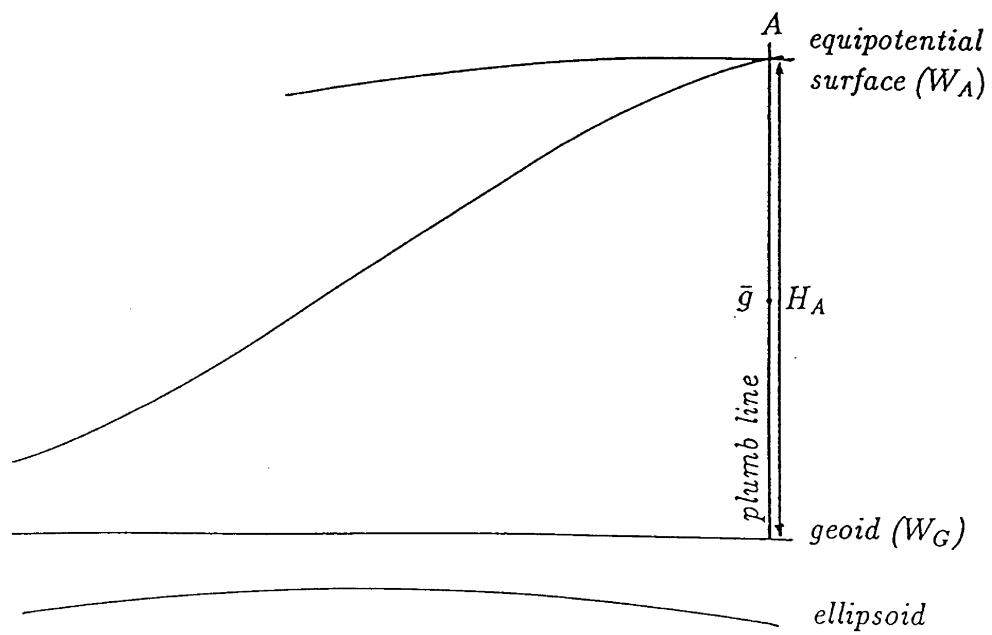


Figure 2.3: The orthometric height of A.

In the system of dynamic heights the value of  $\bar{g}$  is replaced by a constant value,  $G$ :

$$H = \frac{C}{G}, \quad (2.5)$$

where  $G$  may be taken as say, 0.978 kgal. Here, there is no pretence at proportional correction and the main function of  $G$  is to give  $H$  units of length.

The system of normal heights uses the normal gravity on the ellipsoid,  $\gamma$ , to calculate the mean normal gravity along the plumbline,  $\bar{\gamma}$ .

$$H = \frac{C}{\bar{\gamma}}. \quad (2.6)$$

One common method of evaluating  $\bar{\gamma}$  is that by Vignal:

$$\bar{\gamma} = \gamma - 0.1543 H, \quad (2.7)$$

where  $H$  is the approximate height above the quasi-geoid (cf. Figure 2.4) and  $\gamma$  in terms of the International Gravity Formula 1980 is:

$$\begin{aligned} \gamma_\phi = & 978.0327(1 + 0.0052790414\sin^2\phi \\ & + 0.00000232718\sin^4\phi \\ & + 0.0000001262\sin^6\phi)Gal \end{aligned} \quad (2.8)$$

which is a function of the latitude,  $\phi$ , only. Vaníček and Krakiwsky (1986) give a detailed discussion of this height system.

In fact, often observed gravity is not used at all and this yields:

$$H = \frac{1}{\bar{\gamma}} \int_G^A \gamma^* dn, \quad (2.9)$$

where  $\gamma^*$  is an approximation of the actual gravity along the route based on normal gravity.

All of the height systems discussed so far, with the exception of the last one, are scaled, albeit variable, versions of the the geopotential number. Orthometric heights are natural heights and do not depend on the reference ellipsoid used (Heiskanen and

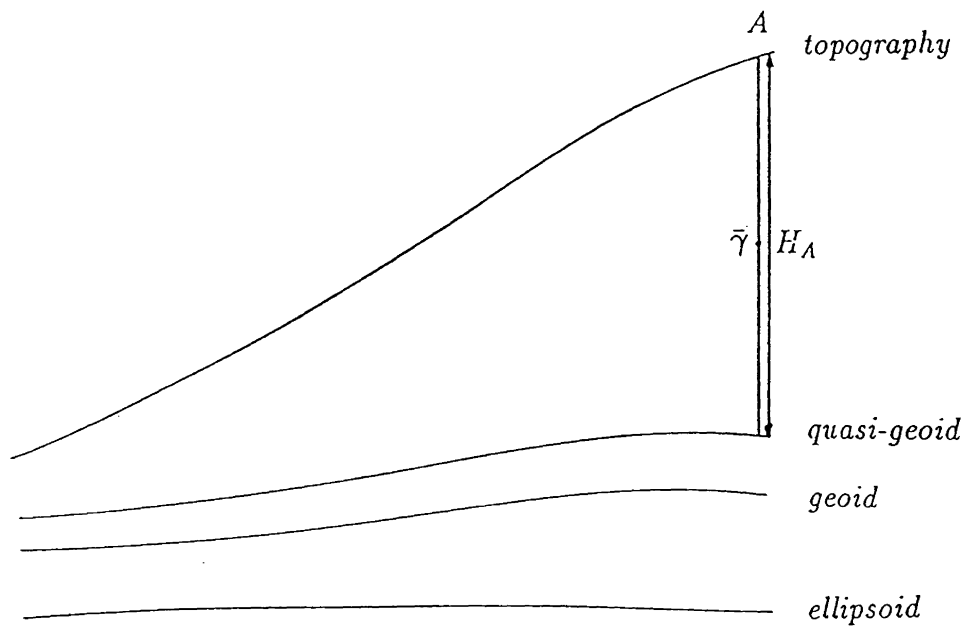


Figure 2.4: The normal height of A.

Moritz, 1967). However, they require a knowledge of gravity and also the gravity gradient between the surface of the earth and the geoid. Normal heights depend on the particular reference figure used and have a more artificial character, but are easier to compute.

## 2.4 Orthometric height correction

In Section 2.3 it was shown that summing height differences measured with a level and a staff in a loop will not sum to zero. A correction must be applied to the measured height differences to convert them to an orthometric difference:

$$\Delta H^{AB} = \sum \delta H^{AB} + OC^{AB}, \quad (2.10)$$

where the orthometric correction,  $OC^{AB}$ , may be evaluated by (Heiskanen and Moritz, 1967):

$$OC^{AB} = \sum_A^B \frac{g - \gamma_\phi}{\gamma_\phi} \delta H + \frac{\bar{g}_A - \gamma_\phi}{\gamma_\phi} H_A - \frac{\bar{g}_B - \gamma_\phi}{\gamma_\phi} H_B, \quad (2.11)$$

where  $\bar{g}_A$  and  $\bar{g}_B$  is the mean value of gravity along the plumb line of A and B respectively and  $\gamma_\phi$  is the normal gravity at a reference latitude.

## 2.5 System used in the Canadian vertical network

The Canadian levelling network made use of an orthometric correction but this correction does not use measured gravity. In this system the height of A is given by (Cannon, 1928):

$$C = \int_G^A \gamma^* dh, \quad (2.12)$$

where  $\gamma^*$  is given by:

$$\gamma^* = \gamma_{45}(1 - \alpha \cos 2\phi + \beta \cos^2 2\phi - rH), \quad (2.13)$$

where  $\gamma_{45}$  is the normal acceleration of gravity at latitude  $45^\circ$ , taken as 980.624 gals,  $\phi$  is the latitude,  $\alpha$  and  $\beta$  are constants equal to 0.002 644 and 0.000 007 respectively,  $r$  is a small constant equal to 0.000 000 314 7 if  $H$  is in metres (Gareau, 1986), and  $H$  is the approximate orthometric height of A. Thus, a mathematically regular form of the earth is adopted where gravity changes with latitude and height.

The approximate orthometric correction to obtain orthometric height differences from differences in potential becomes, after some simplification (Cannon, 1928):

$$OC \doteq -Hd\phi\left(2\alpha \sin 2\phi\left(1 + \left(\alpha - \frac{2\beta}{\alpha} \cos 2\phi\right)\right)\right). \quad (2.14)$$

In practice this formula was simplified to:

$$OC \doteq -\frac{Hd\phi}{700\,000}. \quad (2.15)$$

Hence, it can be seen the original system of levelled heights in Canada falls into the category known by various names –“normal orthometric”, “approximate orthometric”, or “spheroidal orthometric”. No determination of gravity, either on the surface of the earth or reduced to a point between the earth’s surface and the geoid, was used in the reduction of the levelled differences in height. However, in the interests of simplicity, heights in the Canadian system will be referred to as orthometric heights in this discussion.

### 2.5.1 Errors due to neglecting gravity

As a result of using normal gravity instead of observed gravity, a discrepancy between the (Helmerts) height difference,  $\Delta H_{AB}^O$ , and the corresponding height difference,  $\Delta \tilde{H}_{AB}^O$  based on normal gravity is introduced (Vaníček et al., 1980):

$$\Delta H_{AB}^O - \Delta \tilde{H}_{AB}^O = \frac{\bar{H}_{AB}}{\gamma_{45}}(\Delta g_B - \Delta g_A - 0.223\,8\Delta h_{AB}), \quad (2.16)$$

where  $\bar{H}_{AB}$ , is the mean height of A and B and  $\Delta g_A$  and  $\Delta g_B$  are the free air anomalies.

These height differences can be in the order of decimetres. Comparisons between the heights are path dependant.

These discrepancies may tend to cancel for levelling over many thousands of kilometres, but this is not so over shorter distances, where the gravity related differences may be of the same size as the systematic first order levelling errors (Vaníček et al., 1980).

### **2.5.2 Other sources of error**

The Canadian levelling network, like all others, is contaminated by errors from various sources. These errors may be divided, for convenience, into three categories – blunders, random and systematic errors. Blunders are gross errors. An example would be transposing backsight and foresight entries in a field book. They are detected by sound observing and booking procedures. However, it is possible for compensating errors to remain undetected. Random errors tend to cancel themselves out over a large number of set ups. An example would be refractive scintillation causing an image to move in all directions many times per minute. These cannot be eliminated but may be minimized by adhering to correct observing procedures.

It is more difficult to deal with systematic errors, which have a cumulative effect. An example would be unequal refraction that is encountered when levelling up or down hill, due to layering effect of temperature from the surface of the earth. The application of the orthometric correction described in Section 2.4. is an attempt to minimize that particular error. Systematic errors in precise levelling are well documented in many sources including Gareau (1986). Vaníček et al. (1985) attempted to identify and to model rod and instrument settlement, rod miscalibration, residual refraction and rod index error in Canadian first order levelling. Some systematic errors may be resolved by applying suitable corrections. However, not all can be modelled because of the lack of availability of the necessary data. An example of the latter case would be the systematic error known as magnetic error. This is caused by the



influence of the earth's magnetic field on the compensator of a level. The Zeiss Ni1 is particularly susceptible to this and three instruments used by Geodetic Survey of Canada were found to have the errors shown in Table 2.1.

<i>Instrument number</i>	<i>Correction at Ottawa in N-S direction</i>
90778	1.33 mm / km
107288	2.00 mm / km
107299	1.54 mm / km

Table 2.1: Correction for magnetic error (Gareau, 1986).

The error is greatest in the southern part of Canada and for lines which run parallel to the earth's magnetic field. Approximately 50,000 kilometres of levelling was carried out using the Zeiss Ni1. There is no correction that can be applied as the behaviour of the instrument can change with time under the influence of a magnetic field.

Nevertheless, Gareau (1986) found in a study of the closures of 106 loops that only four displayed a misclosure greater than  $4\sqrt{k}$  millimetres where  $k$  is the distance in kilometres.

## 2.6 Trans-Canada levelling lines

By 1971 a line of levels along highways from Halifax to Vancouver had been completed over a distance of about 6,400 kilometres. When this line was compared with one completed in 1916 along railways a discrepancy of 2.2 metres was revealed (cf. Figure 2.5). The original levelling line places the Vancouver tide gauge 1 centimetre higher than that at Halifax. The more recent line places Vancouver 196 centimetres higher. There was a change of elevation at Halifax of 20 centimetres over this

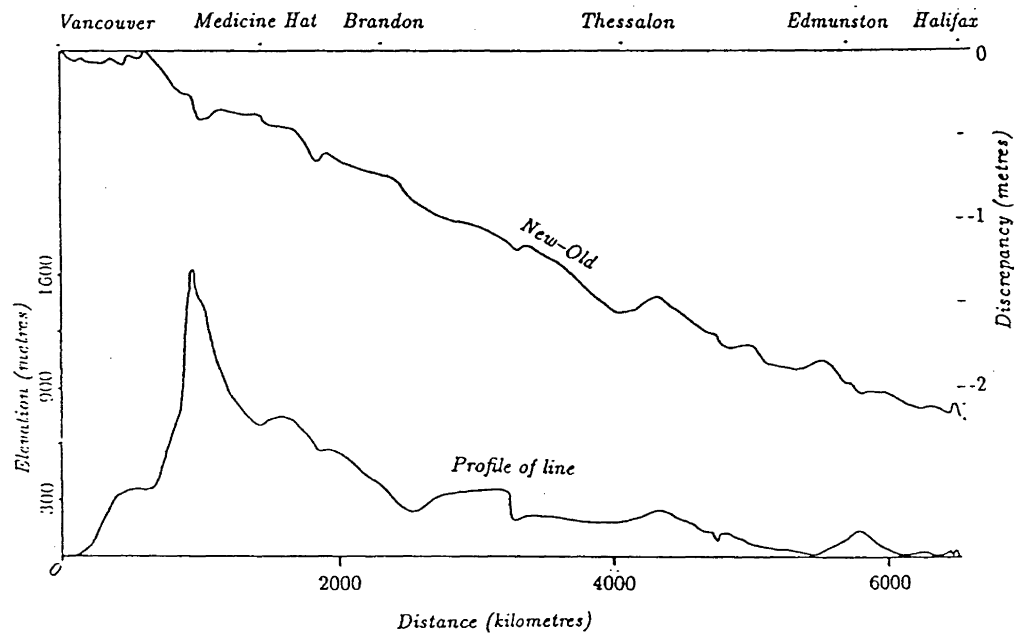


Figure 2.5: Two levelling lines across Canada (After Lachapelle and Whalen, 1979).

period (Lachapelle and Whalen, 1979). The indication here is that levelling lines may be affected by large systematic errors while still meeting the rejection criteria. This discrepancy is most likely due to systematic effects resulting from the different conditions and procedures under which the levellings were performed.

# Chapter 3

## The Canadian vertical datum

### 3.1 Introduction

Orthometric heights are usually referred to mean sea level as the zero reference surface. The assumption is that this surface coincides with the geoid (or with the quasi-geoid in the case of normal heights). It is now realized that these two surfaces are not, in fact, coincident due mainly to sea surface topography which may amount to many decimetres (Vaníček et al., 1980), but until recently the discrepancy was disregarded.

Obtaining the geoid from a tide gauge then simplifies to obtaining local mean sea level at that point. This consists of recording variations of local sea level,  $H_{in}$ , at the tide gauge with respect to some arbitrarily defined reference mark and calculating the local mean sea level,  $H_{mst}$ , from these measurements. If the difference in height between the the tide gauge reference mark and a bench mark is measured to be  $\Delta H$ , then the height of the bench mark above the geoid,  $H_{bm}$ , is given by:

$$H_{bm} = \Delta H + H_{mst} \quad (3.1)$$

(cf. Figure 3.1).

Generally, adjustments for a reference datum are carried out using data from a number of tide gauges. As mentioned, the height of each reference bench mark only

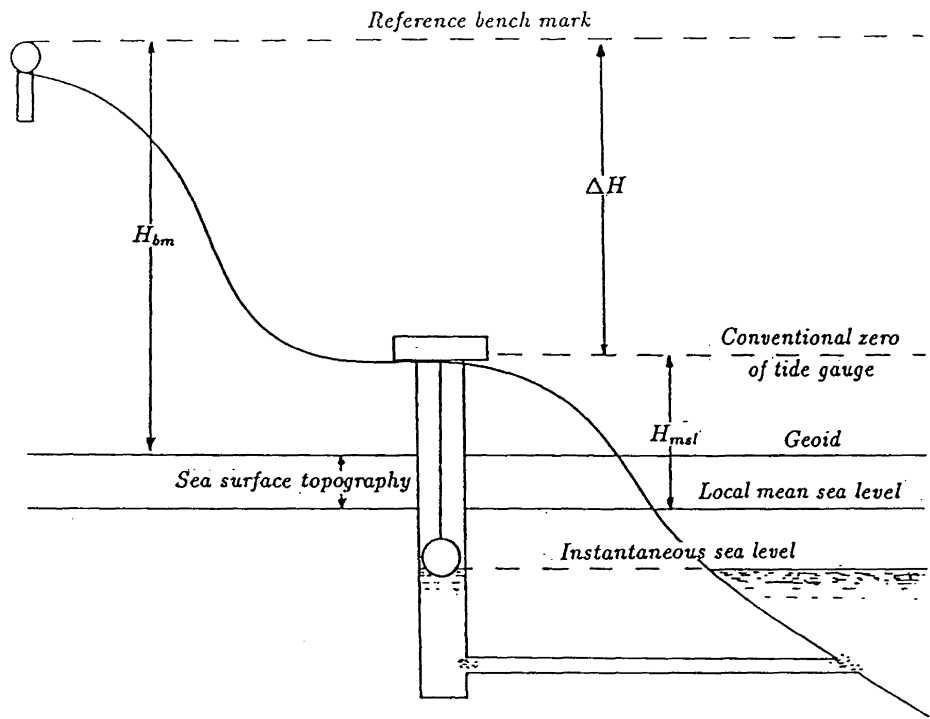


Figure 3.1: Sea level as the local reference surface (After Vaníček et al., 1980).

approximates the height above the geoid, and therefore, if the effect of sea surface topography is not taken into account, the network will become distorted and the heights of all points will be affected. Tide gauges are also subject to error in readings due to settling of their supports. Also of concern is the neglect of eustatic changes in sea level for which estimates vary from 0.5 to 1.5 millimetres per year (Vaníček et al., 1980).

Further problems are encountered due to errors in levelled height differences between tide gauges and possible crustal instability in the region. As discussed in Chapter 2, errors of considerable magnitude may be introduced by using path dependent observed height differences instead of height differences corrected for observed gravity. Other important errors are staff and instrument settlement, staff graduation, and temperature errors (Vaníček et al., 1985).

## **3.2 The Canadian datum**

Canada and the United States are presently cooperating in a project to redefine the heights of bench marks in North America. This will provide a much needed standard as many different datums have been used in the past. Those datums relevant to the areas of study in this thesis (see Chapter 5) will be discussed in detail.

### **3.2.1 The Canadian Geodetic Datum of 1928**

The Department of Public Works began first order leveling in Canada in 1883 when a line was run from a bench mark of the United States Coast and Geodetic Survey at Rouses Point, New York, along the St. Lawrence River and finally connected with a tide gauge in Halifax in 1907 (Young and Murakami, 1989).

The Geodetic Survey of Canada was established in 1905 but because of the large demand for precise heights, the vastness of the country, and the lack of resources work was carried out in a somewhat disjointed manner and five different reference points

were used (Gareau, 1986):

1. Halifax, Nova Scotia,
2. St. Stephen, New Brunswick,
3. Rouses Point, New York,
4. Stephen, Minnesota, and
5. Vancouver, British Columbia.

In 1919 a least squares adjustment of the western Canada levelling network was attempted. This represented the first in a series leading up to the 1928 adjustment known as the Canadian Geodetic Datum which incorporated all precise levelling that had been carried out in Canada. The reference datum chosen was mean sea level as determined by the Canadian Hydrographic Service at Halifax, Yarmouth, Pointe-au-Père, Vancouver, and Prince Rupert. Water transfers across the Great Lakes and Kootenay Lake were used to reinforce the network. The leveling lines included in the adjustment are shown in Figure 3.2.

The adjustment made the following assumptions, all of which are now accepted to be incorrect (Vaníček et al., 1980):

1. mean sea level at each of the tide gauges used was assumed to be coincident with the geoid,
2. the crustal area of which the network was developed was assumed to be stable,
3. and the elevation differences between bench marks were assumed to be contaminated by random errors only, with a symmetrical probability distribution.

Since 1928 new lines have been adjusted to fit the Canadian Geodetic Datum (Lachapelle and Whalen, 1979). A further adjustment of level lines was carried out in 1952 which included the 5 tide gauges used in the 1928 adjustment, plus a further

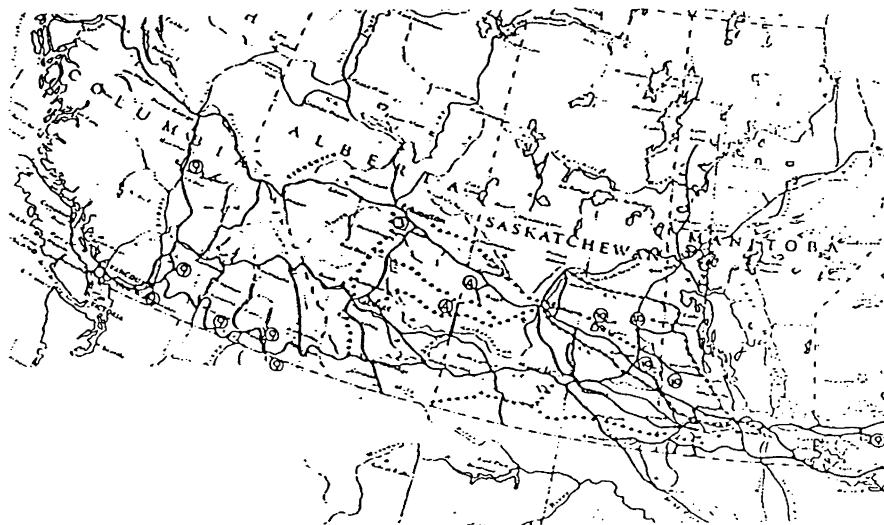
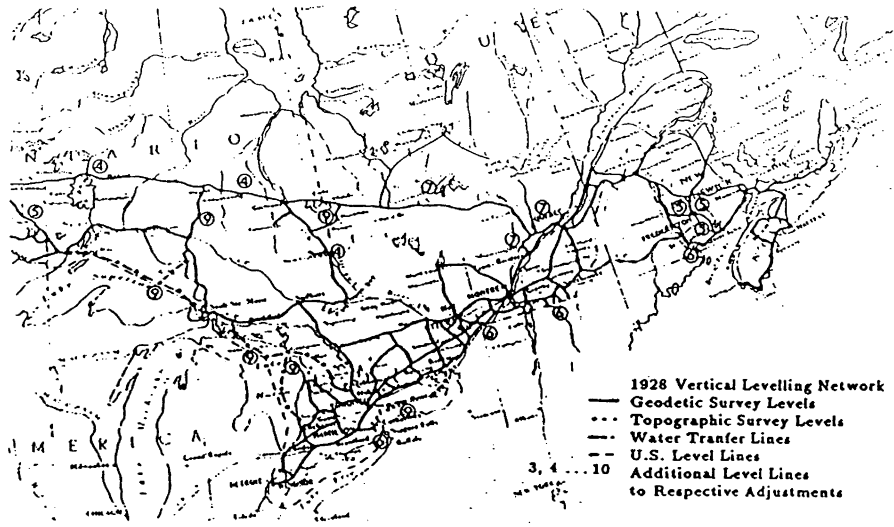


Figure 3.2: The 1928 levelling network (Gareau, 1986).



gauge at Churchill. The previous adjustment was retained as there was no significant change and the new work was “fitted” to it (Young and Murakami, 1989).

### **3.2.2 The International Great Lakes Datum of 1955**

This datum was established for the Great Lakes and the St. Lawrence River system and is shared by both Canada and the United States. Up until 1955, use had been made of six different datums. In order to overcome this confusing situation a joint Canada-United States project was set up to establish a standard datum for the Great Lakes. The reference for this system was chosen as mean sea level at Pointe-au-Père, Quebec. The period of sea level observation used was from 1941 to 1956 in order to counter the effects of crustal movements and long term sea level variations. Lippincott (1985) gives details of the methods of elevation transfer used in the adjustment.

The dynamic height system was chosen as the most useful. The use of dynamic heights rather than normal orthometric heights ensured that all surfaces of a particular lake would have the same elevation and it would also give a true representation of the hydraulic slope of rivers.

The dynamic heights were obtained in the following manner:

1. The elevations of the bench marks along a levelling line were computed using precise levelling.
2. These observed heights were converted to normal orthometric heights by applying an orthometric conversion as a function of latitude.
3. A dynamic correction dependant on both latitude and elevation was applied to obtain the dynamic height.

These were the only corrections applied and details are given in Rappleye (1948).

The extent of the International Great Lakes Datum levelling network is shown in Figure 3.3.

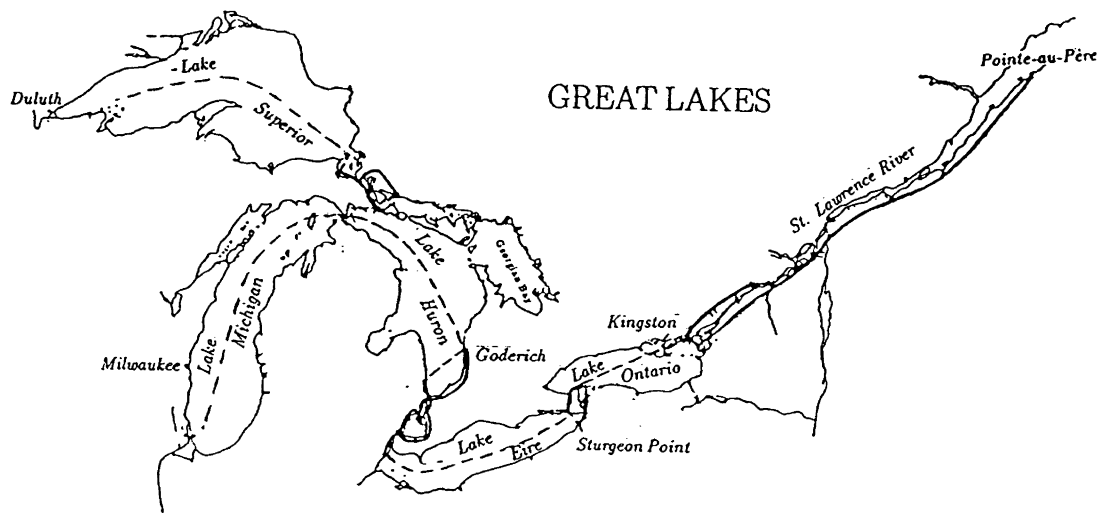


Figure 3.3: The International Great Lakes Datum levelling network (After Lippincott, 1985).

# Chapter 4

## Determination of the Canadian geoid

Many methods of determining the regional geoid exist. All approaches have special qualities and characteristics. Mainville (1987) makes a comparison of some methods as does Holloway (1988). This study will deal with the University of New Brunswick application of Stokes's formula in the "UNB Dec. '86" (Vaníček et al., 1986) and "UNB '90" (Vaníček et al., 1990) versions of the geoid. Ohio State University global geopotential models, OSU86F and OSU89A, are included for comparison purposes.

### 4.1 The evaluation of the geoid using Stokes's formula

#### 4.1.1 Introduction

The disturbing potential,  $T$ , is defined as the difference between the gravity potential on the geoid,  $W$ , and the normal gravity potential on the reference ellipsoid,  $U$ .

$$T = W - U. \tag{4.1}$$

If  $U$  is chosen with a constant value  $U_O$  on the reference ellipsoid and  $W$  with a value  $W_G$  on the geoid such that  $U_O = W_G$ , then Bruns formula applies. If a point,  $G$ , on the geoid is projected onto a point  $O$  on the ellipsoid by means of the ellipsoidal normal then:

$$N = \frac{T_G}{\gamma_O}, \quad (4.2)$$

where  $N$  is the height of the geoid above a “best fitting” ellipsoid or the geoidal undulation,  $T_G$  is the disturbing potential on the geoid and  $\gamma_O$  is the normal gravity on the reference ellipsoid.

If it is assumed that the centrifugal forces affect  $U$  and  $W$  by the same amount, the Laplace equation:

$$\nabla^2 T = 0 \quad (4.3)$$

applies outside the gravitating masses of the earth (Vaníček and Kleusberg, 1987). This last condition obviously does not hold, but, in the process of reducing gravity measurements to the geoid, those masses outside the geoid are removed by computation. A number of corrections must be applied. More detail will be given in Section 4.3.5.

Equation 4.1 can be manipulated to yield:

$$\Delta g \doteq -\frac{\partial T}{\partial H}|_G - \left(\frac{2}{R}\right)T|_G, \quad (4.4)$$

where  $\Delta g$  is the free air gravity anomaly,  $g_G - \gamma_O$ , on the geoid /ellipsoid,  $H$  is the orthometric height and  $R$  is the mean radius of the earth. The expression relates the measured quantity,  $\Delta g$ , to the potential,  $T$ , which is unknown.

### 4.1.2 Stokes’s formula

Equation 4.4 is a spherical approximation of the fundamental gravimetric equation of physical geodesy (Heiskanen and Moritz, 1967).

The solution for  $T$  is given by

$$T \doteq \frac{R}{4\pi} \int \int_{\sigma} \Delta g S(\psi) d\sigma, \quad (4.5)$$

where  $d\sigma$  is the element of surface area over which integration takes place,  $\Delta g$  is the gravity anomaly associated with  $d\sigma$ ,  $\psi$  is the spherical distance between  $G$  and  $d\sigma$ , and  $S(\psi)$  is Stokes's function or kernel:

$$S(\psi) = \sum_{l=2}^{\infty} \frac{(2l+1)}{(l-1)} P_l(\cos \psi), \quad (4.6)$$

where  $P_l$  are the associated Legendre polynomials of degree  $l$ .

By incorporating Bruns formula into the solution, Stokes's formula for geoidal heights is obtained:

$$N = \frac{R}{4\pi\gamma_m} \int \int_{\sigma} \Delta g S(\psi) d\sigma, \quad (4.7)$$

where  $\gamma_m$  is the mean gravity of the earth

Stokes's formula requires a continuous knowledge of gravity anomalies over the entire earth. In practice anomalies are only available for discrete points and the coverage is especially sparse over the water masses, in polar regions, and in the USSR. Evaluation of the formula is usually reduced, therefore, to summation over a limited area in the vicinity of the point of interest.

### 4.1.3 Evaluation of Stokes's formula

Two approaches to the solution of Stokes's formula are commonly followed. One is the subdivision of the area, by means of concentric circles and radii, into smaller and smaller sectors approaching the computation point. The gravity anomalies are replaced by a mean gravity anomaly,  $\Delta\bar{g}$ , which is assigned to the sector. The other approach is the division of the area, usually in terms of geographical co-ordinates, into, say, 10' by 10' blocks. In this case, the mean gravity anomaly is assigned to the block (cf. Figure 4.1).

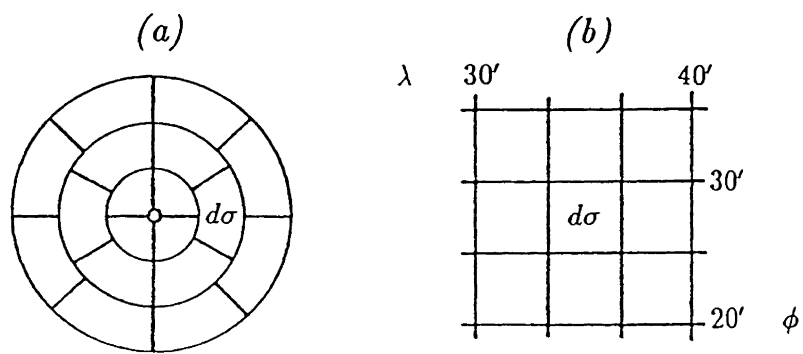


Figure 4.1: Surface area subdivided into (a) sectors and (b) blocks.

The integral then takes the following form:

$$N = \frac{R}{4\pi\gamma_m} \sum S(\psi) \Delta\bar{g} d\sigma. \quad (4.8)$$

As the point of interest is approached Stokes's function,  $S(\psi)$ , changes rapidly and the method which makes use of rings and radii naturally compensates, because the size of the each sector represented by a single mean gravity anomaly becomes smaller.

The advantage of the fixed block system is that the value of each block can be aggregated for use further away from the point. The basic unit remains the same and can be used as the point of interest changes.

A further approach is the Fast Fourier transform technique which is now increasingly being used to compute Stokes's integral. The computation has the form:

$$N = N_l + \frac{1}{2\pi\gamma} \int_{y_i}^{y_{i+1}} \int_{x_i}^{x_{i+1}} \frac{\Delta g - \Delta g_l}{(x^2 + y^2)^{\frac{1}{2}}} dx dy, \quad (4.9)$$

where  $N_l$  and  $\Delta g_l$  are the geoidal undulation and free air anomaly obtained from the satellite reference field with coefficients to degree and order  $l$ . In this method a cartesian rectangular zone  $(x, y)$  of gravity anomalies is integrated to produce a rectangular zone of geoidal undulations. The undulation of a particular station is then interpolated from this grid. The solution is cost effective, but must be used with care as it makes use of a number of approximations (Mainville, 1987).

## 4.2 Global geopotential models

The gravity potential of the earth may be expressed in terms of spherical harmonic coefficients (Vaniček and Krakiwsky, 1986):

$$W(r, \phi, \lambda) = \frac{GM}{r} \sum_{n=2}^{n_{max}} \sum_{m=0}^n \frac{a^n}{r} (J_{nm} Y_{nm}^c(\phi\lambda) + K_{nm} Y_{nm}^s(\phi\lambda)), \quad (4.10)$$

where  $GM$  is the gravitational constant multiplied by the mass of the earth,  $a$  is the mean equatorial radius of the earth,  $n$  and  $m$  refer to the degree and order of the

geopotential model,  $J_{nm}$  and  $K_{nm}$  are the potential coefficients, and  $Y_{nm}^c$  and  $Y_{nm}^s$  are normalized spherical harmonic functions. The expansion may be used to evaluate geoidal heights and gravity anomalies amongst other quantities. This is the frequency domain equivalent of Stokes's formula (Merry and van Gysen, 1987).

The coefficients are usually obtained from a combination of satellite and terrestrial observations. The long wave length coefficients are often obtained from satellite observations while satellite altimetry and terrestrial gravity data may be used to obtain the higher order terms.

Many geopotential models are given to degree and order 180 or 360. The former case will have 16,471 coefficients and the latter will have 65,341.

The models used for comparison purposes in this study are Ohio State University OSU86F and OSU89A, both of which are complete to degree and order 360 and make use of geophysically predicted anomalies in areas which lack data. OSU86F was computed by combining terrestrial data with the GEM-L2 satellite model, while in OSU89A surface data were combined with the GEM-T2 satellite model.

The maximum order of a model is not necessarily a reflection of its accuracy (Kearsley, 1988b). The error in higher order terms comes mainly from the gravity measurements and from the sampling and smoothing techniques which are used (Holloway, 1988). Figure 4.2 shows  $\Delta N_{OSU}$  from OSU89A compared to  $\Delta N_{GPS}$  obtained by comparing the geometric and levelled heights of the ends of a baseline. For a sample of ten baselines  $\delta N$  was calculated for each of  $n = 20, 30, \dots, 180$  using the formula:

$$\delta N = \Delta N_{GPS} - \Delta N_{OSU}. \quad (4.11)$$

$\delta N$  was then compared with the baseline length,  $d$ , and the mean of the baselines was calculated using the formula:

$$mis = \frac{1}{10} \sum_{i=1}^{10} \left| \frac{\delta N_i}{d_i} \right| \times 10^6. \quad (4.12)$$

Although OSU89A is complete to degree and order 360 the model was truncated to



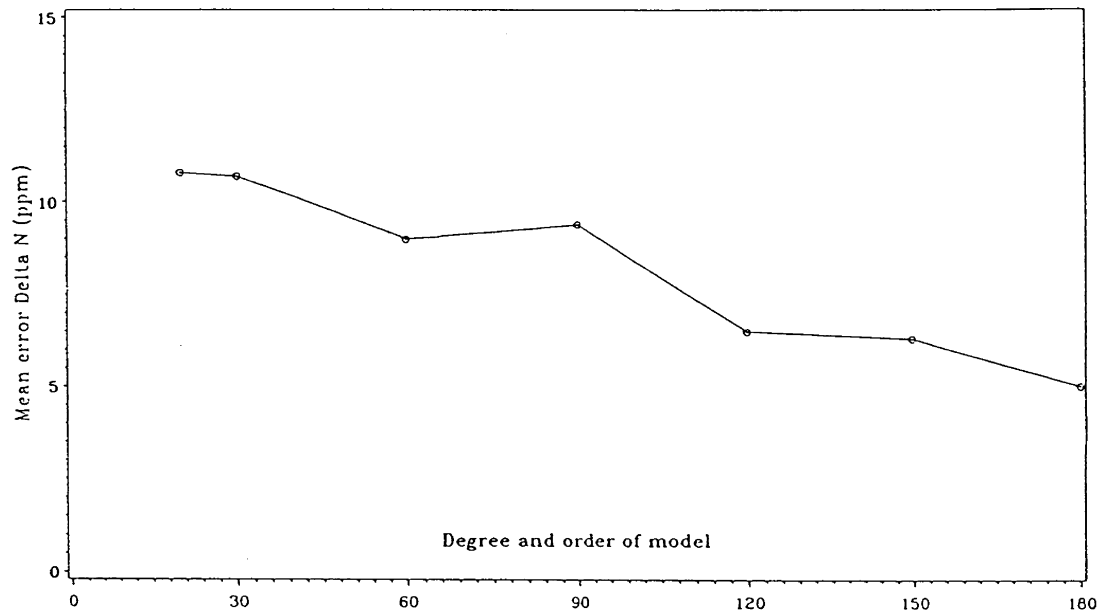


Figure 4.2: Results of test on  $\Delta N$  taken to various  $n_{max}$  with OSU89A.

$n_{max} = 180$  for computational reasons.

According to Schwarz and Sideris (1985) geopotential models are capable of defining geoidal undulations to approximately half a metre over Canada.

## 4.3 The UNB Dec. '86 Geoid

### 4.3.1 Introduction

The “UNB Dec. '86” geoid make uses of the following method to determine the value of geoidal undulations over Canada. If the total separation of geoid and ellipsoid at a point is taken as  $N$  then:

$$N = N_L + dN, \quad (4.13)$$

where the long wave length contribution,  $N_L$ , is obtained, as described in Section 4.3.6, from satellite derived coefficients. This field will only describe features larger than  $180/n_{max}$  where  $n_{max}$  is the maximum degree and order of the coefficients.  $dN$  is the part of the geoidal undulation obtained from terrestrial gravity anomalies and the method of evaluating this contribution involves the use of Stokes’s formula. Figure 4.3 shows this geoid plotted in the form of contours for a  $3^\circ$  by  $7^\circ$  area including the Great Slave Lake in the North West Territories.

### 4.3.2 Computational strategy for the high frequency contribution

For the terrestrial contribution the method of subdivision according to geographical grid lines is used in the “UNB Dec. '86” geoid. The computation strategy is set out in Table 4.1. Integration, in fact, takes place over an “approximate” spherical cap as is shown in Figure 4.4.

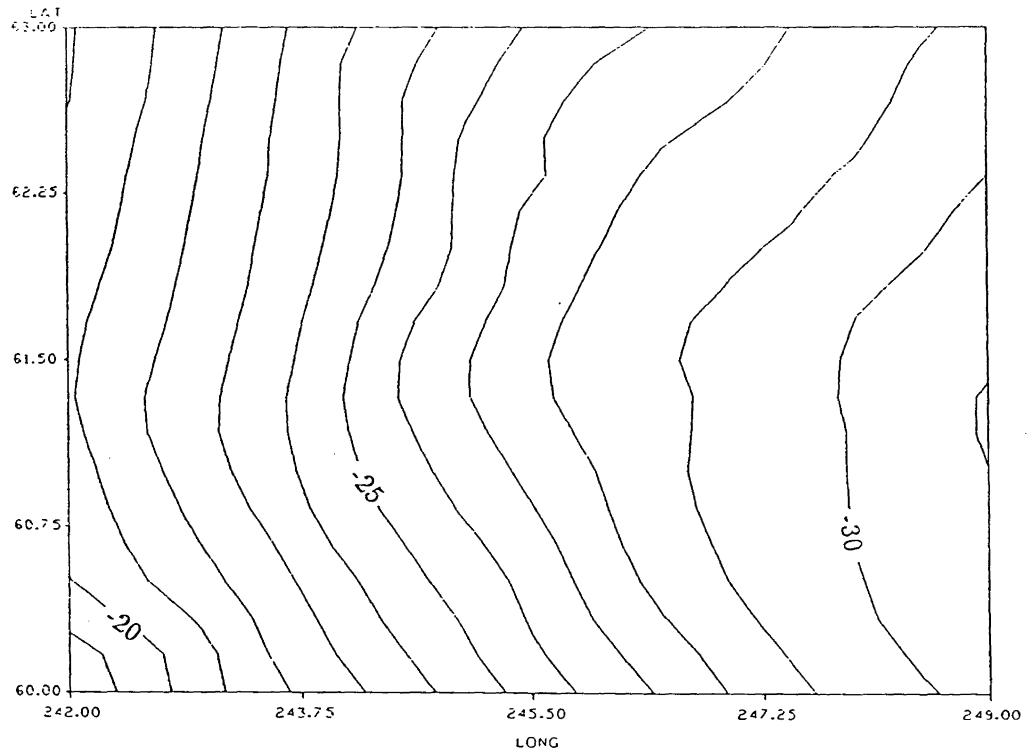


Figure 4.3: "UNB Dec. '86" gravimetric geoidal undulations (in metres) for the Great Slave Lake Area, NWT.

<i>Zone</i>	<i>Size of zone</i>	<i>Boundary of zone</i>
inner-most	10' by 10' (10' by 20' in higher latitudes)	coincides with 5' by 5' gravity anomaly file.
inner	2° by 2° less innermost zone	coincides with 1° by 1° grid lines.
outer	whole integration area $\psi_o = 6^\circ$ less inner zone	see Figure 4.4 for details.

Table 4.1: Computational strategy for “UNB Dec. ’86”.

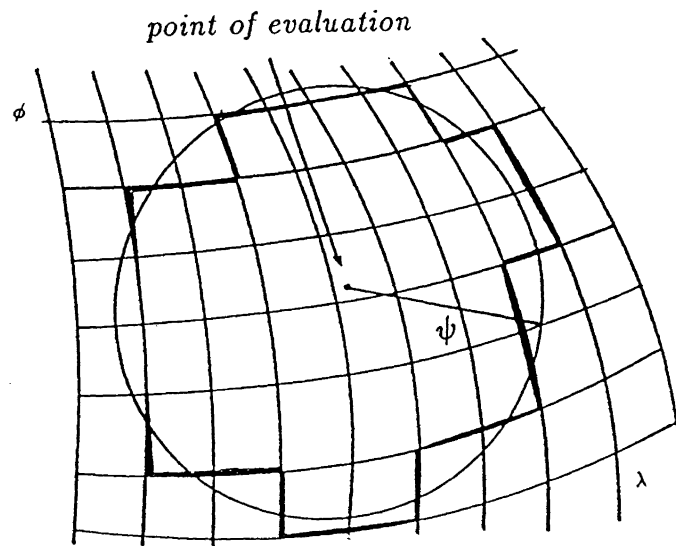


Figure 4.4: The approximate spherical cap used in the UNB Dec. '86 geoid (after Vaníček et al., 1986).

### 4.3.3 Sources of gravity data

The gravity data used for the calculation of the “UNB Dec. ’86” geoid come from two sources and are contained in three files. These consist of the point gravity file, the file containing the 5' by 5' (and to the north the 5' by 10') mean gravity anomalies and, lastly, that containing the 1° by 1° mean gravity anomalies (cf. Table 4.2). The first two files were supplied by the Division of Gravity, Geothermics and Geodynamics of the former Earth Physics Branch of Energy, Mines and Resources Canada. The latter file originated from the Department of Geodetic Science and Surveying of Ohio State University and the data are termed “The January 1983 1 × 1 Degree Mean Free-air Anomaly Data” (Rapp, 1983).

All anomalies are accompanied by their standard deviation. If a 5' by 5' (or 5' by 10') cell had no anomaly associated with it then its value was predicted from the surrounding point anomalies and, if there were none of these, then the value of the corresponding 1° by 1° cell was used for the integration with an assumed standard deviation of 50 mGal.

In the 1° by 1° file, of 185 empty cells, 24 could be predicted from the point gravity anomaly file and the rest were given a value of 0 with a standard deviation of 50 mGal.

### 4.3.4 Modification of Stokes's function

Stokes's formula,  $S(\psi)$ , requires integration to be carried out to  $\psi = 180^\circ$ . Measurements of gravity anomalies are scarce on parts of the earth and apart from this the computational burden would be large. Fortunately, if use is made of a higher order reference field of degree  $l$ , the appropriate Stokes's function,  $S_{l+1}(\psi)$ , displays different characteristics. The integration area can be further reduced by modifying the formula to the form  $S_{l+1}^m(\psi)$ . Stokes's function may be seen as a weighting function and referring to Figure 4.5 it can be clearly seen that the modified version is different

<i>Data file</i>	<i>size of file</i>	<i>source of data</i>
Point gravity data	628 019 free air anomalies (40° to 80° N) (218° to 320° E) corrected for the GEM9 modelled value	Energy, Mines and Resources, Canada.
Mean gravity anomalies	for each 5' by 5' cell (40° to 56° N) 5' by 10' cell (56° to 76° N) (214° to 318° E) mean free air anomalies corrected for GEM9 modelled value	Energy, Mines and Resources, Canada.
Mean gravity anomalies	1° by 1° cell (30° to 80° N) (190° to 340° E) mean anomalies corrected for GEM9 modelled value	Ohio State University (Rapp, 1983).

Table 4.2: Gravity data used in "UNB Dec. '86".

from the original and the higher order unmodified functions.

The modified function makes use of the Molodenskij truncation coefficients and minimizes the resulting truncation error in  $dN$  when the size of the spherical cap is limited. If a reference field of degree and order 20 is adopted the formula for the

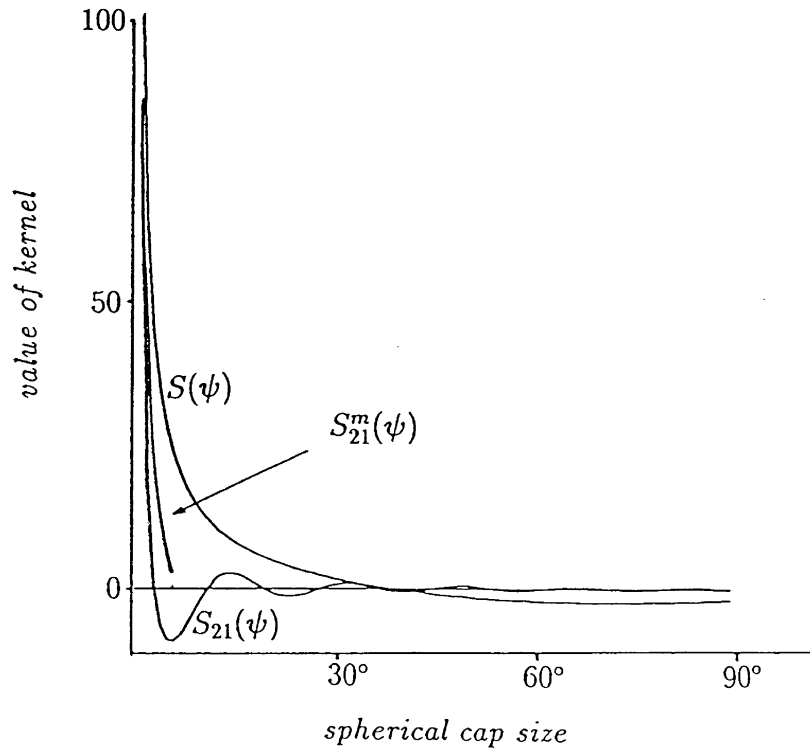


Figure 4.5: Behaviour of Stokes's function in the original version ( $S(\psi)$ ), unmodified higher order version ( $S_{21}(\psi)$ ) and modified higher order version ( $S_{21}^m(\psi)$ ).

modified higher order Stokes's formula becomes:

$$S_{21}^m(\psi) = S_{21}(\psi) - S_{20}^t(\psi), \quad (4.14)$$



where

$$S_{21}(\psi) = \sum_{k=21}^{\infty} \frac{(2k+1)}{(k-1)} P_k(\cos \psi) \quad (4.15)$$

and

$$S_{20}^t = \sum_{i=0}^{20} \frac{(2i+1)}{2} t_i P_i(\cos \psi), \quad (4.16)$$

where  $t_i$  are the Molodenskij truncation coefficients given in Appendix I.

Careful testing in Vaniček et al. (1986) revealed that the best compromise between computer time and accuracy yielded a spherical cap of  $\psi = 6^\circ$ .

In the innermost zone a second order algebraic surface is fitted to the available point gravity anomalies. If none are available, then mean anomalies are used. Stokes's formula is approximated to a series and the eight most significant terms of the product of these two series are integrated term by term and summed.

$$I_{INM} = \sum_{i=1}^8 I_i, \quad (4.17)$$

where  $I_i$  represents the individual contributions.

For the inner and outer zones computation of the modified Stokes's formula was approximated by means of an expression:

$$S^* = \beta_0 + \frac{\beta_1}{\psi} + \beta_2 \ln\left(\frac{\psi}{2}\right) + \beta_3 \psi^2 \ln\left(\frac{\psi}{2}\right), \quad (4.18)$$

such that  $S^*$  fits  $S_{21}^m$  as well as possible over the  $6^\circ$  radius of integration. The constants  $\beta_0$ ,  $\beta_1$ ,  $\beta_2$  and  $\beta_3$  were obtained by numerical computation. The above approximation results in errors of less than 1 centimetre (Vaniček and Kleusberg, 1987) and is necessary because the generation must be carried out at least 650 times for each of 100 000 computation points.

### 4.3.5 Corrections to be applied

The assumption so far has been that all the mass of the earth lies within the geoid. This is obviously not so.

If all masses are moved below the geoid mathematically then this changes the gravity at the surface. This change is called the topographical effect and is expressed as  $\delta g_t$  which must be applied to a free air anomaly before it can be used in Stokes's formula. For areas of up to  $6^\circ$  and height differences of less than 2 kilometres a planar approximation (Vaniček and Kleusberg, 1987) yields:

$$\delta g_t \doteq \frac{1}{2} G \sigma \int_{\alpha=0}^{2\pi} \int_{l=0}^{\infty} \frac{(H_Q^2 - H_A^2)}{l^3} d\alpha dl \quad (4.19)$$

where  $\sigma$  is the constant density of the topographic masses and  $\alpha$  and  $l$  are local coordinates centered on a point below the point of computation,  $P_A$ .  $H_A$  and  $H_Q$  are as defined in Figure 4.6.

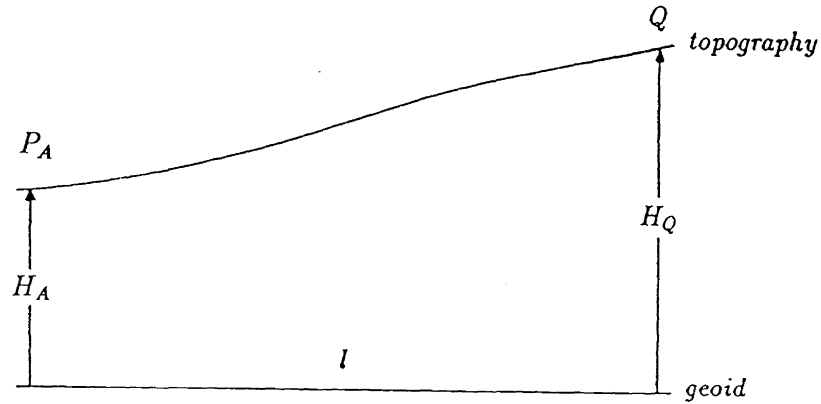


Figure 4.6: Calculation of the topographic and indirect effects (after Vaniček and Kleusberg, 1987).

In practical terms the topographic correction is evaluated using the following

formula:

$$\delta g_t \doteq \frac{1}{2} G \sigma R^2 \sum_i \frac{(H_i^2 - H_A^2)}{l^3} A_i, \quad (4.20)$$

where  $H_i$ ,  $l_i$  and  $A_i$  refer to the mean topographic height of the  $i$ th 5' by 5' cell (or 5' by 10' cell in the north), its distance from the point of interest, and its area. The presence of the  $l^{-3}$  term implies that integration need only be carried out in the close vicinity of the point.

The shifting of the masses will change the gravity potential and hence the geoid. Therefore, the surface computed by Stokes's formula will be slightly different from the geoid. In order to obtain the actual geoid from this other surface,  $N^c$  (the co-geoid), a correction  $\delta N$  must be applied.

Referring once more to Figure 4.6 the approximate correction is given by:

$$\delta N \doteq -\frac{\pi G \sigma}{\gamma} H_A^2 - \frac{G \sigma}{6\gamma} \int_{\alpha=0}^{2\pi} \int_{l=0}^{\infty} \frac{(H_Q^3 - H_A^3)}{l^3} d\alpha dl, \quad (4.21)$$

where  $\gamma$  is the normal gravity on the ellipsoid. In practice the following formula was used:

$$\delta N \doteq \frac{\pi G \sigma}{\gamma} H_A^2 - \frac{G \sigma R^2}{6\gamma} \sum_i \frac{(H_i^2 - H_A^2)}{l^3} A_i, \quad (4.22)$$

where  $H_i$ ,  $l_i$  and  $A_i$  refer to the  $i^{\text{th}}$  5' by 5' cell in Equation 4.20. Again integration does not have to be carried out too far because of the  $l^{-3}$  term.

The masses of the atmosphere are also outside the geoid and hence a correction has to be applied to the observed gravity anomaly. Tables for this effect, which is dependent on height, have been published by the International Association of Gravity. Values for  $\delta g_A$  vary between about -0.5 mGal and -0.9 mGal.

The total terrestrial contribution, with the correction for topographical effect, indirect effect, and atmospheric effect applied are shown in Table 4.3 for a number of stations in the NWT Network.

<i>station</i>	<i>inner-most zone</i>	<i>inner zone</i>	<i>outer zone</i>	<i>total contribution</i>	<i>std. dev.</i>
629102	-0.14	-1.61	-1.17	-2.92	±0.10
699062	-0.21	-1.54	-1.24	-2.99	±0.09
66T035	-0.15	-1.11	-1.26	-2.53	±0.11
66T038	-0.17	-0.82	-1.47	-2.45	±0.11
66T081	-0.04	-0.85	-1.32	-2.20	±0.12
66T086	-0.05	-0.87	-1.36	-2.28	±0.12
66T116	-0.07	-0.80	-1.45	-2.32	±0.16
66T120	-0.10	-0.82	-1.43	-2.35	±0.16
58908	-0.12	-0.90	-1.44	-2.46	±0.15
66T167	-0.09	-1.20	-1.10	-2.39	±0.14
869228	-0.15	-1.37	-1.39	-2.92	±0.12
82T054	-0.15	-1.35	-1.51	-3.01	±0.12
67T064	-0.11	-1.52	-1.39	-3.02	±0.11
809209	-0.10	-1.04	-1.85	-3.00	±0.11
67T095	-0.11	-1.26	-1.44	-2.81	±0.10
869217	-0.13	-1.22	-1.40	-2.75	±0.10
67T042	-0.10	-1.63	-1.54	-3.28	±0.10
82T069	-0.15	-1.58	-1.60	-3.33	±0.10
82T097	-0.19	-2.00	-1.54	-3.73	±0.10
869225	-0.16	-2.01	-1.56	-3.74	±0.10
82T010	±0.00	+0.07	-1.15	-1.08	±0.15
58900	-0.05	+0.17	-1.06	-0.96	±0.15

Table 4.3: The total terrestrial contribution for points in the North West Territories Network.

### 4.3.6 The low frequency contribution

In the UNB solution it was decided to use the GEM9 (Lerch et al., 1979) potential field. At that stage (1986), it was the most complete purely satellite solution available (Vaníček et al., 1986). This potential field model is available to degree and order (20,20), which the physics of orbital analysis indicate should be the limit of a satellite derived field (Vaníček et al., 1990). Thus, only those geoidal features larger than  $9^\circ$  will be distinguished according to the formula  $180/n_{max}$ .

In the following, the superscript  $G9$  refers to the GEM9 potential field and the superscript  $G80$  refers to the Geodetic Reference Spheroid 1980 (GRS80) (Moritz, 1980). The potential field solution for GEM9 is given in the usual form of spherical harmonic coefficients,  $J_{nm}^{G9}$  and  $K_{nm}^{G9}$ . GEM9 was referred to GRS80 in the UNB study by the following procedure. The derivation is given in Vaníček et al. (1986), but, practically, the change of reference involves multiplying the normalised GRS80 potential coefficients by a factor and adding the GEM9 potential coefficients. Only the  $J_{20}^{G9}$ ,  $J_{40}^{G9}$ ,  $J_{60}^{G9}$  and  $J_{80}^{G9}$  potential coefficients are affected and they become, for  $n = 2, 4, 6, 8$ :

$$J_{n0} = J_{n0}^{G9} + \frac{GM^{G80}}{GM^{G9}} \left(\frac{a^{G80}}{a^{G9}}\right)^n J_{n0}^{G80}, \quad (4.23)$$

where  $GM^{G80}$  and  $GM^{G9}$  is the product of the gravitational constant and the mass of the earth for each system and  $a^{G80}$  and  $a^{G9}$  are the two mean earth equatorial radii.

The height of the GEM9 spheroid above the GRS80 ellipsoid is given by:

$$N^{G9} = \frac{GM^{G9} - GM^{G80}}{\gamma r} + \frac{GM^{G9}}{\gamma a^{G9}} \sum_{n=2}^{20} \sum_{m=0}^n \left(\frac{a^{G9}}{r}\right)^{n+1} (J_{nm} Y_{nm}^c(\phi\lambda) + K_{nm} Y_{nm}^s(\phi\lambda)), \quad (4.24)$$

where  $J_{nm}$  and  $K_{nm}$  are taken as equal to the the potential coefficients  $J^{G9}$  and  $K^{G9}$ , except for  $J_{20}$ ,  $J_{40}$ ,  $J_{60}$  and  $J_{80}$ , which are evaluated in Equation 4.23.  $Y_{nm}^c$  and  $Y_{nm}^s$  are the normalized spherical harmonic functions and  $\gamma$  is the normal gravity as

for the ellipsoid. In practice  $N^{G9}$  can be evaluated using the program POT described in Tscherning et al. (1983). This program may be used to evaluate the corrections to the gravity anomalies so that the effects of the GEM9 field can be discounted from the terrestrial or high frequency contribution.

The average standard deviation for the undulation is about 1.75 metres for for GEM9 coefficients taken to degree and order 20 (Lerch et al., 1985) (cf. Figure 4.7). This error applies to wavelengths of greater than 2,000 kilometres and is not of concern

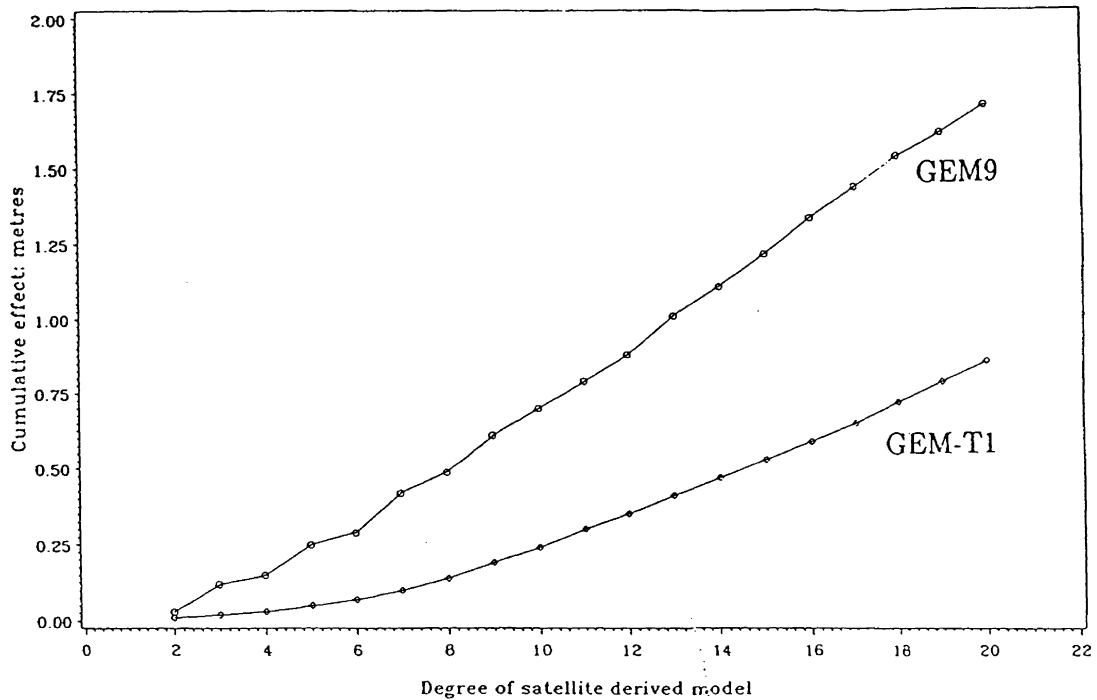


Figure 4.7: Accuracy of the GEM9 and GEM-T1 potential coefficients.

when dealing with the commonly used geoidal height differences because the generally limited length of the baselines will result in both terminals being affected by the same amount.

## 4.4 Changing of the reference field from one geopotential model to another

The procedure for changing the reference field from one earth gravity model to another of a similar degree is fairly simple as has been pointed out by Vaníček and Sjöberg (1989).

The choice of a good earth gravity model for use with the determination of the geoid is important and it is very useful to be able to update to a new model as new solutions become available. The “UNB Dec. ’86” geoid uses the GEM9 reference field. However, additional models have become available including the GEM-T1 model (Marsh et al., 1988).

For replacing an earth gravity model of degree and order 20, such as GEM9, by another, such as GEM-T1, truncated to degree and order 20, the change in reference gravity will be from  $\gamma_{G9}^{20}$  to  $\gamma_{GT1}^{20}$  denoted here by  $D\gamma^{20}$ .

Only the low order gravity anomalies will be affected and so, for  $n$  less than or equal to 20:

$$(\Delta g_n^{20})^{GT1} = (\Delta g_n^{20})^{G9} + D\gamma_n^{20}. \quad (4.25)$$

The correction to the geoidal undulation consists of two parts. The correction to the new reference spheroid, GEM-T1, is obtained from the following formula:

$$DN_2^{20} = \frac{1}{\gamma} \sum_{n=2}^{20} (T_n^{GT1} - T_n^{G9}), \quad (4.26)$$

where  $T_n^{GT1}$  and  $T_n^{G9}$  are the disturbing potential constituents for each reference field and may be obtained from the potential coefficients referred to GRS80. The second correction is to the geoidal height above the reference spheroid due to the change in gravity and is given by:

$$DN_2^{20} \doteq -\frac{R}{2\gamma} \sum_{n=2}^{20} t_n D\gamma_n^{20}, \quad (4.27)$$

where

$$D\gamma_n^{20} = \frac{n-1}{R} DT_n, \quad (4.28)$$

$R$  is the mean radius of the earth, and:

$$DT_n = T_n^{GT1} - T_n^{G9} \quad (4.29)$$

refers to the change in the disturbing potential.

The complete correction,  $DN$ , to the geoidal height above the GRS80 reference figure is therefore:

$$DN = \frac{1}{\gamma} \sum_{n=2}^{20} \frac{2 - (n-1)t_n}{2} DT_n. \quad (4.30)$$

The Molodenskij truncation coefficients are given in Appendix I for the integration cap of  $\psi = 6^\circ$  as used in “UNB Dec. ’86 ” geoid.  $DT_n$  may be obtained by modification to the function POT (Tscherning et al., 1983). A contour map showing the corrections from GEM9 to GEM-T1 for “UNB Dec. 1986” for the Great Slave Lake Area, North West Territories, is shown in Figure 4.8. The truncation coefficients were obtained from the program TRUNC (Chang et al., 1986).

## 4.5 The UNB ’90 geoid

### 4.5.1 Introduction

In 1989 the University of New Brunswick was contracted to recompute the geoid over Canada using the same modified Stokes’s formula used in the 1986 version but with updated gravity data sets. The Geodetic Survey of Canada undertook to provide:

- a set of point free-air gravity anomalies updated to January 1989,
- a set of mean free-air anomalies on a geographical grid of 5’ by 5’, and
- a set of mean free-air anomalies on a geographical grids of 1° by 1°.

The reference spheroid chosen was the model GEM-T1 of the NASA Goddard Space Flight Center, given in the form of potential coefficients (Marsh et al., 1988), truncated to (20, 20).



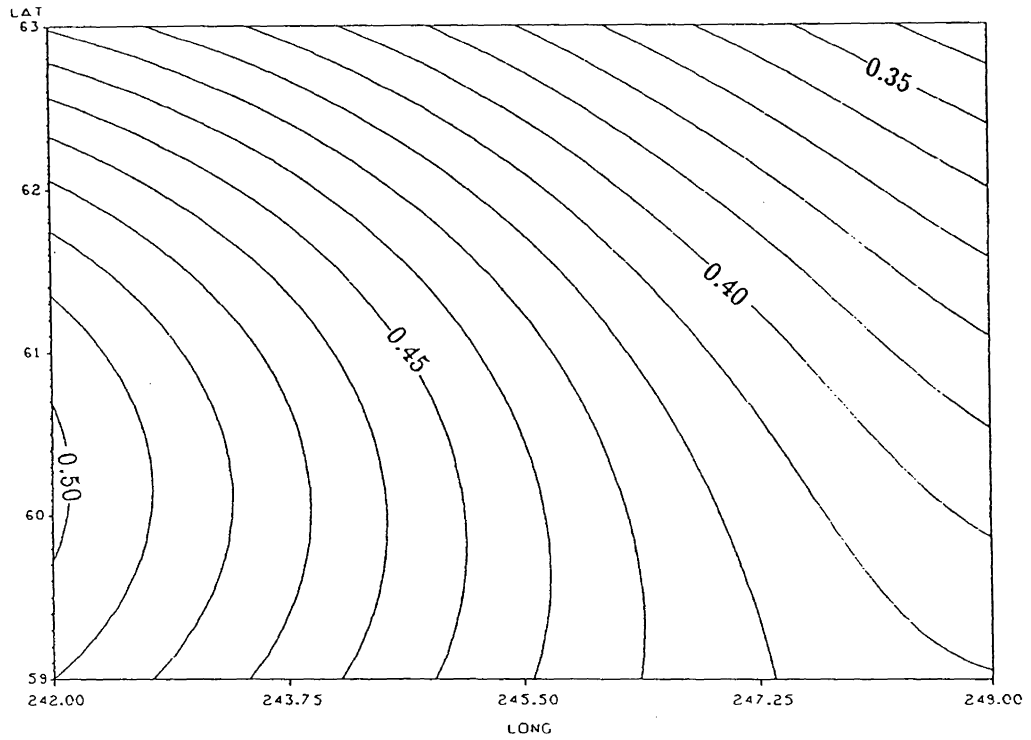


Figure 4.8: *DN* to be applied to “UNB Dec. '86” to convert from reference field GEM9 to GEM-T1 for the Great Slave Lake area.

Computation was again carried out with the GIN program, which was adapted to take the new data sets.

#### **4.5.2 Computational strategy for the high frequency contribution**

The same computational strategy was used in this version of the geoid as in the "UNB Dec. '86" version (cf. Table 4.1).

#### **4.5.3 Sources of gravity data**

The gravity data used for the calculation of the "UNB '90" geoid were all supplied by the Geodetic Survey of Canada and are contained in three files. These are the point gravity file, the file containing the 5' by 5' mean gravity anomalies, and, lastly, that containing the 1° by 1° mean gravity anomalies (cf. Table 4.4). Bouguer anomalies were used to produce representative gravity values for 5' by 5' cells over the land and free anomalies were used over the water areas. Interpolation was carried out by means of least squares collocation. The terrain heights for the Bouguer anomaly were obtained from a digital elevation model also with 5' by 5' grid spacing.

In the 1° by 1° file there were a number of empty cells. These were regarded as having a gravity anomaly of 0 mGal and a standard deviation of 50 mGal.

The contribution of the GEM-T1 value to the point gravity anomalies was discounted by generating a 5' by 5' grid of contributions and interpolating individual values by means of a quadratic surface fitted to 9 adjacent grid values. This technique yielded an excellent agreement with individually generated corrections.

#### **4.5.4 Modification of Stokes's function**

The same form of the modified Stokes's formula was used as was used in the 1986 version of the geoid (cf. Section 4.3.4).

<i>Data file</i>	<i>size of file</i>	<i>source of file</i>
Point gravity data	588 874 free air anomalies corrected for atmospheric attraction effect and the GEM-T1 contribution	Geological Survey of Canada.
Mean gravity anomalies	for each 5' by 5' cell (40° to 76° N) (214° to 318° E) mean free air anomalies corrected for atmospheric attraction effect and the GEM-T1 contribution	created by Contract Authority (Mainville and Veronneau, 1989).
Mean gravity anomalies	1° by 1° (35° to 90° N) (190° to 340° E) mean anomalies corrected for atmospheric attraction effect and the GEM-T1 contribution	created by Contract Authority (Mainville and Veronneau, 1989).

Table 4.4: Gravity data used in “UNB ’90”.

### 4.5.5 Corrections to be applied

In the “UNB Dec. ’86” geoid the topographic correction was applied by first correcting the gravity anomalies and then integrating these anomalies (cf. Section 4.3.5). The approach used in the 1990 version is to generate geoidal height corrections directly by means of a two dimensional Fourier transform. Mean topographic heights on a 5’ by 5’ grid were used for this purpose.

The atmospheric correction and indirect effect were applied as in Section 4.3.5.

### 4.5.6 The low frequency contribution

In the updated solution it was decided to use the GEM-T1 (Marsh et al., 1988) potential coefficient field. It was supposed to be the most accurate purely satellite solution available at the beginning of 1989. Its accuracy is estimated at nearly twice that of the GEM9 reference field used in 1986. This potential field is available to degree and order (36,36). It makes use of “Kaula’s rule”. This approximate rule which is based on previous studies yields the degree variance per coefficient as:

$$\sigma_l = \frac{10^{-5}}{l^2} \quad (4.31)$$

(cf. Section 4.9). The satellite data set does not have the sensitivity to resolve all the coefficients to degree 36 and so this external estimate of the coefficients was used to stabilize the solution. The application of this rule is equivalent to introducing a set of additional observations of the coefficients where each has an expected value of zero, with Kaula’s estimate being used as the variance of the “observations”. Marsh et al. (1988) have found that this has caused coefficients above degree 25 to have about 1/3 to 1/2 of the power of fields that have been obtained from altimetry or surface gravity. It was felt, therefore, by Vaniček et al. (1990) that the physics of orbit analysis set the upper limit of a satellite derived field to (20,20). Therefore, the GEM-T1 field was truncated to this latter limit, which is possible because of the

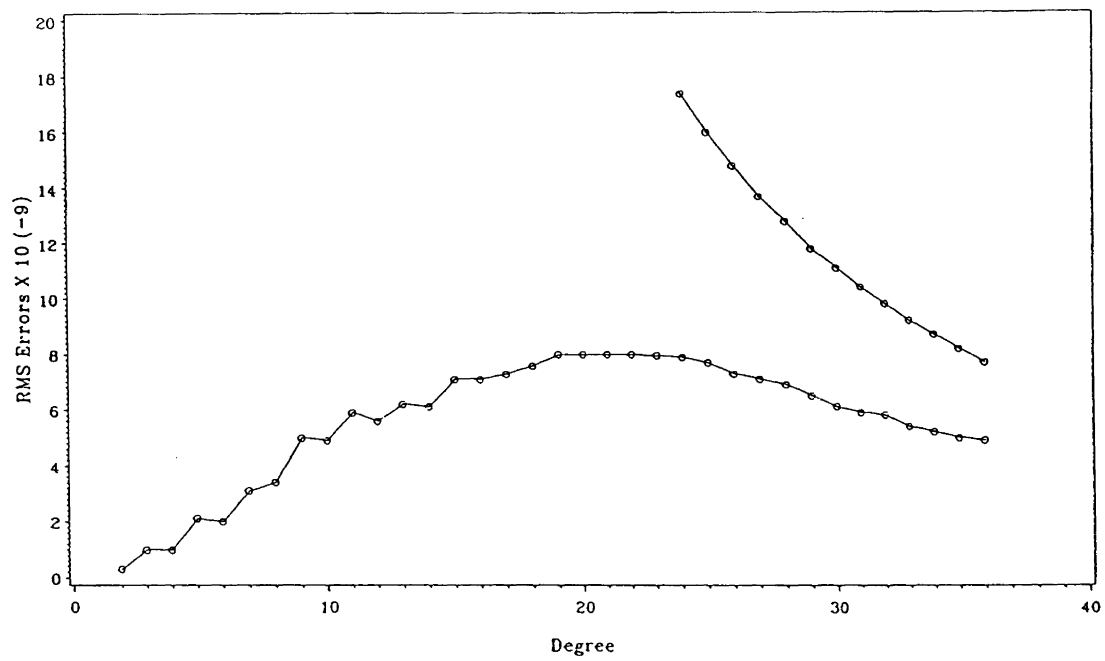


Figure 4.9: The application of Kaula's rule (after Marsh et al.,1988).

orthogonality of spherical harmonics. However, it is important to note that biases may be introduced by the application of “Kaulas rule”.

The potential coefficients were related to GRS80 by means of the same procedure as outlined in Section 4.3.6.

The average standard deviation for the undulation is about .85 metre for the GEM-T1 coefficients taken to degree and order 20 (cf. Figure 4.7).

## 4.6 Comparison between geoidal models

Figure 4.10 shows a comparison between the “UNB '90” geoid and the “UNB Dec. '86” geoid. This difference should be equal, approximately, to Figure 4.8 as the largest difference between the two models (apart from updated gravity) is due to the use of the GEM-T1 reference field in the 1990 model and the use of GEM9 in the 1986 model. The difference between the two is clearly greater than expected and this is due to a change in gravity data sets.

In the Figures 4.11 and 4.12 is shown the difference between the UNB86 and OSU86F as well as the difference between the UNB90 and the OSU86F.

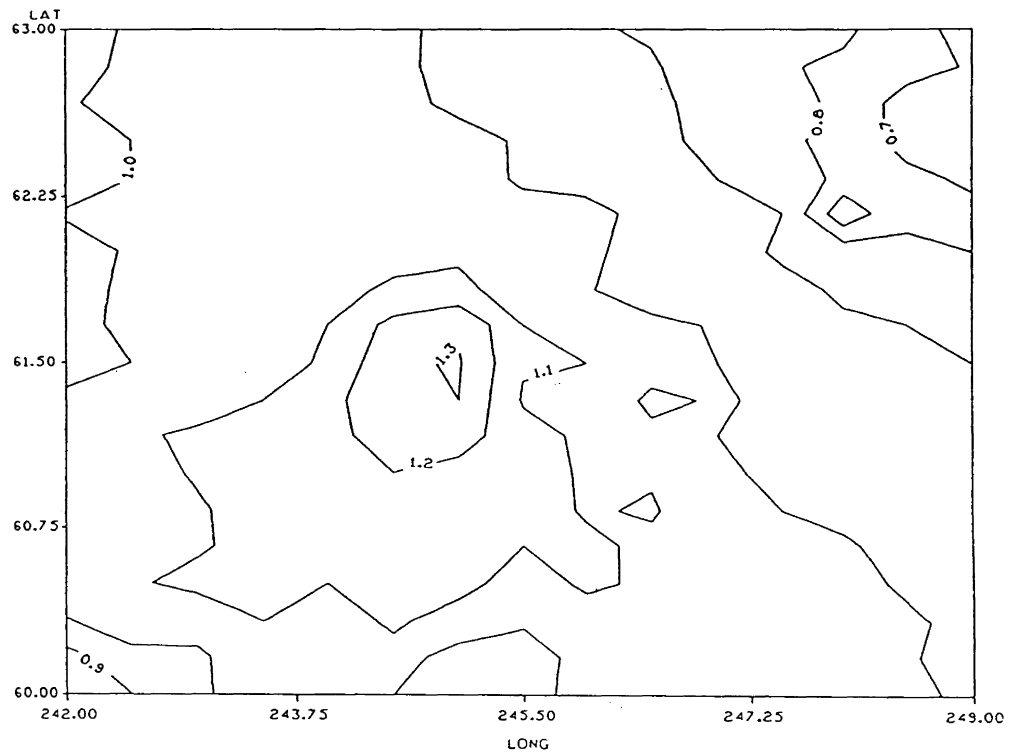


Figure 4.10: The difference between UNB90 and UNB86 for the Great Slave Lake Area.

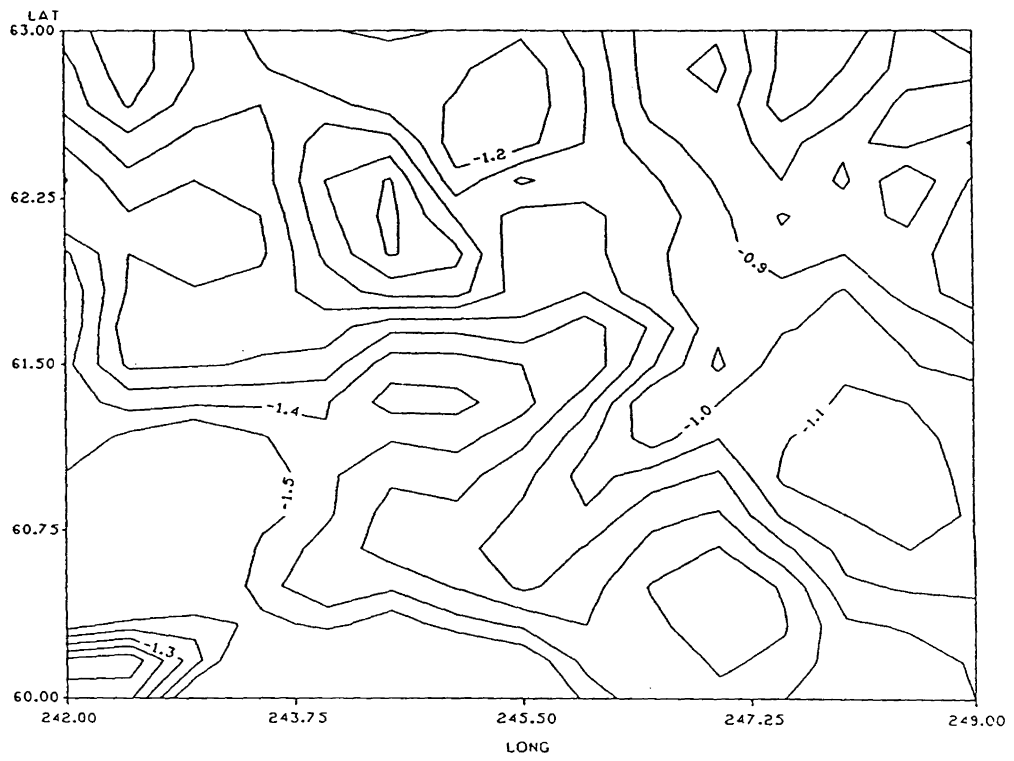


Figure 4.11: Difference between UNB86 and OSU86F for the Great Slave Lake Area.



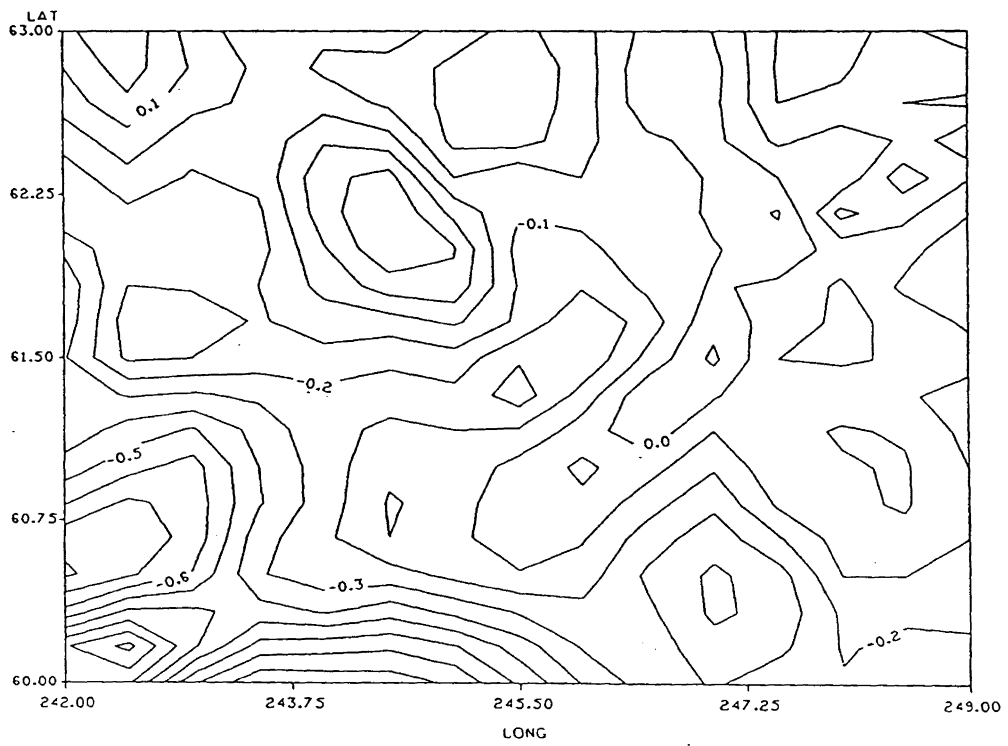


Figure 4.12: Difference between UNB90 and OSU86F for the Great Slave Lake Area.

## Chapter 5

# Biases and errors in GPS height differences

### 5.1 The Global Positioning System

The Navigation Satellite Timing and Ranging Global Positioning System (NAVSTAR/ GPS) has been under development by the US Defense Department since the mid-1970's. It is intended to replace the aging TRANSIT system. The GPS was designed primarily as a navigation system.

Ranges measured to four known satellite positions will allow an observer to obtain his position as well as a "nuisance" parameter which is the arbitrary receiver clock offset. Higher accuracy is achievable when GPS receivers are used in a differential mode—that is simultaneous range measurements are made to the same satellites from both terminals of a baseline. Biases, such as the uncertainty in satellite position and inadequate refraction corrections, are highly correlated and will tend to equally affect both stations. Therefore, far greater relative than absolute accuracies are obtainable.

The C/A (Coarse Acquisition) Code has a wavelength of approximately 293 metres. For the P (Precise) Code, it is 29.3 metres. As a rule, resolution can be performed to about 1% of the wavelength (Wells et al., 1986).

## 5.2 Carrier phase observations

For surveying applications, use is made of the  $L_1$  and  $L_2$  carrier signals, which have nominal wavelengths of 19 centimetres and 24 centimetres. The principle of carrier wave phase measurement is that the range between the satellite and the receiver consists of an integer number of carrier waves and the residual fractional part of a cycle –this fractional part is found by comparing or “beating” the received carrier signal and the signal generated by the receiver oscillator:

$$\Phi_i^j = \Phi_i(T) - \Phi^j(t). \quad (5.1)$$

The signal is transmitted at time,  $t$ , from satellite,  $j$ , and received at receiver,  $i$ , at time,  $T$ . The equation, thus, compares the receiver signal phase,  $\Phi_i(T)$ , with the transmitter signal phase,  $\Phi^j(t)$ .

The difference in phase,  $\Phi_i^j$ , is dependent on transmission time from satellite to receiver. This, in turn, depends on the range as well as the ionospheric and tropospheric delays. When multiplied by the wavelength of  $L_1$  or  $L_2$ ,  $\lambda$ , in order to transform the phase difference to units of length, the carrier phase observation equation becomes:

$$\lambda\Phi_i^j = \rho_i^j - d_{ion} + d_{trop} + cdt^j - c\delta t_i + \lambda N_i^j + \varepsilon, \quad (5.2)$$

where the receivers position,  $x_i$ ,  $y_i$  and  $z_i$ , is contained in the range,  $\rho_i^j$ ,  $d_{ion}$  and  $d_{trop}$  are ionospheric and tropospheric delays,  $dt^j$  is the satellite clock error,  $\delta t_i$  is the receiver clock error,  $N_i^j$  is the integer cycle ambiguity at the start of the measurement, and  $\varepsilon$  is the error associated with the observation.

Clearly, error sources such as satellite orbit uncertainty, receiver and satellite clock, and atmospheric propagation errors, will be strongly correlated between receiver sites. If the measurements are differenced between receivers, satellites, or epochs, much of the error will be removed. Most software packages make use of “double difference”

observation processing (Santerre, 1989). This method results in the removal, or reduction, of the effects of satellite clock error and receiver clock error, as well as the reduction of the effects of orbit uncertainty and ionospheric and tropospheric delays. The double difference carrier phase observation equation is:

$$\lambda \nabla \Delta \Phi = \nabla \Delta \rho + \nabla \Delta N + \nabla \Delta d_{ion} + \nabla \Delta d_{trop} + \nabla \Delta \varepsilon, \quad (5.3)$$

where  $\nabla \Delta \Phi$  is the double difference carrier phase observable,  $\nabla \Delta \rho$  is the geometric double difference range,  $\nabla \Delta N$  is the integer double difference phase ambiguity,  $\nabla \Delta d_{ion}$  is the double difference range error due to ionospheric delay,  $\nabla \Delta d_{trop}$  is the double difference range error due to tropospheric delay, and  $\nabla \Delta \varepsilon$  is the double difference carrier phase observation noise and the remaining unmodelled effects.

A number of investigators (i.e. Wells et al., 1987) have found that whether undifferenced or one of the various forms of differenced carrier beat phase observations is used, the results are the same and hence the methods are equivalent, providing extra parameters are included to account for biases when using undifferenced observables. This means that so long as the equations are correctly implemented in the software, it does not matter what approach is used. Single difference and triple difference observation equations are given in most texts on GPS (i.e. Wells et al., 1986).

Some residual error, however, will remain and propagate into the solution. In Section 5.4 the errors affecting GPS derived geometric heights will be identified and quantified.

### 5.3 The GPS Networks

The following GPS networks were observed by the Geodetic Survey of Canada as part of an ongoing project of implementing GPS for control surveys in Canada. Wherever possible connections have been made to bench marks with orthometric heights from differential leveling (Mainville, 1987). At these stations, where both the GPS derived

geometric heights and the orthometric heights are known, geoidal undulation can be obtained to check gravimetric geoid solutions. The networks are described in the following sections.

### 5.3.1 The North West Territories network

This network was observed during the months of September and October, 1986. Ninety three GPS stations were established along the roads that circle the Great Slave Lake, which is located in the North West Territories (NWT) and lies between  $60^{\circ}$  and  $63^{\circ}$  N and  $242^{\circ}$  and  $249^{\circ}$  E. The GPS stations were at intervals of approximately 10 kilometres and 83 were set up at or connected to first order leveling network bench marks (Mainville and Veronneau, 1989) (cf. Figure 5.1).

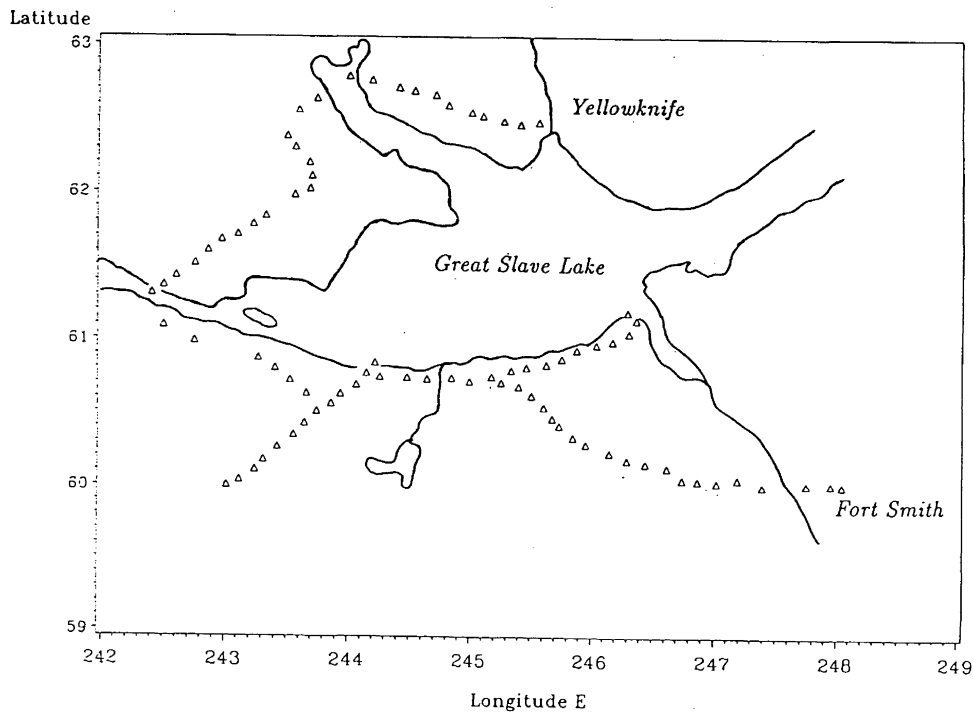


Figure 5.1: The North West Territories network.

Baselines were observed for an average of about 1 hour and always for more than 45 minutes. Four Wild-Magnavox WM101 GPS receivers were used simultaneously and at least four common satellites were observed from each of these stations. All observations were made during two daytime sessions, as it was found that sessions at night yielded poor results.

Positions were determined using the WM's *POPS* program. Double difference carrier phase equations were used from the WM101's single frequency observations to determine  $\Delta x$ ,  $\Delta y$  and  $\Delta z$  components for 356 baselines. The tropospheric model used was HOPFIELD II. These results were then processed in a least squares network adjustment using the GHOST adjustment program (Penney, 1990) with a single station at Yellowknife held fixed.

### **5.3.2 The Ontario network**

During the summer of 1985, a network of 45 stations was established by GPS (Mainville, 1987). These points are in the vicinity of Lake Ontario and lie between 43° and 48° N, and between 275° and 284° E (cf. Figure 5.2). Of 45 stations, 25 stations were tied to primary vertical control. Kearsley (1988b), after testing, found that five of these were less reliable.

Dual frequency observations were made using Texas Instrument TI-4100 receivers.

Observations were reduced using the PHASAR program (Penney, 1990) to obtain the baselines and the results were processed in the GHOST network adjustment program. The HOPFIELD tropospheric correction model was used. Station 683100A was held fixed.

### **5.3.3 The Manitoba network**

This network, consisting of 22 stations, was observed in the summer of 1983. It lies in central Manitoba between 50° and 51° N and between 261° and 264° E (cf.

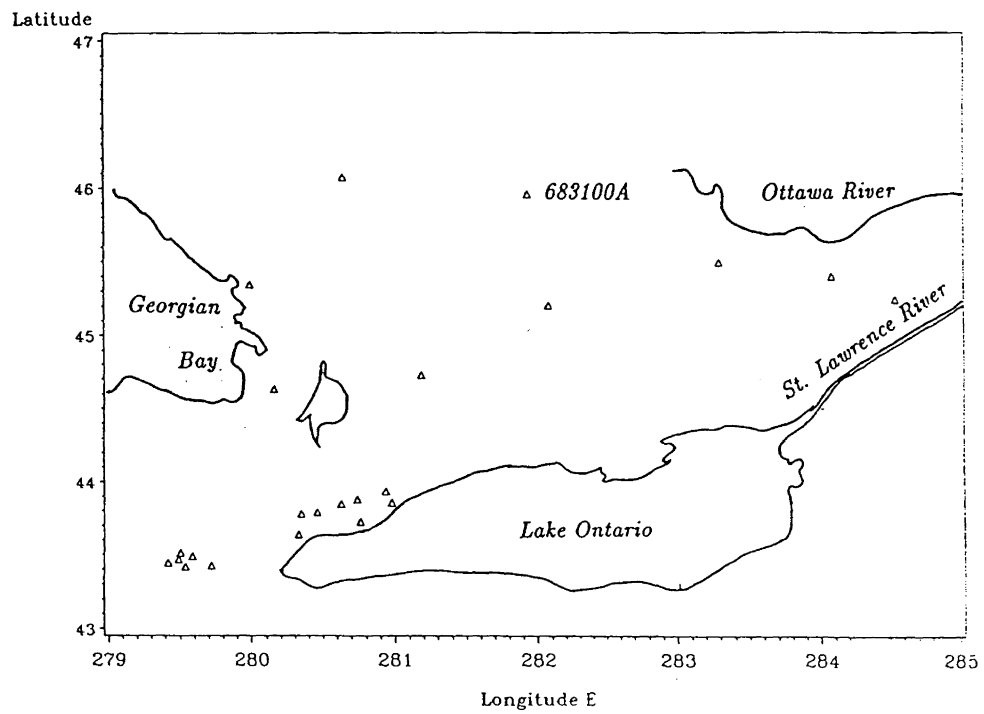


Figure 5.2: The Ontario Network.

Figure 5.3). Of the 22 stations, 11 were connected to the primary vertical network.

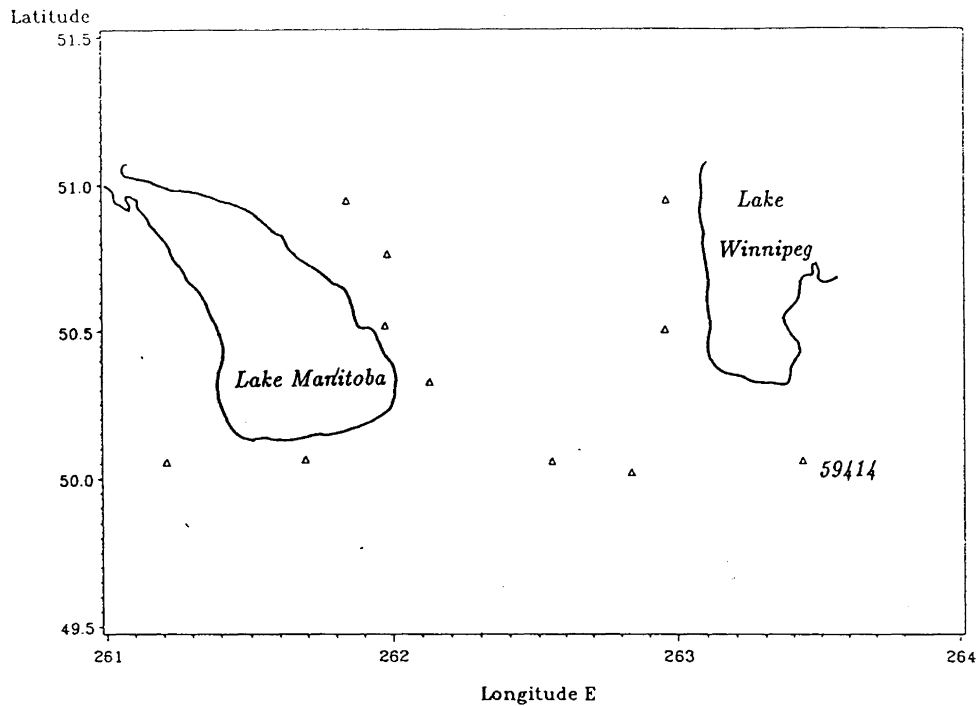


Figure 5.3: The Manitoba network

Kearsley (1988b) found one station to be less reliable after testing.

The receivers used in this survey were Macrometer V-1000's, which are capable of collecting single frequency data.

Observations were reduced using the Macrometer suite of programs and the base-lines were processed in the GHOST network adjustment program. The values were obtained by holding the station 58419 fixed.

The accuracy of the orthometric heights quoted for this network are generally inferior to those of the other networks.



## 5.4 Sources of errors in GPS relative height determination.

The accuracy of heights obtained from GPS are influenced by random errors due to the observation process and biases due to incorrect or incomplete mathematical modelling. The geometry of the satellites determines how the errors propagate into the final solution. Biases, such as those due to orbit error and delays, will influence the observations.

### 5.4.1 The geometry of the satellite configuration

Santerre (1989) conducted an investigation of the impact of GPS satellite sky distribution on the propagation of errors in precise relative positioning by studying the behaviour of the covariance matrix, the confidence ellipsoid, and correlation coefficients in a least squares solution as functions of the following – satellite sky distribution, station co-ordinates, clock and tropospheric zenith delay. He found that even when the system is fully operational unmodelled biases will still significantly effect the final solution. With the GPS still in its developmental stage, the poor distribution of satellites, as experienced during these three campaigns, will result in unmodelled biases propagating strongly into the final solution, depending on the particular geometry during each period of observation.

### 5.4.2 Orbit biases

The estimated uncertainty in the broadcast ephemeris is in the order of 20 metres. The error is due to the following uncertainties (Holloway, 1988):

- in the defining elements of the reference ellipsoid (GRS80),
- in the position of satellite tracking stations,

- initial state of the satellite, and
- force models used for the gravitational and non-gravitational disturbing effects acting on the satellite.

By making use of a relative positioning the effect is reduced. As a “rule of thumb” the orbit biases will propagate into a baseline as follows (Wells et al., 1986):

$$\vec{\rho} d\vec{B} = \vec{B} d\vec{\rho}, \quad (5.4)$$

where  $\vec{B}$  is the baseline vector joining the receivers,  $\vec{\rho}$  is the range vector to the satellite, and  $d\vec{B}$  and  $d\vec{\rho}$  are the error vectors.

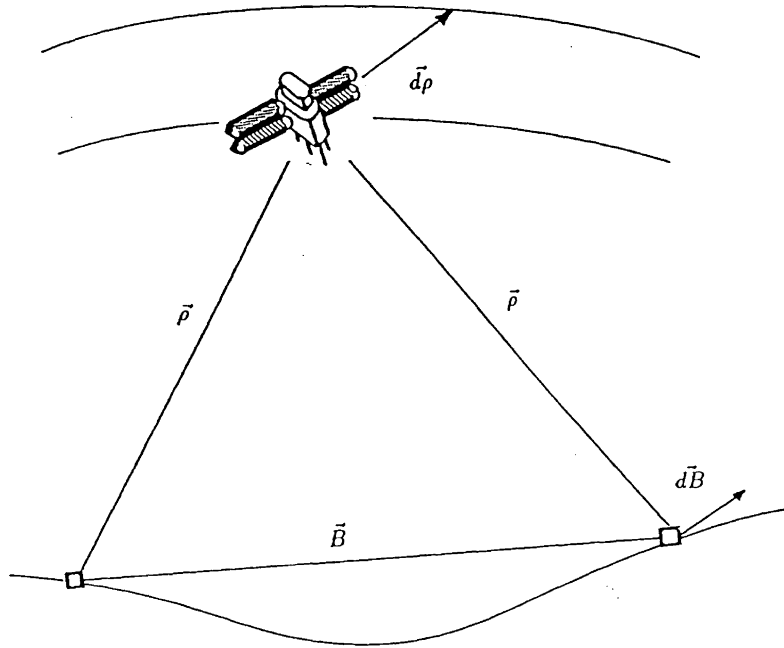


Figure 5.4: The effect of orbit uncertainty on a baseline.

An error in the satellites orbit may be described by means of its along track (direction of motion), radial (direction from satellite to earth), and across track (perpendicular to the other two) components. Due mainly to difficulties in modelling

solar radiation pressure, the along track error is the greatest of the three. The effect of the along track error was determined by Beutler et al. (1989) to have the most significant effect on the height. The error is a maximum when the direction of the baseline is the same as the direction of the orbit plane. The magnitude of the height error,  $e_{\Delta h}$ , may be expressed as:

$$e_{\Delta h} = \cos(Az_s - Az_b) \frac{\Delta s}{\rho} b, \quad (5.5)$$

where  $Az_s$  is the azimuth of the orbital plane of the satellite being tracked,  $Az_b$  is the azimuth of the baseline,  $\Delta s$  is the along track error,  $\rho$  is the range of the satellite and  $b$  is the baseline length. For a the worst case scenario for a baseline of any length Table 5.1 would apply.

$\Delta s$	$\rho$	height error
20m	20 000km	1ppm
40m	20 000km	2ppm

Table 5.1: Effect of orbit uncertainty on baseline height difference.

### 5.4.3 Atmospheric refraction

The effect of the atmosphere on the GPS signal takes two very different forms. The troposphere, which makes up the layer from the earth's surface to approximately 40 kilometres above its surface, is a non-dispersive medium for which the delay is dependent on the refractive index of the medium along the path of the signal. On the other hand, the ionosphere, which lies between 40 to 1000 kilometres, is a region where the the delay of the satellite signal is due to its interaction with ionised gas molecules and is frequency dependent.

## Tropospheric refraction

The differential residual error in the tropospheric correction between two stations is often the major source of error when using GPS for obtaining geometric heights. Beutler et al. (1987b) report that a bias of 1 millimetre in the zenith distance of the relative tropospheric refraction will cause a height bias of approximately 3 millimetres.

The total tropospheric effect can be separated into two parts – the more stable dry component, which accounts for about 90% of the bias, and the variable wet component, which depends on humidity. The dry component usually accounts for about 80 -90% of the zenith range delay of about 2.3 metres within the first 7 kilometres of troposphere above the earths surface (Holloway, 1988). The effect increases as the secant of the zenith distance and may reach to 20 metres at 20° above the horizon. Providing, however, that low altitude observations are neglected, it is possible to model the dry component to about 1% and the wet component to 10 -20% using surface meteorological data.

The wet component is more difficult to model, because it depends on the temperature and water vapour content from the surface of the earth to the upper regions of the troposphere. Obviously surface meteorological conditions do not accurately reflect this, especially when weather conditions, such as fog, occur.

When processing GPS data, the tropospheric correction is sometimes ignored, hoping that it will cancel out. This may be reasonable for shorter baselines, where the topography is flat and weather conditions are fairly stable. For greater accuracy, one of the standard tropospheric correction models is used. The latest models are able, dependent on the amount and quality of atmospheric information available, to account for 92 -95 % of the combined wet and dry effect or equivalently leave a residual of 2 -5 centimetres (Delikaraoglou, 1989). In many GPS processing packages tropospheric delay is statistically estimated using a spatially and temporally averaged troposphere. The actual variations of the wet troposphere around these average values will show up as baseline and height difference errors. Kouba (1987) has adapted experience

with VLBI measurements to arrive at the following model to describe the effect of the wet troposphere on baseline height differences:

$$\sigma_{\delta h} = s^2 \sqrt{\frac{1 - \exp \frac{-b^2}{d^2}}{b^2}}. \quad (5.6)$$

The error in height difference is given in parts per million (i.e. millimetres per kilometre). The constant,  $s$ , is taken as 80 millimetres, which corresponds to uncorrelated tropospheric conditions as experienced in VLBI observations. The baseline length,  $b$ , is in kilometres and the correlation distance,  $d$ , is usually taken as 30 kilometres. The effect is shown in Figure 5.5.

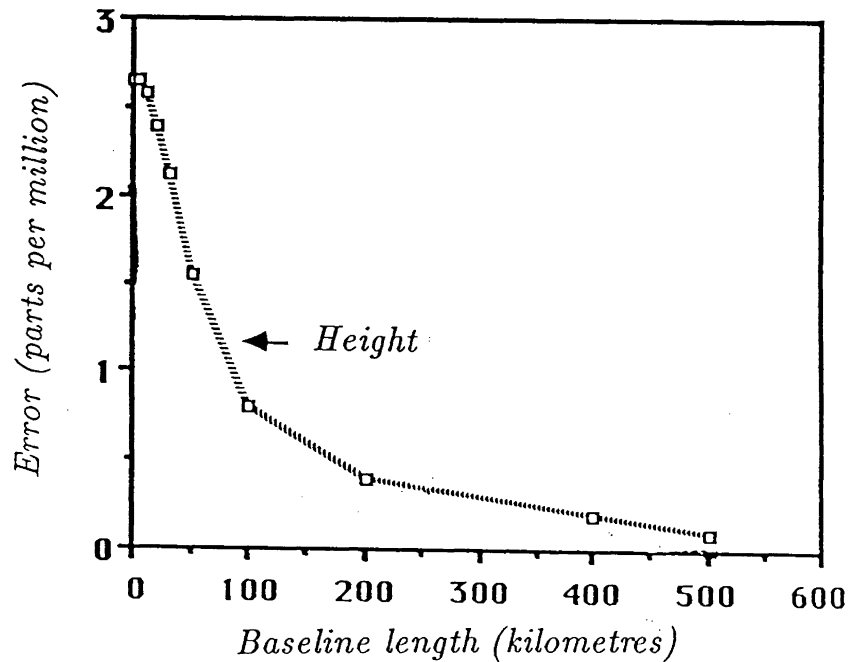


Figure 5.5: The effect of modelling errors of wet tropospheric refraction on GPS height differences (after Delikaraoglou, 1989).

GPS processing software generally gives a choice of correction model to be used. For example, the *POPS* package by the Wild-Magnavox company used for the North West Territories Network gives a choice of:

- Hopfield I,
- Hopfield II,
- Saastamonien, or
- no model.

The user enters the temperature, relative humidity, and pressure or the default option will use a standard atmosphere.

### **Ionospheric effect**

The ionosphere tends to disperse the GPS signal, the code signal used for the ranging technique is less than the velocity of light in a vacuum, but the phase delay is negative (an apparent increase in velocity):

$$d\Phi_{ion} = \frac{-8.442TEC}{f}, \quad (5.7)$$

where  $d\Phi_{ion}$  is the phase delay in radians, TEC is the total electron content per metre squared ( $elm^{-2}$ ) and varies typically from  $2000 \times 10^{15}$  to  $10 \times 10^{15} elm^{-2}$  (Holloway, 1988).

The TEC is a function of latitude –it has a maximum near the equator and in the Auroral regions (Leal, 1989). It is also dependent on the time of day. A maximum is experienced in the early afternoon and this falls to a minimum in the early morning (cf. Figure 5.6). The TEC varies according to an eleven year cycle, depending on solar sunspot activity. When the observations described in this report were taken for the North West Territories network, a low in the cycle was being experienced. Both the Ontario and Manitoba Networks were observed in the intermediate stage between a maximum and a low (cf. Figure 5.7). There are also isolated sudden ionospheric disturbances.

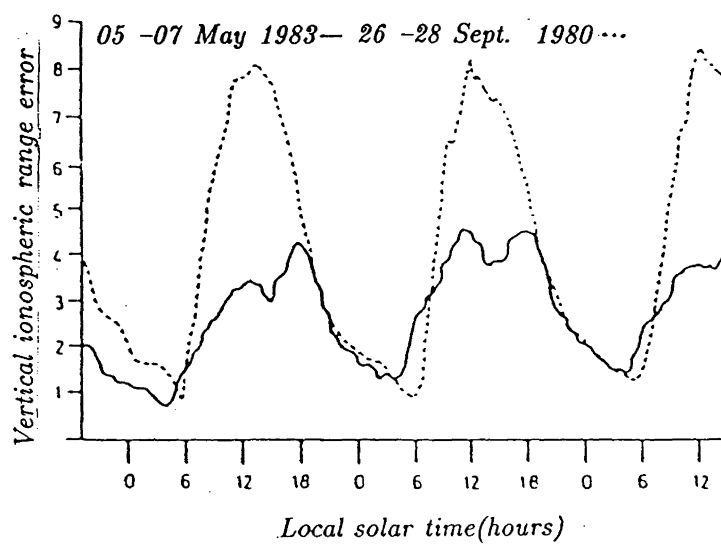


Figure 5.6: Typical diurnal variations in the Total Electron Content (TEC) (Holloway, 1988).

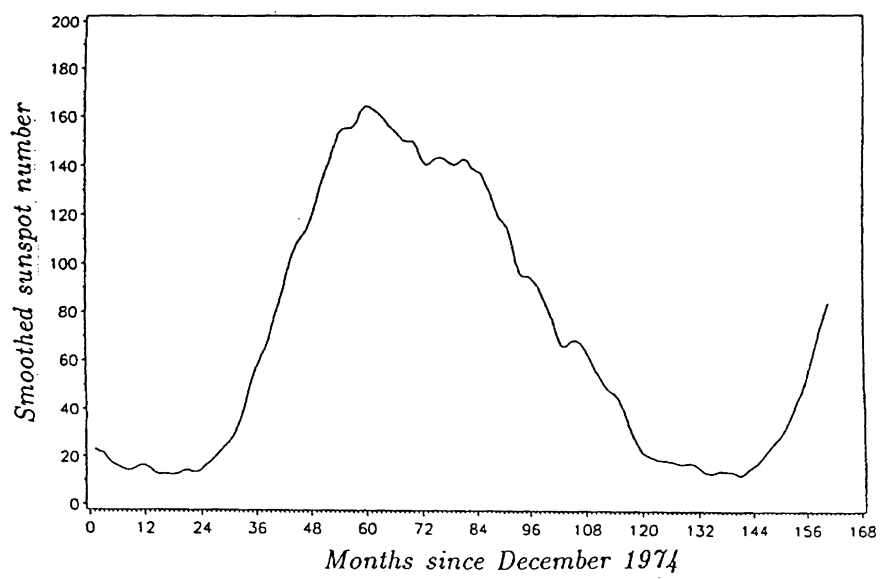


Figure 5.7: Sunspot activity.



According to Buetler et al. (1987b), the following formula may be used to calculate the effect of the ionosphere on the  $L_1$  carrier:

$$\frac{\Delta e}{b} = -0.7 \times 10^{-17} TEC. \quad (5.8)$$

The observations for the NWT network and those in Manitoba were taken with a single frequency receivers.

This effect of the ionospheric delay reaches a maximum when the satellite is near the horizon and is at a minimum at the zenith. The bias effect is greatly decreased from a maximum of up to 150 metres when differenced between the two ends of the baseline.

The amount by which a GPS signal is dispersed by the ionosphere depends on its frequency and so, if measurements are made simultaneously on both the  $L_1$  and  $L_2$  signals, almost all of the ionospheric delay can be removed.

The correction to be applied to the  $L_1$  signal is given by:

$$d\Phi_{ion} = \frac{f_2^2}{f_2^2 - f_1^2} (\Phi_{L_1} - \Phi_{L_2} \frac{f_1}{f_2} - N_{L_1} - N_{L_2} \frac{f_1}{f_2}), \quad (5.9)$$

where  $f_1$  and  $f_2$  are the frequencies of the  $L_1$  and  $L_2$  carriers, respectively, and  $N_{L_1}$  and  $N_{L_2}$  are their cycle ambiguities. This correction becomes more important as the length of the baseline increases, as ionospheric delay is not correlated over long distances. The frequency dependence of the ionosphere allows a correction to be applied in the case of the Ontario network, as dual frequency observations were made. This is the most accurate method of correcting differential carrier beat phase measurements for this delay. Some error may be left in times of high TEC, resulting in a non-homogeneous signal path from a satellite to the receivers on either end of a baseline. The same effect is likely to occur, even in times of low TEC, for longer baselines. The residual ionospheric delay tends to affect a baseline or a network more as a scale error than a height error. Longer baselines, especially those with a north-south orientation, will have an error in height (Santerre, 1989). Kleusberg (1986) reports that the dual frequency correction increases the noise of the observations by a factor of 3.3.

#### 5.4.4 Antenna phase centre variations

All GPS measurements refer to the antenna phase centre. The geometrical phase centre will not, in general, coincide with the electrical phase centre. The error is dependent on the design of the antenna (which is often the result of a compromise between high gain and multipath reduction) and the direction of the incoming signal.

The practice of mounting an antenna in the same orientation on its tripod may greatly reduce the variation of the phase centre with azimuth when differential measurements are made. However, the phase center may also be dependent on the vertical angle to a satellite and this will affect height determination. Calibration is performed by mapping the antenna pattern for a full range of azimuths and elevations. Wells and Tranquilla (1986) have reported phase centre variations of 2 to 10 centimetres depending on the antenna type. Kleusberg (1986) has found a variation of phase centre for a TI 4100 antenna to be 1.9 centimetre for the  $L_1$  frequency and 3.3 centimetre for the  $L_2$  frequency.

#### 5.4.5 Multipath and antenna imaging

Both a direct and reflected signal arrive at the receiver and introduce a bias into phase difference for carrier phase observations. This effect depends on the antenna design and the location of the reflecting surface. It is not possible to calculate the magnitude of this effect as it will vary according to location, but Tranquilla (1988) has found that due to its cyclic nature, if observation periods are kept long, it will tend to randomise.

The phenomenon known as antenna imaging is similar to multipath and results from conducting objects in the vicinity of the antenna coupling with it and defining an image of it. The resultant amplitude and phase characteristics will be significantly different from those of the isolated antenna (Delikaraoglou, 1989).

#### 5.4.6 Bias due to errors in station co-ordinates

If the GPS baseline solution is with respect to a fixed station whose geocentric position is not well determined, significant errors in heighting can occur. Holloway (1988), in a simulated study, found that for a six satellite scenario, when error values of  $\delta_\phi$ ,  $\delta_\lambda$ ,  $\delta_h = 10$  metres were assumed, the resultant error in height was 2 parts per million for both a 5 kilometre and a 50 kilometre baseline. With a simulated shift of  $\delta_\phi$ ,  $\delta_\lambda = 100\text{m}$ , Chrzanowski et al. (1988) reported an error of 8 parts per million.

#### 5.4.7 Ambiguity resolution and clock biases

In double differencing, which is the most commonly used software calculation technique, the ambiguity  $\nabla\Delta N$ , which is an integer number of wavelengths of the carrier signal, must be solved for in the calculation. The ambiguity remains constant for each combination of satellite and receiver unless there is a loss of lock, commonly referred to as cycle slip. If this does occur, then the ambiguity must again be obtained from a new calculation.

The cycle slips are repaired initially by trial and error or by the triple difference technique. When the cycle ambiguity is solved for, the solution does not recognise that it is an integer and it may be difficult to estimate the correct integer from the real number solution, especially for longer baselines. Correct resolution of the ambiguity will result in an increase in the precision of the geodetic co-ordinates, but incorrect resolution will degrade it. Holloway (1988) found in his simulated study that, while correct ambiguity resolution did increase the precision of the horizontal co-ordinates, the improvement to the height was minimal and it appears that this does not justify risking the degraded accuracy that would result from unsuccessful resolution.

Each satellite has four atomic frequency standards and the best of these is used for GPS time and for generating the fundamental frequency. Even when using the second order degree correction polynomial which is broadcast by the satellite, a significant

bias remains. This is dealt with by differencing between receivers in most software packages that calculate precise relative positions.

The receivers generally have quartz crystal oscillators and the same method is used to eliminate their inaccuracies as are used for the satellite clock. All biases and stabilities of both clocks are cancelled out.

# Chapter 6

## Analysis of sample data

### 6.1 Introduction

As mentioned in Chapter 2 errors are usually classified as blunders, random or systematic errors. Blunders or gross errors may be detected by sound observing and recording procedures. Random errors are normally regarded as being statistically independent and follow the Gaussian probability density function with zero mean. Systematic errors are statistically dependent. There is a functional relationship between the observation and some influencing factor or factors. There remains in almost any kind of observation some residual systematic error which depends on the measuring technique (Craymer, 1984).

If all possible statistical moments of a data series (mean, variance etc.) are independent of the argument then the process is stationary. In other words, the statistical moments describing the behaviour of the sample are identical for all values of the argument. This condition is not satisfied when the process is non-stationary. Degrees of stationarity exist –if only the first few statistical moments are independent of the argument then the process is weakly stationary. The autocorrelation function may be used to detect statistical dependence between data series values and any specific argument. Further information is gained by the decomposition of the signal into its

spectral components using the technique of least squares spectral analysis (LSSA) (Wells et al., 1985) allowing unknown periods to be estimated. This technique is capable of simultaneously removing any datum bias or linear trend that may be present in the data. The data series may be ordered with respect to any argument i.e.  $\phi, \lambda, H$  etc. in order to detect statistical dependence between values and this argument. A significant trend in the autocorrelation will point to the presence of systematic errors.

## 6.2 The autocorrelation function

A data series,  $x_i$ , ordered according to the argument,  $a$ , providing it is stationary, has:

1. mean:  $E\{x_i\} = \bar{x}$ ,
2. variance:  $E\{x_i - \bar{x}\} = \sigma^2$ , and
3. autocovariance:  $E\{(x_i - \bar{x})(x_j - \bar{x})\} = \mu_{i-j}$ ,

where  $E$  is the expectation operator. The autocovariance is therefore defined as the expected value of the random variable multiplied by itself, lagged by a given number of the argument,  $i - j$ . Non-zero values for  $i \neq j$  will indicate that the variable is autocorrelated.

If the datum bias mean is removed (the LSSA program will do this) from the data series the residual series,  $e_i$ , has:

$$E\{e_i\} = 0 \tag{6.1}$$

and the autocovariance reduces to:

$$E\{e_i e_j\} = \mu_{i-j} \tag{6.2}$$

The autocorrelation,  $C$ , of a data series,  $e_i$ , is simply the normalised autocovariance of the variable where normalisation is based on the autocovariance at zero lag,  $\mu_0$ ,

so:

$$C(b) = \frac{\mu_b}{\mu_0} \quad (6.3)$$

for  $b = i - j = 0, 1, 2 \dots m$ . The implication is that the data series is equally spaced. The data series dealt with in this discussion are unequally spaced. Vaníček and Craymer (1983) proposed a method of overcoming this problem. The method is similar to the histogram used in statistics. This “binning” technique consists of evaluating  $C(b)$ , not for the discrete values  $b$ , but for all  $b_l$  in the interval  $(b_l, b_l + db)$ . The direct estimate of the autocorrelation function,  $C(b_l)$ , is given by (Vaníček et al., 1985):

$$C(b_l) = \frac{1}{N\mu_0} \sum_{i=1}^N e(a_i)e(a_j), \quad (6.4)$$

for all  $b_l = |a_i - a_j| \in (b_l, b_l + db)$ .  $N$  is the number of values in the series. The value of  $b$  must be reasonably large, ensuring that  $C(b_l)$  provides a meaningful average for each bin (cf. Figure 6.1).

The computed autocorrelations usually display short period fluctuations due to the finite length of the data. This noise may be reduced, for example, by means of a weighted, moving average filter. The Gaussian filter used in this study is described in Craymer (1984). The equation defining the filter is given by:

$$C(b_l) = \frac{\sum_{i=-k}^k C(b_{i-l})W_{i-l}}{\sum_{i=-k}^k W_{i-l}}, \quad (6.5)$$

where  $C(b_l)$  is the smoothed autocorrelation and  $k$  is the width of the filter on either side of  $b_l$  included in the averaging process. The weight of each  $C(b_{i-l})$  in the direct estimation is given by:

$$W_{i-l} = N_l G_l, \quad (6.6)$$

for  $l = -k, -k + 1, \dots k$ , where  $N_l$  is the number of products used to compute  $C(b_{i-l})$  and  $G_l$  are the Gaussian coefficients. A value of  $k = 3$  was used in this study and the corresponding Gaussian coefficients are:

$$G_0 = 1.0000$$

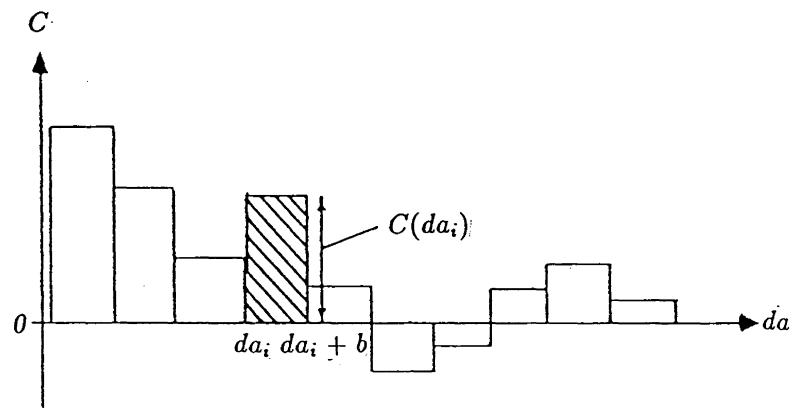


Figure 6.1: The direct interval estimation method (after Craymer, 1984).



$$\begin{aligned}
G_{1/-1} &= 0.8825 \\
G_{2/-2} &= 0.6065 \\
G_{3/-3} &= 0.3247.
\end{aligned}$$

For the first three lags there is little smoothing in order to maintain the value  $C(0) = 1$ , but these values are generally obtained from a large number of products and are thus less susceptible to large variations. For the two values at the end of the series, the filtered values were made equal to the unfiltered values.

### 6.3 Least squares spectral analysis

It is possible to describe a data series in the frequency domain by means of its spectral density function, which is the Fourier transform of the autocorrelation function (Craymer, 1984). This, however, has only been applied in the case of equally spaced data. In order to make provision for unequally spaced data, Vaníček (1971) applied the method of least squares to obtain the spectral density function. This method simultaneously obtains the best estimates of the datum bias and linear trend amongst other values.

The LSSA problem may be described as follows. For a data series,  $\mathbf{e}$ , ordered according to an argument,  $\mathbf{a}$ , a vector of spectral densities,  $\mathbf{s}$ , is required corresponding to a vector of frequencies,  $\boldsymbol{\omega}$ .

According to the method of least squares:

$$\hat{\mathbf{c}} = (\boldsymbol{\Phi}^T \mathbf{W} \boldsymbol{\Phi})^{-1} \boldsymbol{\Phi}^T \mathbf{W} \mathbf{e}, \quad (6.7)$$

where  $\hat{\mathbf{c}}$  is the vector of the unknown parameters,  $(\hat{c}_1, \hat{c}_2)^T$ .  $\boldsymbol{\Phi}$  is the design matrix which models the relationship between the unknown parameters,  $\mathbf{c}$ , by means of the observation equation,  $\mathbf{e} = \boldsymbol{\Phi} \mathbf{c}$ . As a simplification the weight matrix,  $\mathbf{W}$ , is assumed to be an identity matrix.

The best fitting approximant of  $\mathbf{p}$  to  $\mathbf{e}$  may be computed for each  $\omega_j$ :

$$p(\omega_j) = \hat{c}_1 \cos \omega_j a + \hat{c}_2 \sin \omega_j a \quad (6.8)$$

If  $p(\omega_j)$  represents  $e$  exactly then the spectral value,  $s$ , will be 100. If  $\hat{\mathbf{c}} = 0$  then  $p(\omega_j) = 0$  and  $s$  will be 0. In general therefore:

$$s = \frac{\text{orthogonal projection of } \mathbf{p} \text{ onto } \mathbf{e}}{\text{length of } \mathbf{e}} * 100 \quad (6.9)$$

or in vector notation:

$$s(\omega_j) = \frac{\mathbf{e}^T \mathbf{p}(\omega_j)}{\mathbf{e}^T \mathbf{e}} * 100. \quad (6.10)$$

In order to compute the least squares spectrum,  $s(\omega_j)$   $j = 1 \dots m$ , a least squares approximation is carried out  $m$  times, each time obtaining  $\mathbf{p}(\omega_j)$  for a specific  $\omega_j$ .

This is a simplified case. In practice the program removes the datum bias and, optionally, the linear trend (and other values) and the spectral analysis is carried out on the residual time series. The derivation of this is more lengthy and may be found in Wells et al. (1985).

## 6.4 Analyses of simulated data series

In order to test the LSSA, direct interval estimation autocorrelation function (DIAF) and smoothing programs, four series, consisting of a random data series and three random series to each of which was introduced a different trend (or statistical dependency), were generated. The first data series may be regarded as statistically independent (normally distributed), and the other series may be thought of as partially statistically dependent (normally distributed with a trend). The DIAF program was used to detect the presence of any systematic effect and the LSSA program was used to recover the period of the trend. The random series were created using the International Mathematical and Statistical Library (IMSL) random number generator routine.

### 6.4.1 Random data series

A series of 84 points between 0 and 6 argument (“distance”) units was obtained using the IMSL random number generator. A total of 84 was chosen as this represents the size of the largest series considered in this study. The “misclosure” has a mean very close to zero and a maximum deviation of 0.25 which is approximately the magnitude of the misclosures to found in the actual data series considered later. The data series, its autocorrelation function, and its spectrum are shown in Figure 6.2.

The autocorrelation function is close to zero, as expected. This is the desired form of an autocorrelation function for random data. The slight periodicity about the zero line may be attributed to the artificial method in which the series was obtained. A smoothed version of the function is shown by the dashed lines in the same plot.

The spectrum of the data series has the 95% significance level indicated by the dashed lines. Any variances below this line are not significant. As expected, there appears to be little significant periodicity. There is a marginally significant peak at a frequency of 0.68 which corresponds reciprocally to a period of about 1.5 argument units of the data series plot but this is most likely due to a bias in the generator.

### 6.4.2 Random data series with trend

In the second test a random series with a maximum deviation of  $\pm 0.25$  was superimposed on a sine trend with a period of 1.5 argument units and an amplitude of 0.25. Again a series of 84 points between 0 and 6 argument units was generated. The data series, its autocorrelation function, and its spectrum are shown in Figure 6.3.

The trend is somewhat obscured by the superimposed random series, but is still clearly visible. The autocorrelation function shows a substantial periodicity as is to be expected. The spectrum has a very well defined peak at a frequency of 0.67 which corresponds, reciprocally, to a period of 1.5 argument units. Hence the LSSA program has accurately determined the period of the trend. A secondary peak of much less

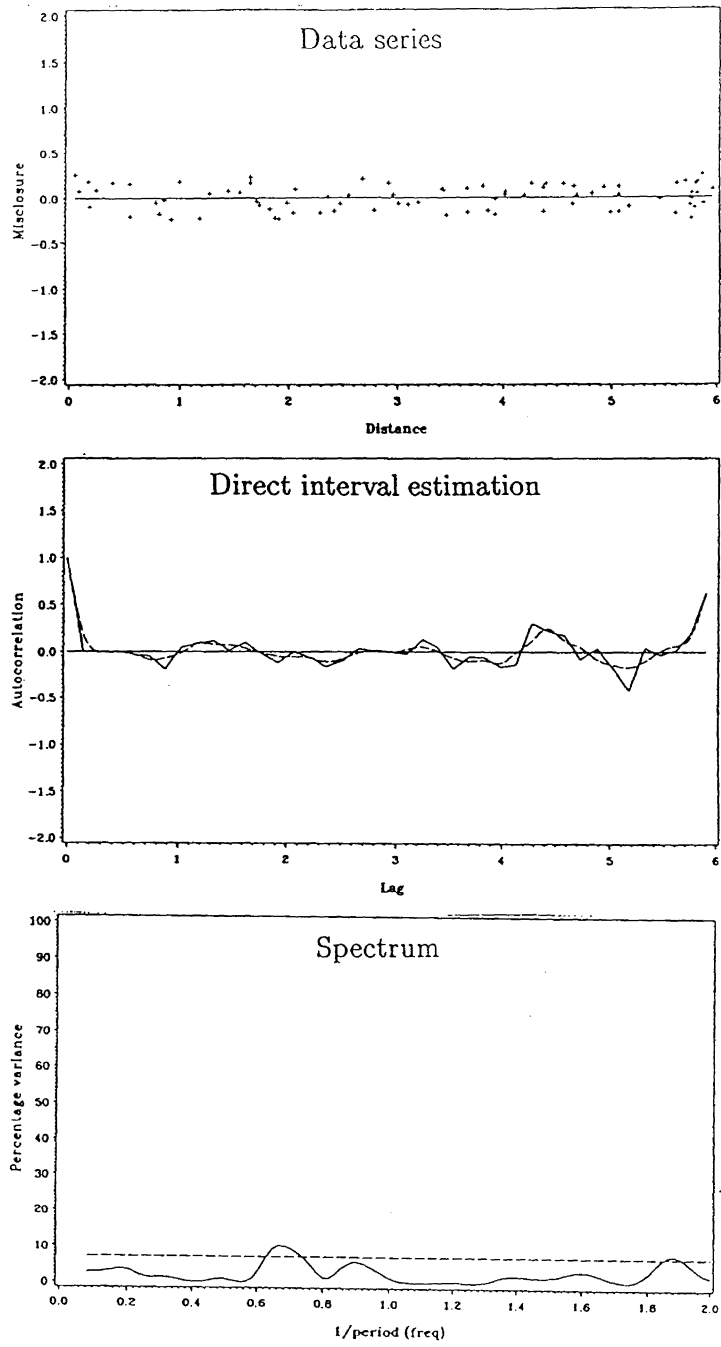


Figure 6.2: Analysis of the purely random data series.

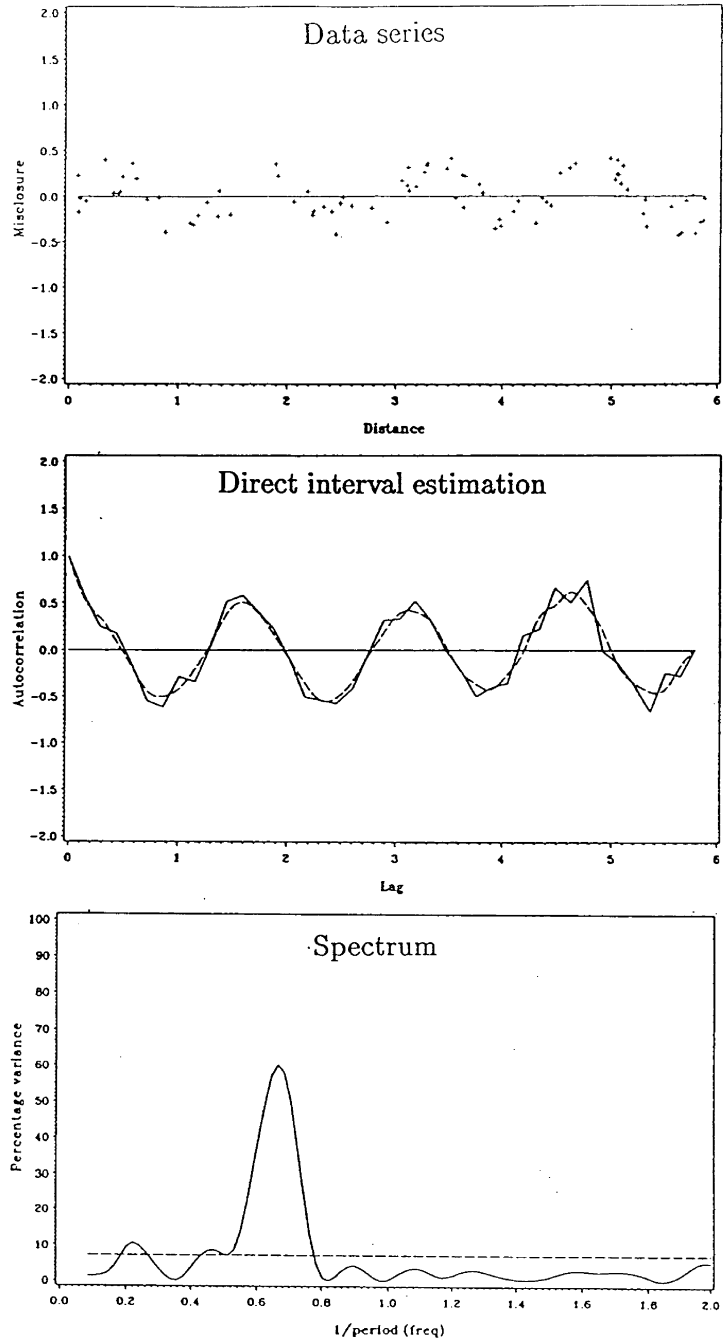


Figure 6.3: Analyses of data series with period 1.5 units.

statistical significance at a lower frequency of 0.22 may again likely be attributed to the small data series or a bias in the generator. It is also, at period 4.5, a multiple of the larger peak.

As a further test a random series with a maximum deviation of 0.5 was superimposed on a sine trend with a period of 4.5 argument units and an amplitude of 0.2. The three plots are shown in Figure 6.4

The autocorrelation function clearly indicates statistical dependency but, as is to be expected, this is not as pronounced as in the previous example. The significant peak at a frequency of 0.22 yields, as its reciprocal, a period of 4.5 argument units.

The effectiveness of the autocorrelation function and of least squares spectral analysis has been demonstrated, but in practice the signal to noise ratio is likely to be less pronounced.

Therefore, as a final test a random series with a maximum deviation of 0.25 was superimposed on a quadratic trend. This series is shown in Figure 6.5. By making use of the relevant option in the LSSA program the linear trend in this series was removed and the residual series, together with its autocorrelation function, and its spectrum are shown in Figure 6.6.

The autocorrelation function gives a clear indication, by its behaviour, of the statistical dependence of the data series. The residual quadratic trend shows up in the spectrum as an ill defined peak at a low frequency. The smaller peak which gives, reciprocally, a period of 0.8 argument units may be disregarded for the reasons given above. The LSSA was able to detect the presence of this trend, which aliases as a low frequency peak. This example, especially, illustrates the suitability of this technique for the detection of systematic effect in any data series.

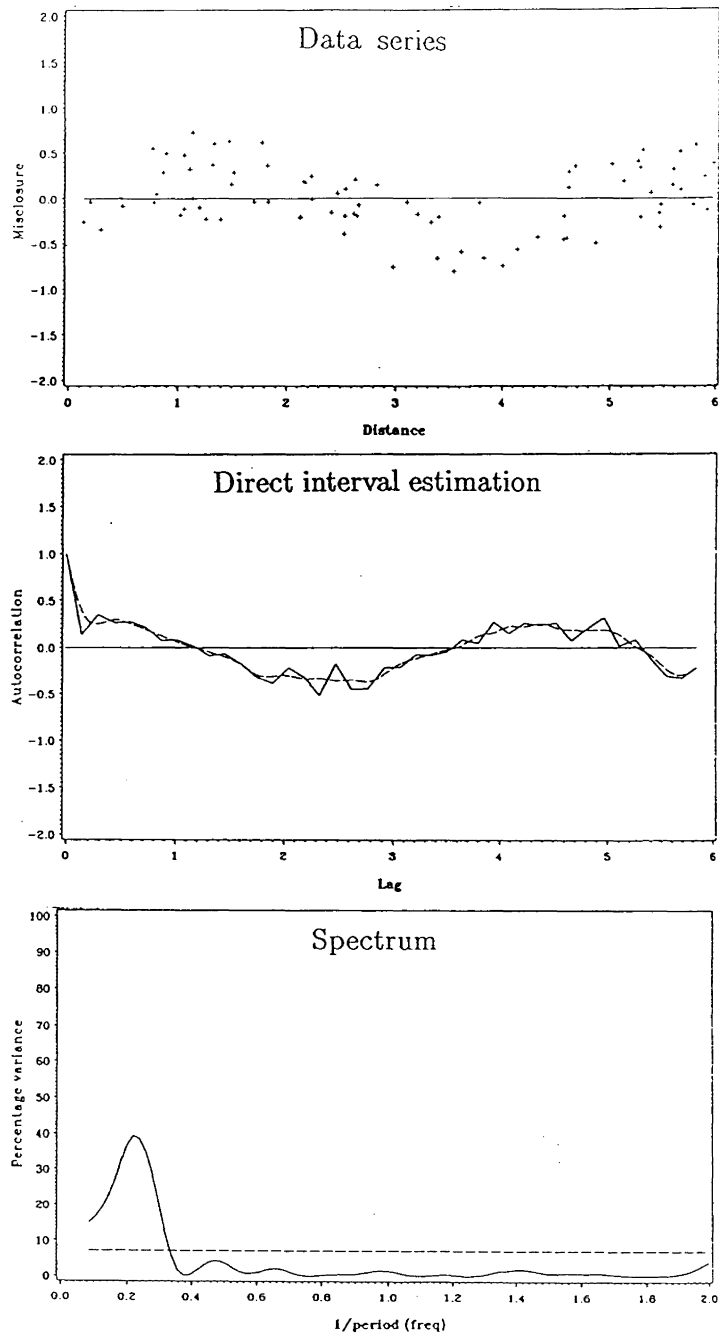


Figure 6.4: Analysis of data series with period 4.5 units.

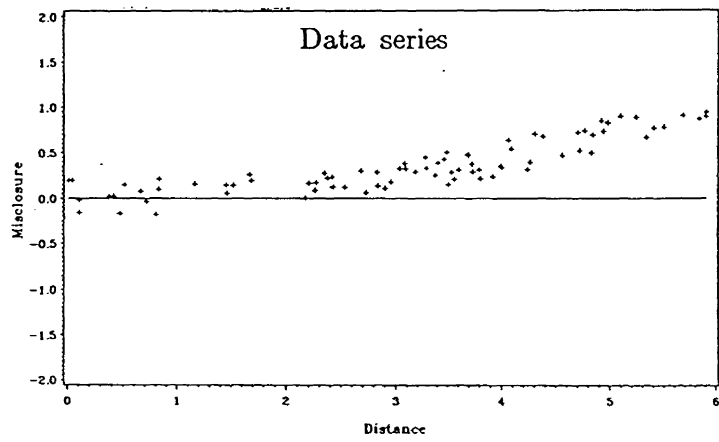


Figure 6.5: Data series with quadratic trend.



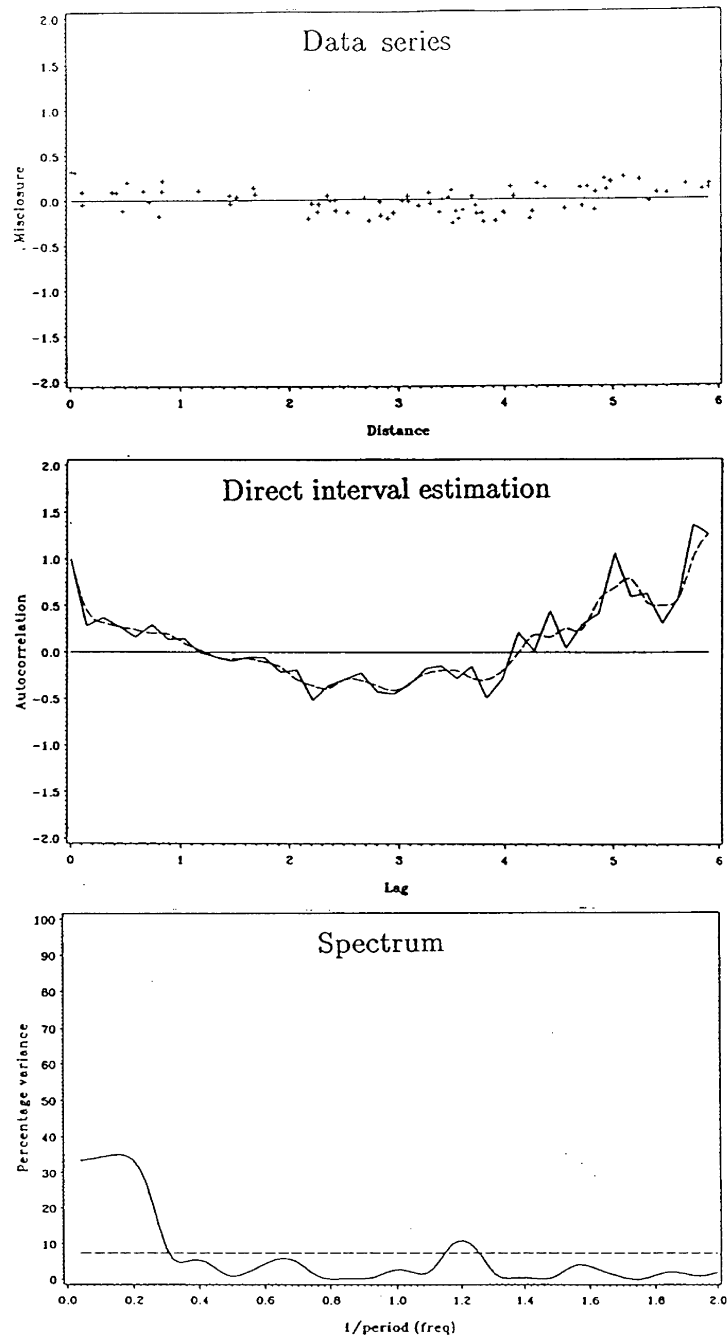


Figure 6.6: Analysis of the data series with residual quadratic trend.

# Chapter 7

## Analysis of field data

### 7.1 Introduction

The discussion has, so far, focussed on the various sources of error to be expected when comparing calculated gravimetric geoidal undulations (or differences in undulation) with those derived from the comparison of orthometric heights and geometric heights from GPS observations (cf. Table 7.1). In the following section an attempt is made to quantify these errors.

### 7.2 Evaluation of data sources

#### 7.2.1 Levelled heights

According to NASA's global empirical formula the standard deviation in height for first order control points propagates according to:

$$\sigma_H = 1.8 \times 10^{-3} S^{\frac{2}{3}} \text{metres}, \quad (7.1)$$

where  $S$  is the distance in kilometres (Vaníček and Krakiwsky, 1986). This would imply that the standard deviation of the height in the middle longitude of southern Canada would be about 0.4 metres. The tolerance prescribed in the specifications for

<i>Component</i>	<i>Error source</i>
Computed geoidal height	(1) satellite derived reference field. (2) computational technique (3) distribution and accuracy of gravity data
Computed geoidal height difference	(1) computational technique (2) distribution and accuracy of gravity data
Orthometric height	(1) datum errors (2) systematic errors (3) undetected, compensating gross errors
Orthometric height differences	(1) systematic errors (2) undetected, compensating gross errors
GPS height and height differences	(1) satellite constellation o number available o geometric distribution (2) atmospheric refraction o troposphere o ionosphere (3) Antenna o phase centre o multipath (4) Satellite ephemeris accuracy (5) length of observing session (6) software o baseline o network adjustment (7) spacing between stations (8) errors in station coordinates (9) receiver noise

Table 7.1: Sources of error when using GPS and orthometric heights to verify a gravimetric geoid.

first order levelling is  $4\sqrt{k}$  millimetres where  $k$  is the levelled distance in kilometres which yields a value of about 0.2 metres. However, both these are likely to be exceeded as can be seen from a comparison between the two trans-Canada levelling lines (cf. Figure 2.5). Here, the total discrepancy was 2.2 metres while the specifications for first order levelling would allow about 0.3 metres.

Vaniček et al. (1985) assert that the elevation difference between Mean Sea Level along the west coast and that along the east coast is about .2 metres, a value which agrees with oceanographic estimates. In the Canadian Geodetic Datum of 1928 it was assumed that Mean Sea Level at all tide gauges was coincident with the geoid and consequently the network is affected by a bias in that direction.

For the most part what is of concern is orthometric height differences over short distances. Double run levelling has always been used for first order heighting. Numerical tests show that the precision for first order levelling in southern Canada show a standard deviation of the mean of less than 1.36 millimetres per kilometre since 1973 (Gareau, 1986). Systematic errors such as rod and instrument settlement, rod miscalibration, residual refraction and rod index error are known to be present in Canadian levelling. These errors are likely to be larger for lower orders of accuracy due to the generally less stringent procedures adopted. Vaniček et al. (1985) conducted an investigation using the autocorrelation function on 15 Canadian first order levelling lines, ordered according to arguments such as elevation difference and length of section. They estimated that turning point settlement was about 0.02 millimetres /turning point. The effect will tend to cancel where the number of set ups in the forward and back direction is balanced. This requirement was not met in most cases. A trend of  $\pm 15$  parts per million in some lines was attributed to rod miscalibration. Residual refraction appeared to have a relatively small effect, but the lack of temperature measurements made further investigation impossible. The systematic effects behaved differently, apparently according to the characteristics of the particular line, and this makes it difficult to draw conclusions about first order Canadian levelling

in general. The application of the approximate orthometric correction as opposed to a rigid correction will introduce an appreciable error (Vaníček et al., 1980). In the levelling lines analysed by Vaníček et al. (1985), an estimate of precision was obtained by finding the standard deviation of each line. In 13 out of 15 the standard deviation was found to be significantly smaller than  $2.8\sqrt{k}$  millimetres which is the expected value for Canadian first order levelling (Nassar, 1971 as quoted in Vaníček et al. (1985)).

A study of the loop closures of 106 loops (Gareau, 1986) revealed that only 4 loops showed a misclosure of greater than  $4\sqrt{k}$  millimetres. There remains a possibility that undetected compensating gross errors are present in the network although there is no evidence to support this at present.

## 7.2.2 GPS geometric heights

An estimate of the precision of GPS derived geometric height differences has been obtained by many researchers, usually after examination of height loop misclosures. These estimates are usually quoted as error in height over baseline length in parts per million (ppm). A selection is shown in Table 7.2.

It is also possible to estimate the contribution of each of the biases and errors and hence approximate the quality of the final height difference. A bar chart of the most important biases and errors is shown in Figure 7.1 for two baselines, one 5 kilometres in length and the other 50 kilometres. The tropospheric contribution,  $\sigma_{trop}$ , is estimated using Equation 5.6. The value of 2 parts per million for ionospheric delay,  $\sigma_{ion}$ , is estimated using the Juan de Fuca and CERN networks reported in Santerre (1989). The satellite ephemeris is assumed to have an along track error of 20 metres and the effect on height,  $\sigma_{orb}$ , is estimated using Equation 5.5. The effect of an assumed co-ordinate error of 5 metres in  $\phi$ ,  $\lambda$  and  $h$  on GPS height determination,  $\sigma_{cord}$ , is estimated from a computer simulation carried out by Holloway (1988). Receiver noise and any residual errors and biases,  $\sigma_{nois}$ , is estimated as 5

<i>Claimed precision</i>	<i>Author(s)</i>
about 1.6 ppm	Engelis and Rapp (1984)
3 ppm	Schwarz and Sederis (1985)
to 3.2 ppm	Holloway (1988)
$\pm (0.5 \text{ mm} + 1 -2 \text{ ppm})$	Zilkoski and Hothem (1988)
1 to 3 ppm	Kearsley, 1988b
to 3.5 ppm	Leal (1989)
1 to 2.5 ppm	Kleusberg, (1990)

Table 7.2: Estimates of the precision of baseline height differences from differential GPS observations.

millimetres irrespective of baseline length. The total uncertainty of each baseline height,  $\sigma_{\Delta h}$ , is then calculated from:

$$\sigma_{\Delta h}^2 = \sigma_{trop}^2 + \sigma_{ion}^2 + \sigma_{orb}^2 + \sigma_{cord}^2 + \sigma_{nois}^2. \quad (7.2)$$

It should be borne in mind that circumstances encountered during specific campaigns could cause these values to vary considerably (cf. Table 7.2).

An estimate of the internal precision of each height difference is one result of the network adjustment of the independent baseline solutions.

### 7.2.3 The regional geoidal models “UNB Dec. ’86” and “UNB ’90”

Part of the regional geoidal solution “UNB Dec. ’86” includes an estimate of the internal precision of the undulations and differences in undulations. Computation of the “UNB 90” regional geoidal model was only recently completed and estimates of its internal precision are not as yet available.

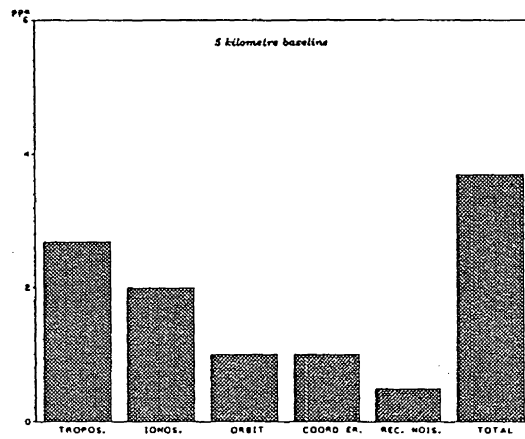
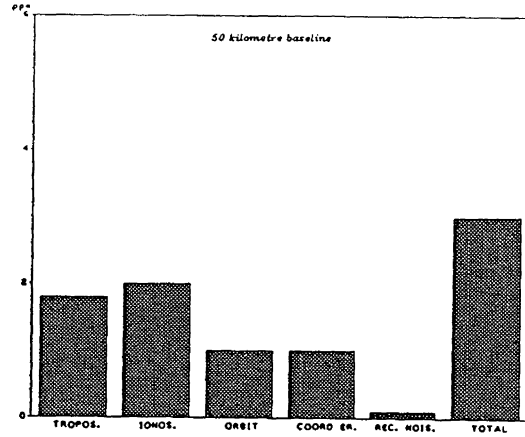


Figure 7.1: The estimated magnitude of errors (in parts per million) of GPS baselines height differences.

### 7.3 Analysis of point data

A comparison for the data series,  $h - H - N$ , using the “UNB Dec. ’86” point values is given in Table 7.3. and for the “UNB ’90” geoidal model in Table 7.4. The standard

<i>Network</i>	<i>No. of points</i>	<i>Mean diff.</i>	<i>Std. dev.</i>	<i>R.M.S.</i>
NWT	64	1.15	±0.23	±1.17
Ontario	23	0.62	±0.22	±0.75
Manitoba	11	1.22	±0.22	±1.23

Table 7.3: Analysis of the misclosures obtained from UNB86 and GPS/ orthometric levelling.

deviations for both sets of data are similar, the change in the mean can be largely

<i>Network</i>	<i>No. of points</i>	<i>Mean diff.</i>	<i>Std. dev.</i>	<i>R.M.S.</i>
NWT	64	0.08	±0.23	±0.25
Ontario	23	0.85	±0.24	±0.96
Manitoba	11	-0.61	±0.20	±0.64

Table 7.4: Analysis of the misclosures obtained from UNB90 and GPS/ orthometric levelling.

attributed to the two regional geoidal models using different reference fields. The “UNB ’90” solution giving improved absolute accuracy.



Histograms have been constructed for each data series of the North West Territories network (cf. Figure 7.2), the Ontario network (cf. Figure 7.3) and the Manitoba network (cf. Figure 7.4). The shape of these bar charts suggest the presence of

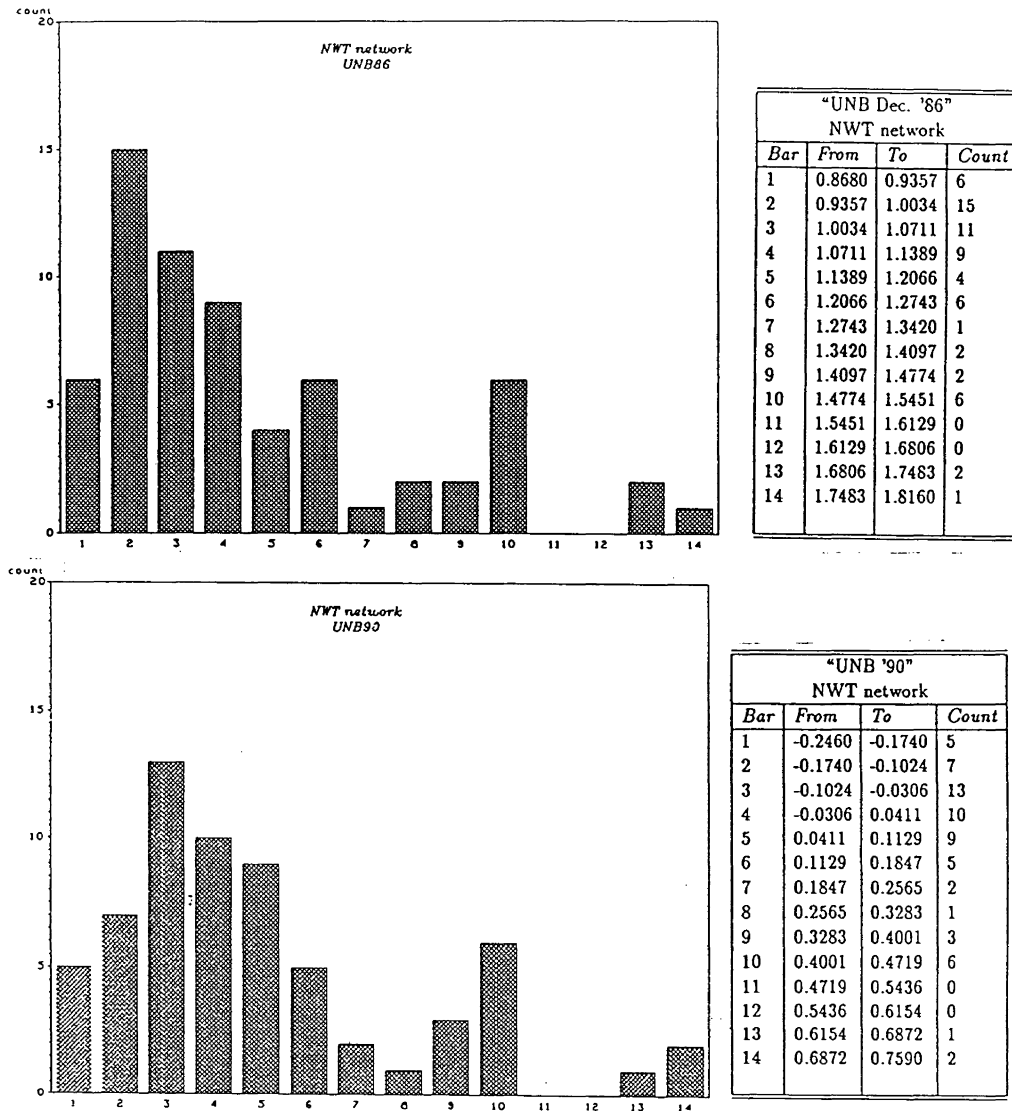
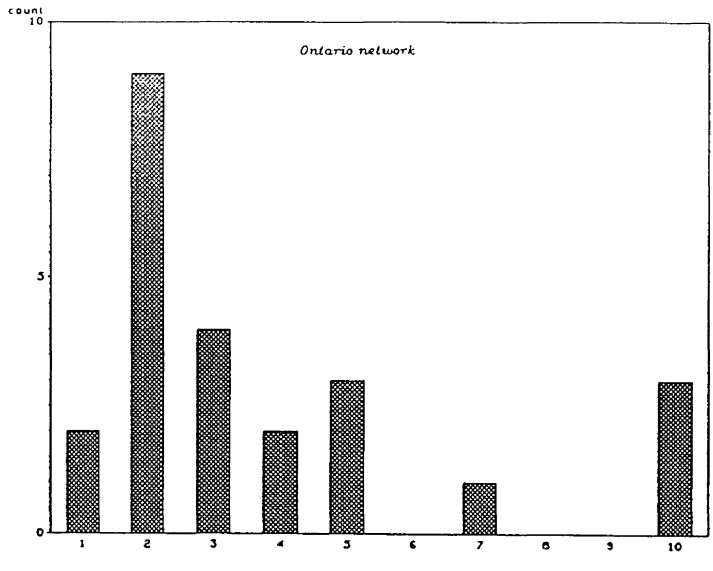


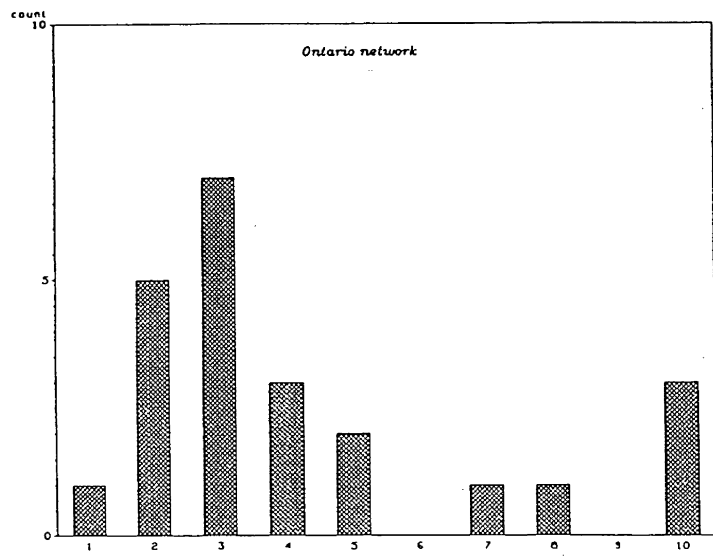
Figure 7.2: Histogram for the North West Territories network.

systematic error.

The variance of an individual point value may be obtained from the formula  $\sigma^2 = \sigma_h^2 + \sigma_H^2 + \sigma_N^2$ , where for example for the North West Territories network,  $\sigma_N$  is



"UNB Dec. '86" Ontario network			
Bar	From	To	Count
1	0.130	0.276	2
2	0.276	0.422	9
3	0.422	0.568	4
4	0.568	0.714	2
5	0.714	0.860	3
6	0.860	1.006	0
7	1.006	1.152	1
8	1.152	1.298	0
9	1.298	1.444	0
10	1.444	1.590	3



"UNB '90" Ontario network			
Bar	From	To	Count
1	0.260	0.417	1
2	0.417	0.574	5
3	0.574	0.731	7
4	0.731	0.888	3
5	0.888	1.045	2
6	1.045	1.202	0
7	1.202	1.359	1
8	1.359	1.516	1
9	1.516	1.673	0
10	1.673	1.830	3

Figure 7.3: Histogram for the Ontario network.

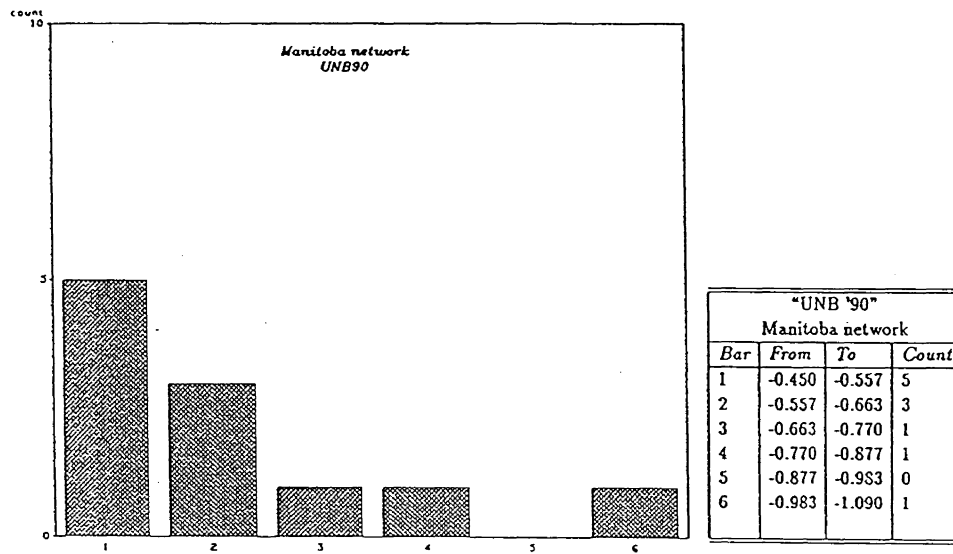
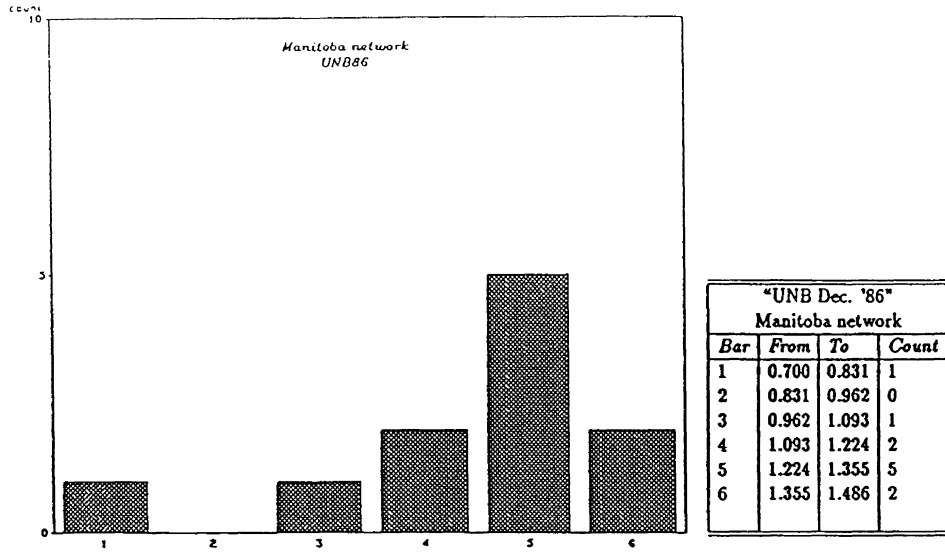


Figure 7.4: Histogram for the Manitoba network.

about 1.3 metres for “UNB Dec. ’86”,  $\sigma_H$  may be estimated at about .3 metres (cf. Section 7.2.1) and  $\sigma_h$  may be estimated at 1.5 metres (Merry, 1988). The expected value of the mean is 0. However, the data values are highly correlated and so the field data yields a standard deviation of  $\pm 0.23$  metres. The mean is 1.15 metres. The results of this are illustrated in Figure 7.5. The positive correlations between

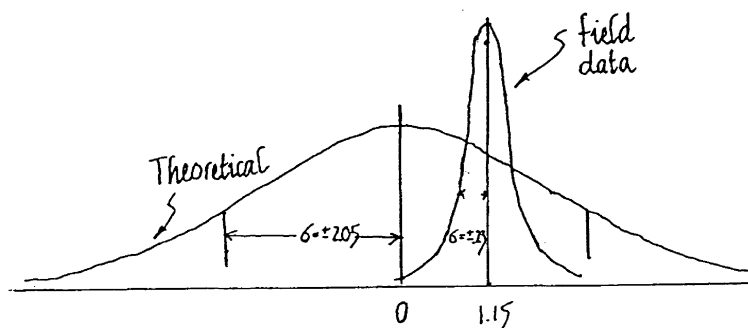


Figure 7.5: The data distributions for the North West Territories network.

the orthometric levelling values, the GPS heights and the geoidal undulations have combined to give a greater precision than expected.

It has already been established that the data are highly correlated, nevertheless, it may be useful to test each of the distributions against a normal distribution. As an example the data series from the NWT network ( $h - H - N$ ) that uses “UNB Dec. ’86” to obtain the undulation,  $N$ , is tested. The size of the intervals have been doubled from those shown in the histogram because it is important to have as many intervals as possible having observed counts of greater than five (Bethea et al., 1985).

The test may be formulated with null hypothesis,  $H_0$ :

$H_0$	the data are normally distributed with mean 1.15 and standard deviation $\pm 0.23$ .
-------	--

The class boundaries are standardized according to:  $z = \frac{(x_i - 1.15)}{0.23}$ . If  $O_i$  is the number of variates in class  $i$  and the expected number of variates, computed from standard distribution, is  $E_i$  then the information needed to conduct the test is in Table 7.5.

<i>Class</i>	<i>Observed</i>	<i>Expected</i>
<i>(z)</i>	<i>(O<sub>i</sub>)</i>	<i>(E<sub>i</sub>)</i>
-1.243 ↔ -0.655	21	9.555
-0.655 ↔ -0.066	19	13.917
-0.066 ↔ 0.523	10	14.453
0.523 ↔ 1.112	3	10.714
1.112 ↔ 1.700	8	5.665
1.700 ↔ 2.290	0	2.148
2.290 ↔ 2.858	3	0.568

Table 7.5: Goodness of fit test for NWT data series (“UNB Dec. ’86”).

It can be shown that:

$$\chi^2 = \sum_{i=1}^7 \frac{(O_i - E_i)^2}{E_i} \tag{7.3}$$

has a  $\chi^2$  distribution with  $7 - 1 - 2 = 4$  degrees of freedom (the two statistics, the mean and standard deviation were drawn from the hypothesized distribution). If a level of significance of 10% is selected for the test the  $\chi^2$  table gives:  $\chi^2_{4,0.90} = 7.8$ . As Equation 7.3 yields 36.0, the null hypothesis is rejected ( $\chi^2 > \chi^2_{4,0.90}$ ) and the underlying distribution of the data may be regarded as not being normal.

The Ontario network will also fail the test. The Manitoba sample is too small to yield any meaningful result. The data series constructed using “UNB ’90” gives similar results.

The results of all tests are summarized in Table 7.6. Clearly, therefore there is some non-random influence in the data and this will be investigated further, later in

<i>Test</i>	<i>Goodness of fit</i>
<i>Level of significance</i>	10 %
<i>"UNB Dec. '86"</i>	
<i>NWT</i>	Fail
<i>Ontario</i>	Fail
<i>Manitoba</i>	–
<i>"UNB '90"</i>	
<i>NWT</i>	Fail
<i>Ontario</i>	Fail
<i>Manitoba</i>	–

Table 7.6: Summary of the results of the statistical tests carried out on the point data series.

the chapter.

## 7.4 Analysis of baseline data

A simple equation may be used to obtain an estimate of the quality of  $\Delta(h - H - N)$ :

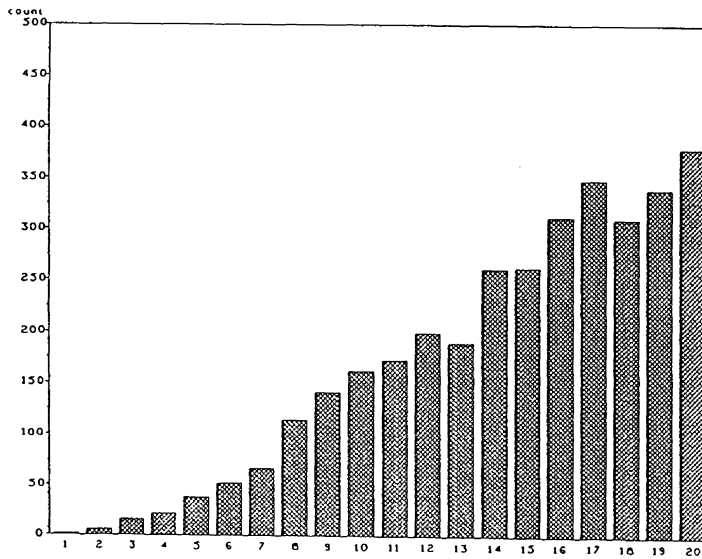
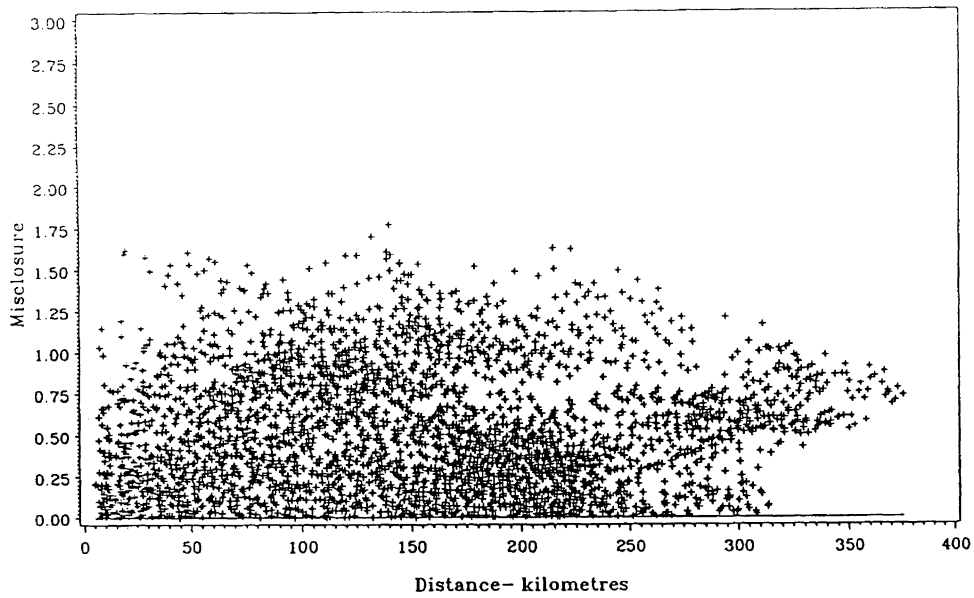
$$\sigma_{\Delta(h-H-N)}^2 = \sigma_{\Delta h}^2 + \sigma_{\Delta H}^2 + \sigma_{\Delta N}^2, \quad (7.4)$$

where  $\sigma_{\Delta h}$  is the standard deviation of the GPS levelling,  $\sigma_{\Delta H}$  of the orthometric levelling and  $\sigma_{\Delta N}$  of the regional geoidal model.

In the North West Territories network 58 bench marks are levelled to first order accuracy while connections were made from these to further stations (Mainville and Veronneau, 1989) and therefore a reasonable value to assume for levelling accuracy will be  $1.4\sqrt{k}$  millimetres (Gareau, 1986). Estimates for the GPS levelling are available from the variance-covariance matrix of the network adjustment (approximately 2.5

parts per million) and estimates for the differences in undulation from the “UNB Dec. ’86” regional geoidal model. Misclosures for each of 3403 baselines in the North West Territories network ( $\Delta(h - H - N)$ ) have been normalised using these estimates for GPS levelling, orthometric height differences, and relative geoidal height accuracy. In order to maintain consistency, the height differences were always taken as a positive value. This data series, ordered according to baseline length, is shown in Figure 7.6. The values are, of course, highly correlated. Also shown is a histogram of the misclosures. The standard deviation is  $\pm 0.37$  suggesting that the values obtained in the construction of the data series may be better than those expected from the estimates of each component. The “jackknife” technique was applied and as a result the equivalent uncorrelated estimate of the standard deviation was found to be  $\pm 0.31$  (cf. Appendix II). The GPS estimates, used for normalisation, agree closely with the values found in practice by other researchers (cf. Table 7.2) and the values used for first order levelling have also been well established (Vaníček et al. (1985), Gareau (1986)). One or more of the components is therefore of considerably better quality than assumed.

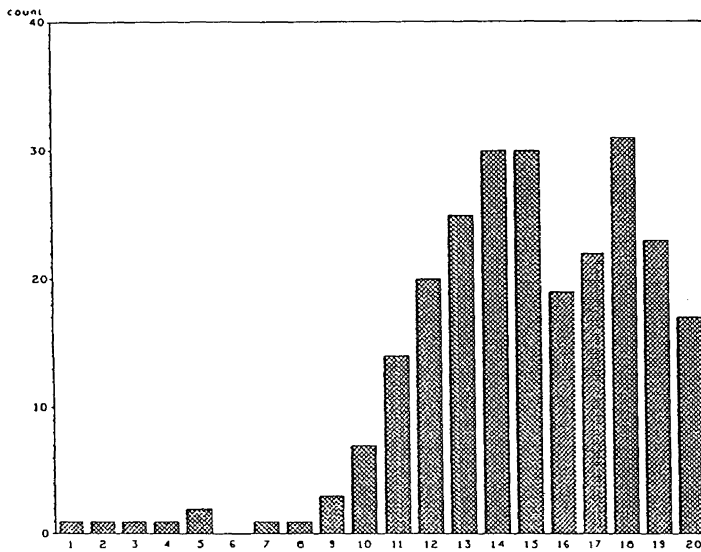
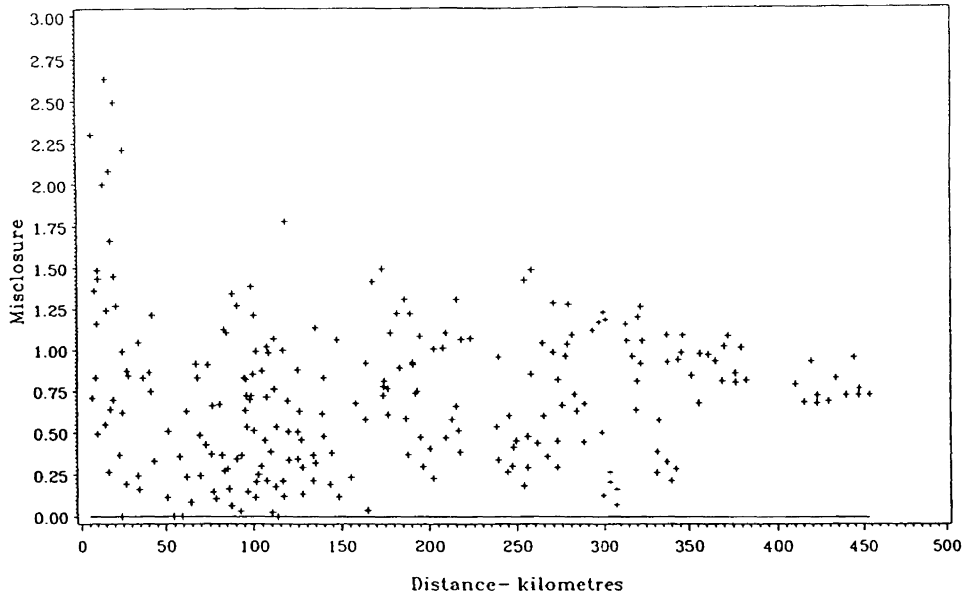
In the Ontario network 14 stations are levelled to first order accuracy, 8 to second order accuracy while a lower order is quoted for 3 points (Mainville, 1987) and so  $1.4\sqrt{k}$  is again assumed for the first order benchmarks while progressively worse values are assumed for lower order levelling. Estimates for the GPS levelling are obtained from the variance-covariance matrix for the network (Mainville, 1987) and is approximately 1 part per million and estimates for the differences in undulation are obtained in the same manner as for the NWT network. The baseline differences were all obtained by taking the positive value to ensure consistency. The normalised data series, again obtained by dividing the misclosure obtained for each network in practice by the expected GPS, orthometric levelling and geoidal model values, are ordered according to baseline length in Figure 7.7. A histogram of these highly correlated values is also shown. The series has a standard deviation of  $\pm 0.46$ . Again,



"UNB Dec. '86" NWT network			
Bar	From	To	Count
1	1.6833	1.7719	2
2	1.5947	1.6833	6
3	1.5061	1.5947	16
4	1.4175	1.5061	22
5	1.3289	1.4175	38
6	1.2403	1.3289	52
7	1.1517	1.2403	67
8	1.0631	1.1517	115
9	0.9745	1.0631	142
10	0.8859	0.9745	162
11	0.7974	0.8859	173
12	0.7088	0.7974	200
13	0.6202	0.7088	190
14	0.5316	0.6202	262
15	0.4430	0.5316	263
16	0.3544	0.4430	313
17	0.2658	0.3544	349
18	0.1772	0.2658	311
19	0.0886	0.1772	340
20	0.0000	0.0886	380

Figure 7.6: The normalised data series of baseline misclosures for the North West Territories network (ordered according to length of baseline).





"UNB Dec. '86" Ontario network			
Bar	From	To	Count
1	2.5065	2.6384	1
2	2.3746	2.5065	1
3	2.2426	2.3746	1
4	2.1107	2.2426	1
5	1.9788	2.1107	2
6	1.8469	1.9788	0
7	1.7150	1.8469	1
8	1.5830	1.7150	1
9	1.4511	1.5830	3
10	1.3192	1.4511	7
11	1.1873	1.3192	14
12	1.0554	1.1873	20
13	0.9234	1.0554	25
14	0.7915	0.9234	30
15	0.6596	0.7915	30
16	0.5277	0.6596	19
17	0.3958	0.5277	22
18	0.2638	0.3958	31
19	0.1319	0.2638	23
20	0.0000	0.1319	17

Figure 7.7: The normalised data series of baseline misclosures for the Ontario network ordered (according to length of baseline).

it appears that one or more of the components is of better than expected quality.

The Manitoba network has all points levelled to lower order accuracy-  $8.4\sqrt{k}$  (Mainville, 1987). Estimates for the GPS levelling are from the network adjustment (approximately 3 parts per million) and values for the differences in undulation from the “UNB Dec. ’86” regional geoidal model. The normalised data series, with its histogram, is shown in Figure 7.8. The series has standard deviation of  $\pm 0.26$ . The data are highly correlated in both a negative and positive sense.

The results of the statistical tests carried out on the baseline data is shown in Table 7.7 The test for comparison of the variances,  $\sigma^2$ , (assuming for the moment the

<i>Test</i>	<i>Comparison of variances</i>
<i>Level of significance</i>	10 %
<i>“UNB Dec. ’86”</i>	
<i>NWT</i>	Fail
<i>Ontario</i>	Fail
<i>Manitoba</i>	Fail

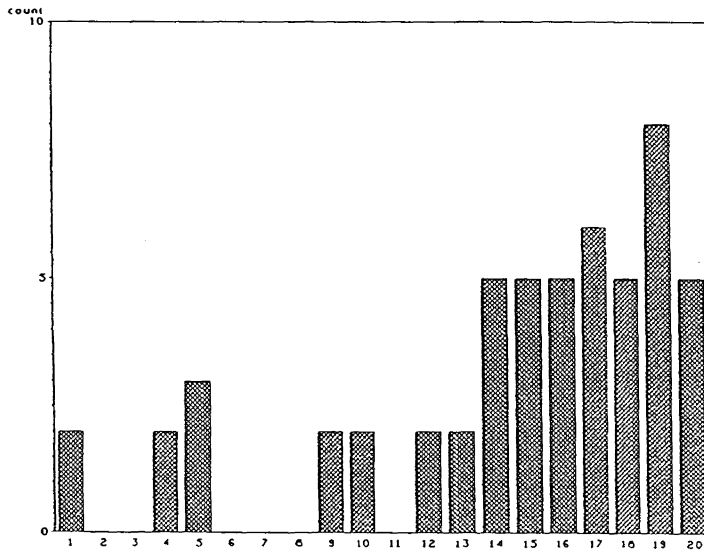
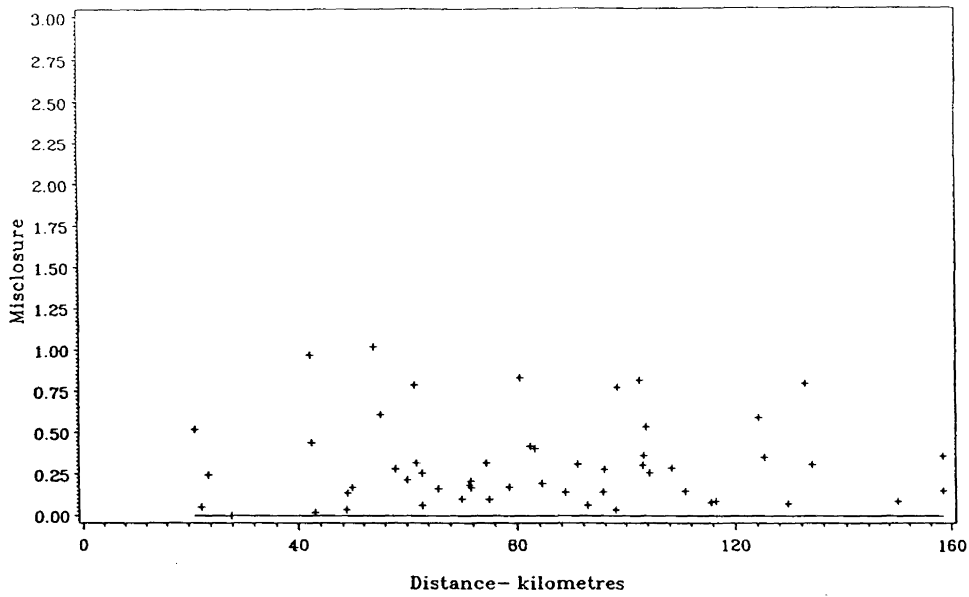
Table 7.7: Summary of the results of the statistical tests carried out on the baseline data series.

data to be uncorrelated) may be formulated with null hypothesis,  $H_0$ :

$$H_0 \quad \sigma^2 = 1.$$

The test statistic is (Bethea et al., 1985) is  $\chi^2 = \frac{(n-1)}{s^2\sigma_0^2}$ , where  $s$  is the sample standard deviation and  $\sigma_0 = 1$ . In, for example, the Manitoba baseline series  $\chi^2 = 798$ . The null hypothesis is rejected (at the 10% level) if  $\chi^2 < \chi_{53,.05} = 38$  or if  $\chi^2 > \chi_{53,.95} = 72$ . Clearly, this is the case.

Although the data are highly correlated, the *a priori* estimates of the individual values are consistently high for all networks and it appears, therefore, that the values obtained from field measurements are better than anticipated.



"UNB Dec. '86" Manitoba network			
Bar	From	To	Count
1	0.9655	1.0163	2
2	0.9147	0.9655	0
3	0.8639	0.9147	0
4	0.8130	0.8639	2
5	0.7622	0.8130	3
6	0.7114	0.7622	0
7	0.6606	0.7114	0
8	0.6098	0.6606	0
9	0.5590	0.6098	2
10	0.5082	0.5590	2
11	0.4573	0.5082	0
12	0.4065	0.4573	2
13	0.3557	0.4065	2
14	0.3049	0.3557	5
15	0.2541	0.3049	5
16	0.2033	0.2541	5
17	0.1524	0.2033	6
18	0.1016	0.1524	5
19	0.0508	0.1016	8
20	0.0000	0.0508	5

Figure 7.8: The normalised data series of baseline misclosures for the Manitoba network (ordered according to length of baseline).

The results of the tests and the shape of each of the histograms suggest the presence of systematic error.

## 7.5 Profiles of the North West Territories network

The closely spaced profile of GPS stations in the NWT network lends itself to a graphical display. In Figure 7.9 may be seen the orthometric height (H) profile of these stations. The main profile is 700 kilometres long and begins at Yellowknife and ends at Fort Smith. A profile of the gravimetric geoidal heights from "UNB Dec. '86"

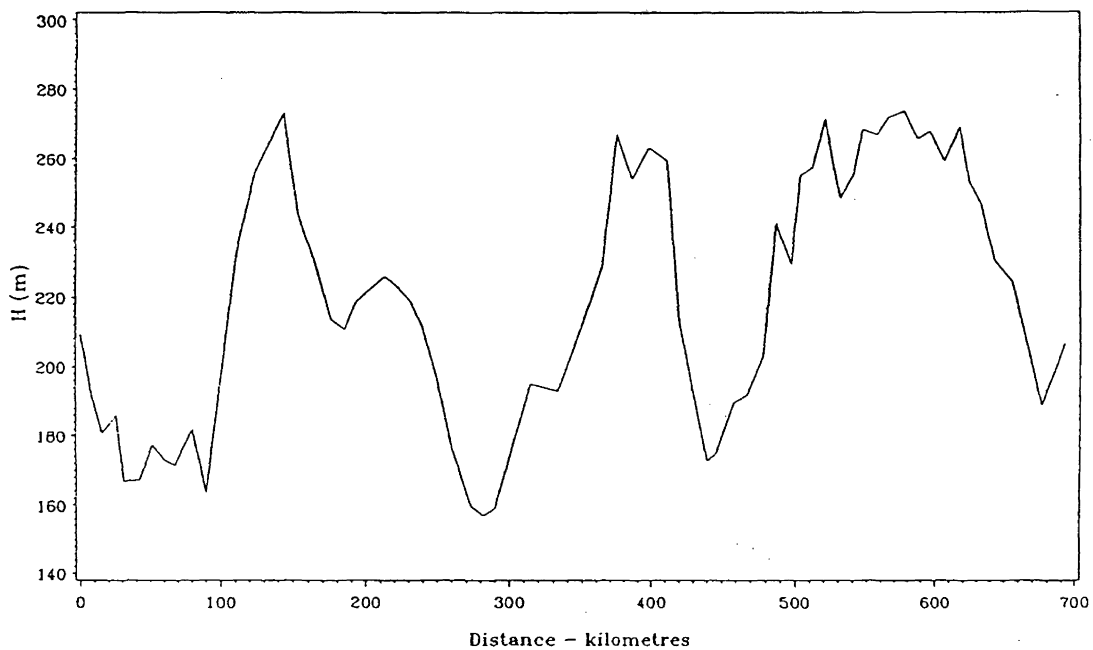


Figure 7.9: Profile of orthometric heights from Yellowknife to Fort Smith (after Mainville and Veronneau, 1989).

(N) as well as the GPS derived geoidal heights ( $h-H$ ) is shown in Figure 7.10. It can

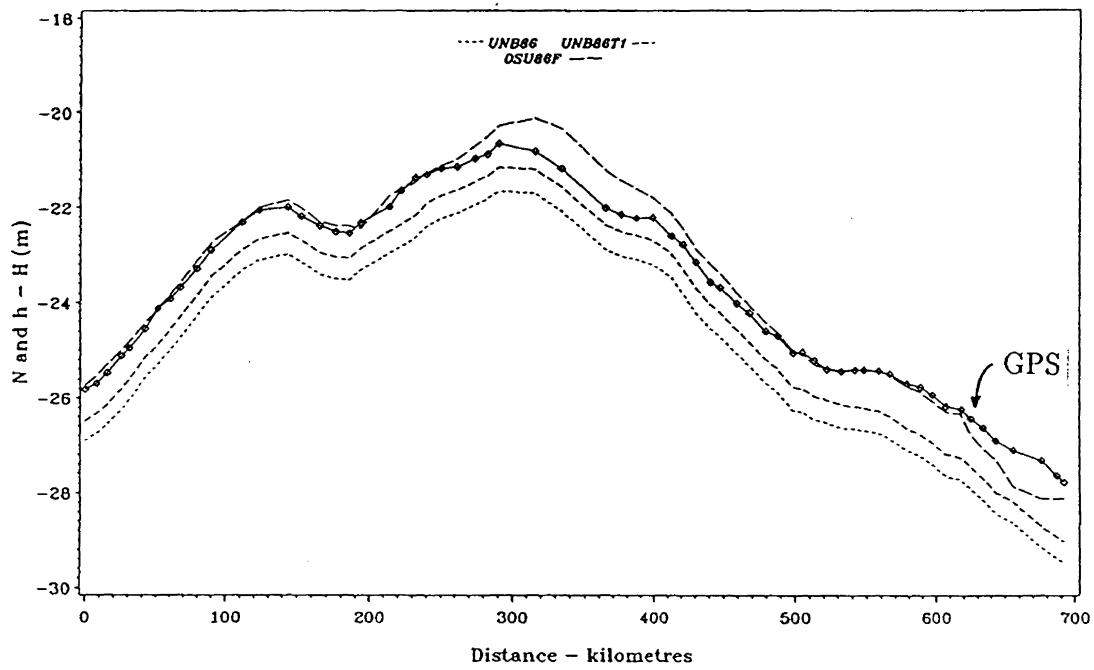


Figure 7.10: Profile of geoidal undulations from Yellowknife to Fort Smith -“UNB Dec. '86”, “UNB Dec. '86” with reference field changed from GEM9 to GEM-T1 and OSU86F (after Mainville and Veronneau, 1989).

be seen that the profiles, if the long periodic effect is discounted, are fairly close to each other, but that the separation increases toward Fort Smith. This separation can be clearly seen in Figure 7.11 which was obtained by taking the difference  $h - H - N$  and making an allowance for a “datum shift” of 1.15 metres. An equivalent set of

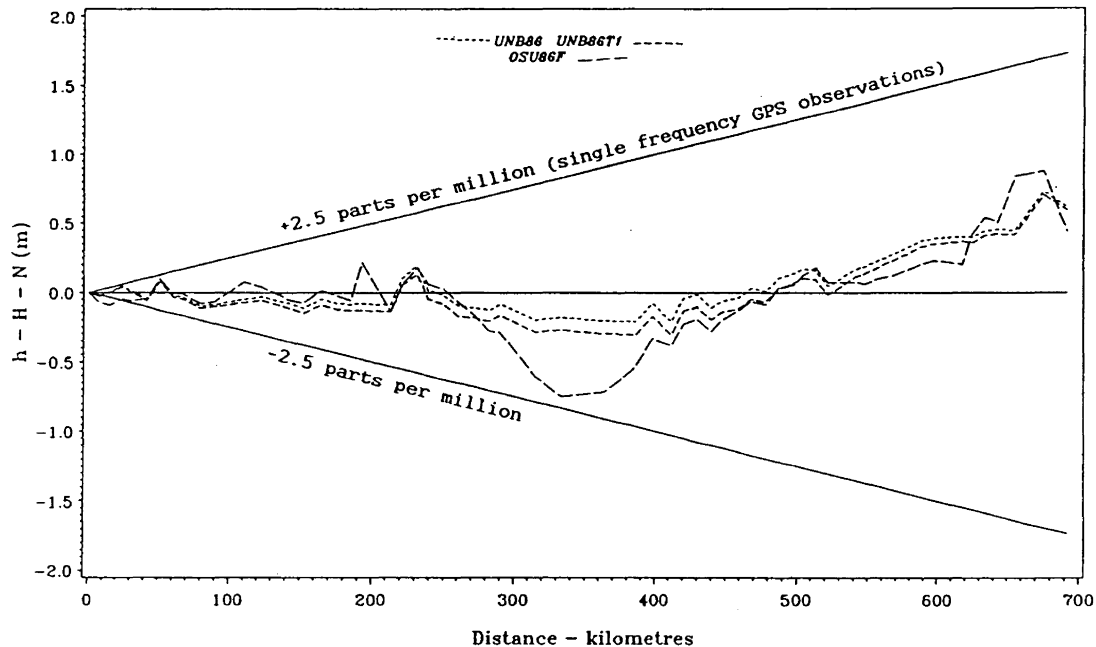


Figure 7.11: Profile of the difference between the GPS/orthometric derived profile and that obtained from “UNB Dec. ’86” with envelope showing limits of GPS heighting accuracy (after Mainville and Veronneau, 1989).

diagrams may be constructed for the “UNB ’90” geoidal model and these are shown in Figure 7.12 and Figure 7.13. The most noticeable difference is that the long periodic effect is much reduced. This is partly due to using GEM-T1 in the solution as opposed to GEM9. However the increasing separation between the GPS /orthometric geoidal profile and the “UNB ’90” profile towards Fort Smith is still apparent.

Clearly, the agreement between the geoidal model undulations and those obtained

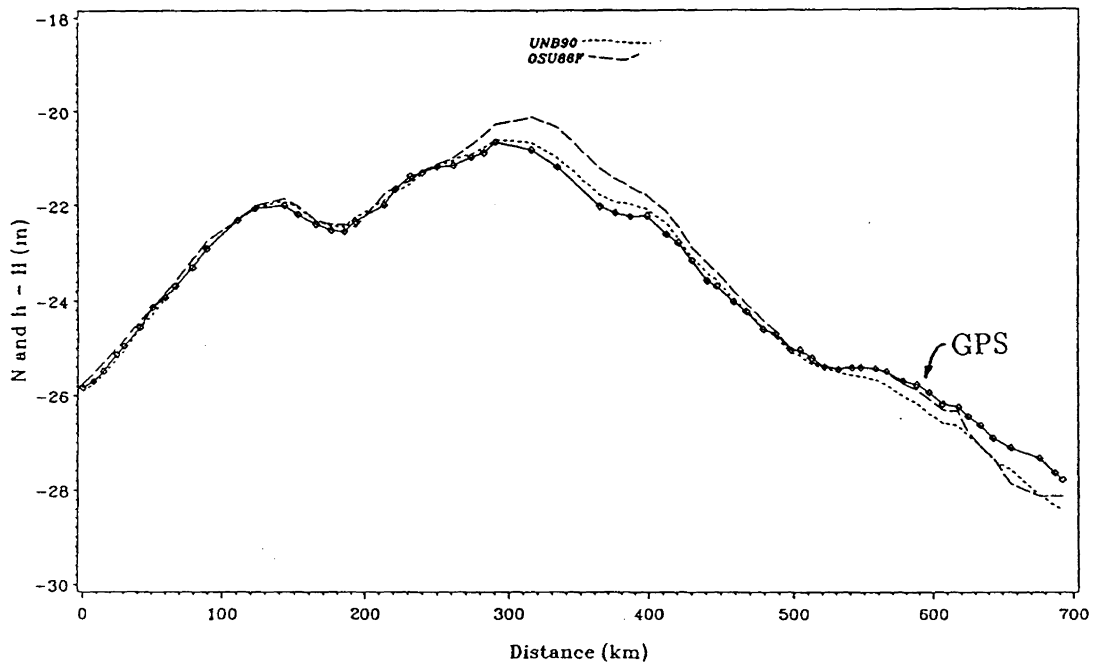


Figure 7.12: Profile of geoidal undulations from Yellowknife to Fort Smith - "UNB '90" and OSU86F.

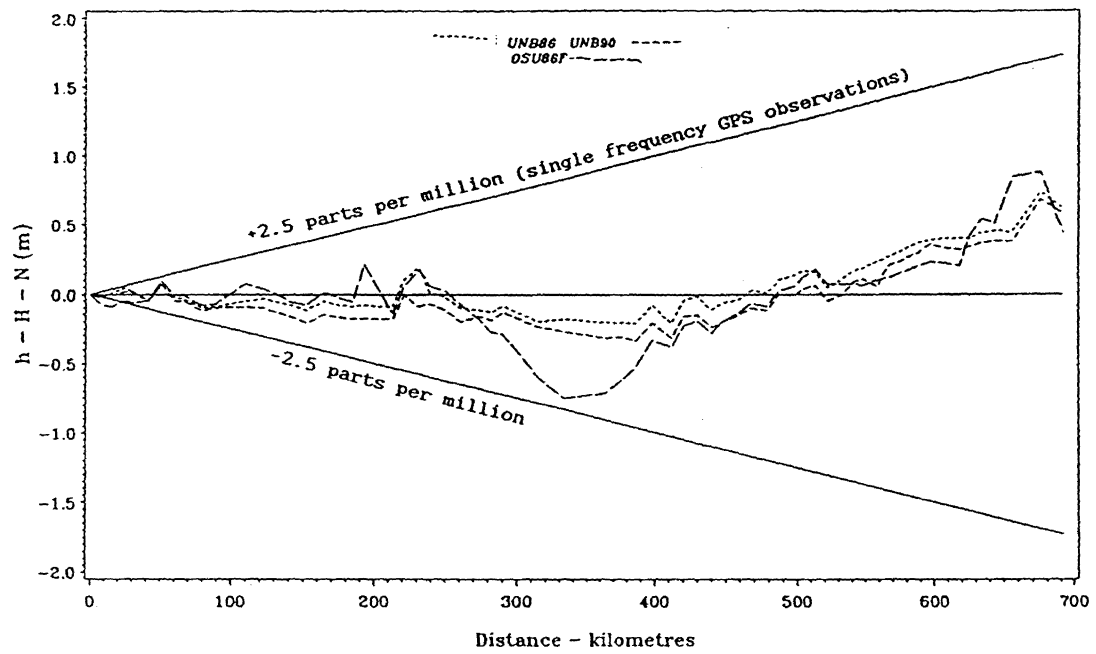


Figure 7.13: Profile of the difference between the GPS/ orthometric derived profile and that obtained from UNB90.



from GPS/ orthometric levelling is very good. However, there are obviously some systematic effects and in the following sections the autocorrelation function and LSSA are used to in order to obtain some insight into these errors. It must be noted that only the NWT network provides sufficient data for analysis –the Ontario and Manitoba networks are more sparse and therefore results of the analyses undertaken on these networks can only be regarded as an indication of the possible presence of systematic effect.

The data series were obtained by subtracting the mathematical geoidal model undulation from the appropriate GPS/ orthometric levelling geoidal undulation ( $h - H - N$ ). The series may then be ordered according to any suitable argument on which it is suspected of having a statistical dependency. In the case of data series ordered according to baseline length and azimuth the misclosures were obtained by from  $\Delta(h - H - N)$ .

## 7.6 Analysis of the UNB Dec. '86 geoid

### 7.6.1 The North West Territories Network

The series of misclosures, ( $h - H - N$ ), ordered according to increasing latitude, as well as its autocorrelation function and spectrum are shown in Figure 7.14. The autocorrelation function shows some evidence of systematic effect. It should be remembered that the autocorrelation function becomes less reliable towards the high end of the scale.

The spectrum shows significant peaks almost continuously from frequency 0.1 to 2.0 which corresponds reciprocally to a period of between greater than  $10^\circ$  and  $0.5^\circ$ . This could be the result of a linear trend aliasing as a low frequency peak. A period of  $10^\circ$  and greater could indicate the effect of the reference field, GEM9, which is sensitive to features larger than  $9^\circ$ . The lower periods indicate that there may be some shortcoming in the gravity data, as this will be influenced by the smaller

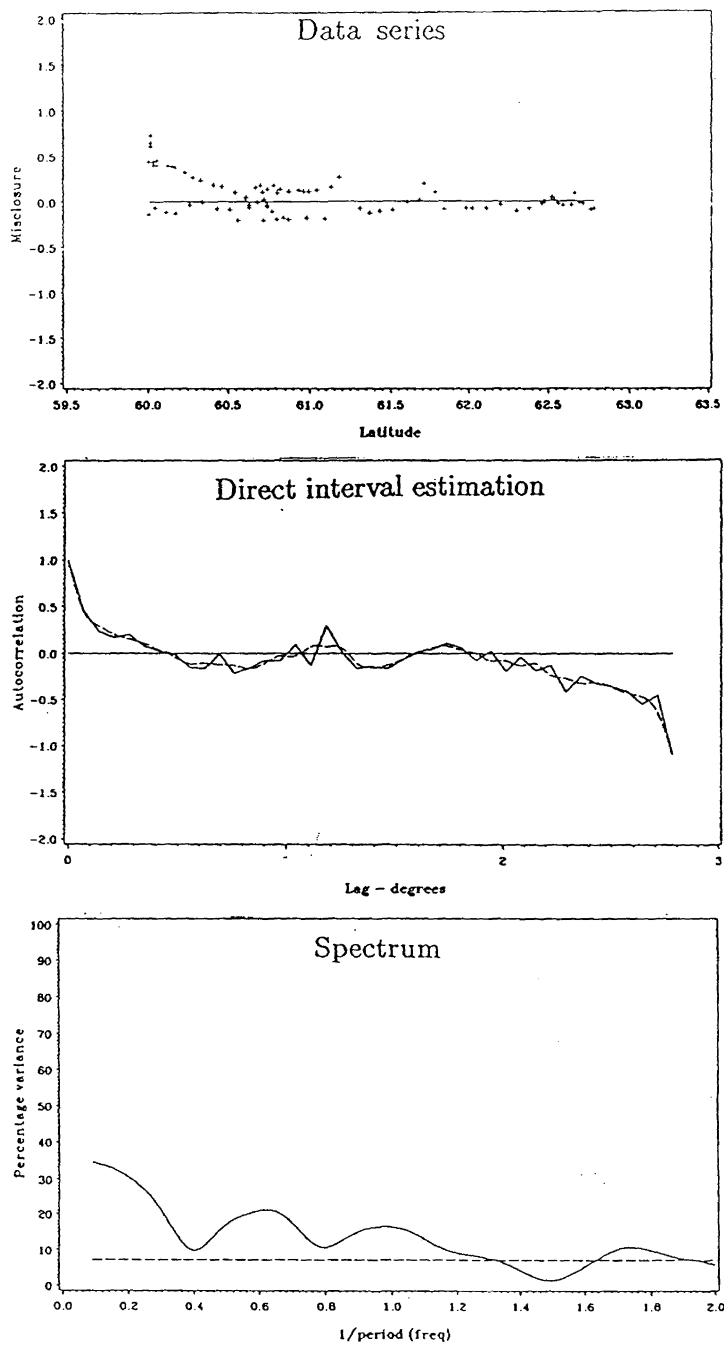


Figure 7.14: Analysis of the North West Territories UNB86 data series (ordered according to latitude).

gravimetric features. The two distinct lines of misclosures in the data series from latitude  $60^\circ$  to  $60.6^\circ$  are, in the case of the upper main profile to Fort Smith, and in the case of the lower, from the spur at approximate azimuth of  $225^\circ$  (cf. Figure 5.1). This suggests that the systematic effect at work is not latitude dependent as it has influenced the main profile but not the spur.

The series of misclosures are then ordered according to increasing longitude as is shown in Figure 7.15. There is clearly evidence of a linear trend and it is convenient

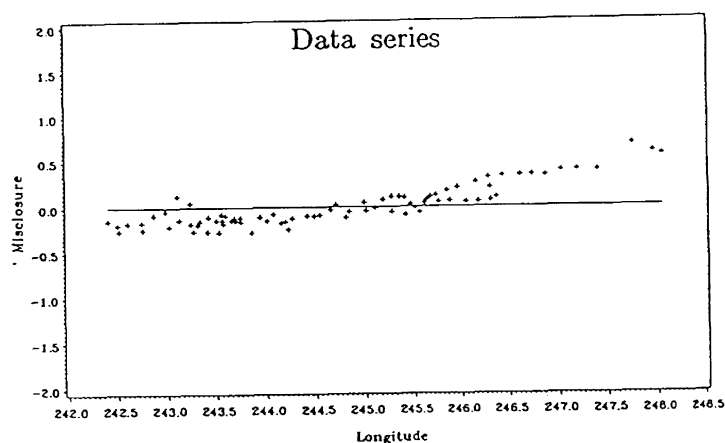


Figure 7.15: The North West Territories UNB86 data series (ordered according to longitude).

to remove this using the option in the LSSA program otherwise it will overpower the autocorrelation function and tend to “drown” the spectrum. The linear trend was determined to be  $\cong 2$  part per million (127 millimetres per  $1^\circ$ ).

This very distinctive trend suggests that there is a relationship between the systematic effect and longitude. It is possible to speculate about the cause of this. If data were available, it would be interesting to order the series according to date of observation because the changing time of the GPS window, when satellite configuration is optimal, by four minutes per day may have aliased into a longitude trend as observations progressed along the profile. Further information could perhaps be derived by using as argument atmospheric parameters, which may reflect the condition of the ionosphere or troposphere at the time of observation. It is also possible that the trend is due to a long wavelength (satellite reference field) deficiency in the geoidal model, and that this has, due to its large size and limited longitude extent of the series, been reflected as a linear trend.

The residual series, its autocorrelation function and spectrum are shown in Figure 7.16.

It becomes clear that even after the considerable linear trend was removed the autocorrelation function still gives evidence of low periodic systematic error. From a visual inspection there appears to be a quadratic trend to the data series. The spectrum has a number of marginally significant peaks at high frequency but is dominated by a peak at low frequency. The length of this period is larger than  $7^\circ$  which implies that it may be due to the satellite reference field GEM9. It is also possible that some systematic error has crept into the GPS heights due to the method of observation or processing. A marginal peak correspond reciprocally to a period of  $1.7^\circ$  which could be a reflection on the terrestrial contribution to the regional geoidal model. It should be noted that  $1.7^\circ$  is a harmonic of  $7^\circ$ .

In Figure 7.17 the data series is ordered according to orthometric height and is shown together with its autocorrelation function and spectrum. Clearly there is no sign of systematic effect, except, marginally, at the very high end of the analysis, but due to the way in which the function is calculated, the top end is less significant. As  $H$  is closely related to  $h$ , this analysis also suggests that there will be little systematic

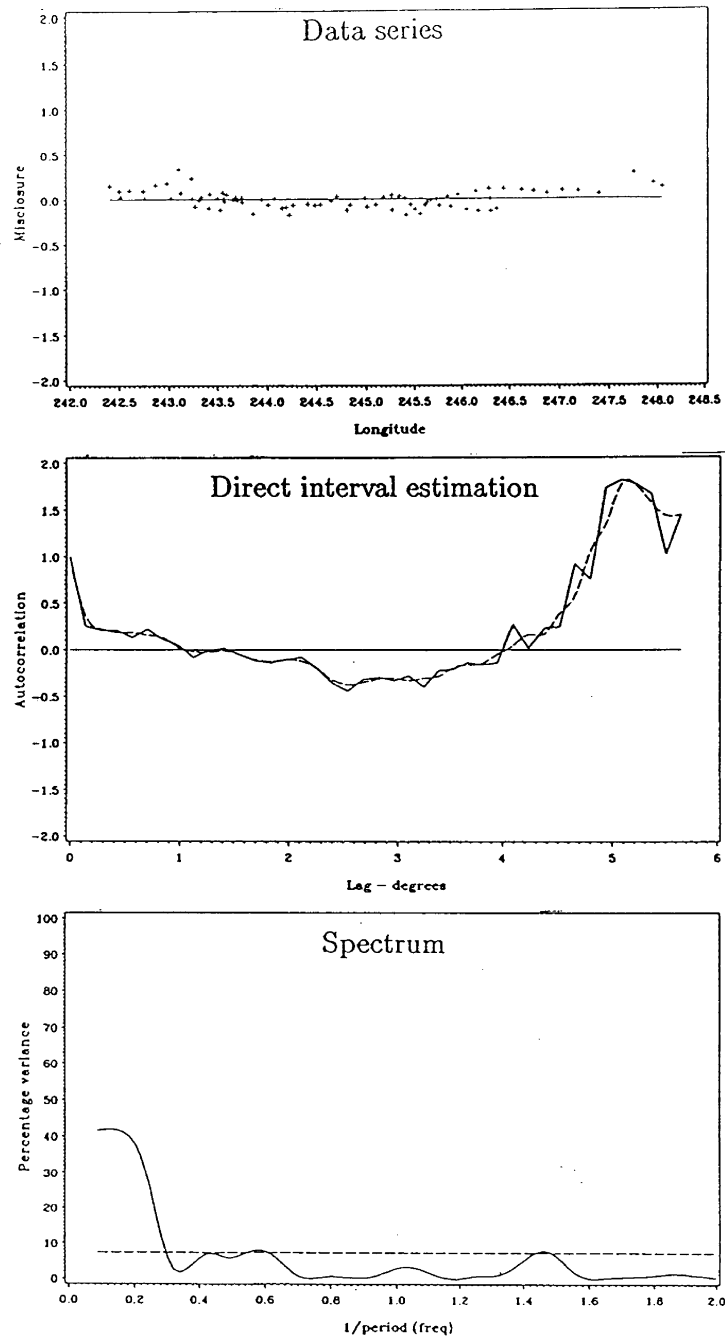


Figure 7.16: Analysis of the North West Territories UNB86 data series ordered according to longitude).

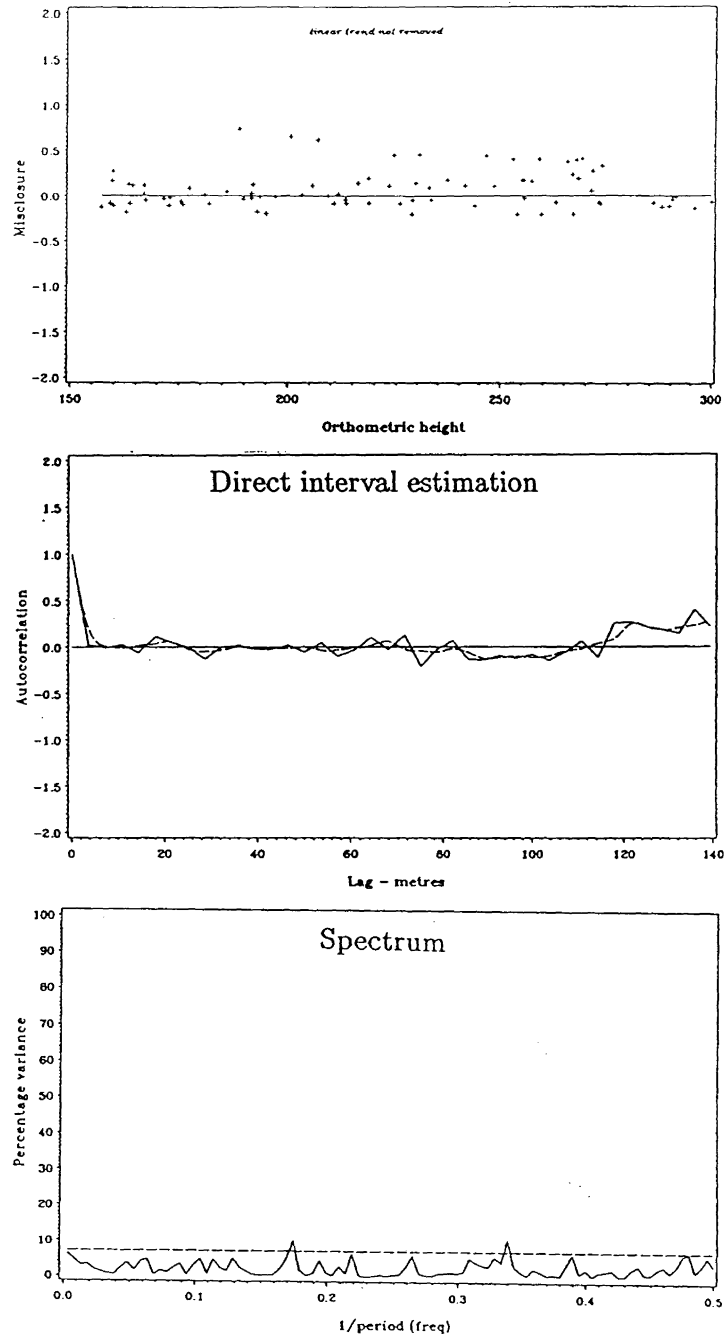


Figure 7.17: Analysis of the North West Territories UNB86 data series (ordered according to orthometric height).

error if the series is ordered according to  $h$  and this was confirmed by the appropriate calculations.

The series was then ordered according to the absolute value of the change in orthometric height associated with each baseline. This series, its autocorrelation function and spectrum are shown in Figure 7.18. The autocorrelation function shows almost no evidence of systematic effect and there are no significant peaks in the spectrum.

The series of baseline misclosures was ordered according to baseline length and is shown in Figure 7.19. The misclosures were again taken as always positive in order to ensure consistency. The variance of the series plainly has a strong dependency on the length of the baseline and so the data series has been normalised. The correlation function shows strong evidence of systematic effect and the spectrum is dominated by a low frequency peak at frequency 0.045 (period 222 kilometres). There is a secondary peak at frequency 0.012 (period 83 kilometres). The low frequency peak is within the sphere of influence of the terrestrial gravity contribution to the gravity model and may be due to a deficiency of the gravity data used in the partial (terrestrial) solution of Stokes formula.

Finally, the series of baseline misclosures was ordered according to the azimuth associated with each baseline. Azimuths were regarded as running between  $0^\circ$  and  $180^\circ$ , the reciprocal of larger azimuths was used. The series, its autocorrelation function and spectrum are shown in Figure 7.20. There is evidence of periodicity in the series and this reaches a peak at  $90^\circ$  approximately. The autocorrelation function shows evidence of systematic effect and the spectrum has a large peak at low frequency as well as peaks at 0.028 (period  $36^\circ$ ) and 0.042 ( $24^\circ$ ). The systematic effect seen here is partially due to the dependency of GPS errors on baseline azimuths.

The results of these analyses are summarised in Table 7.8.

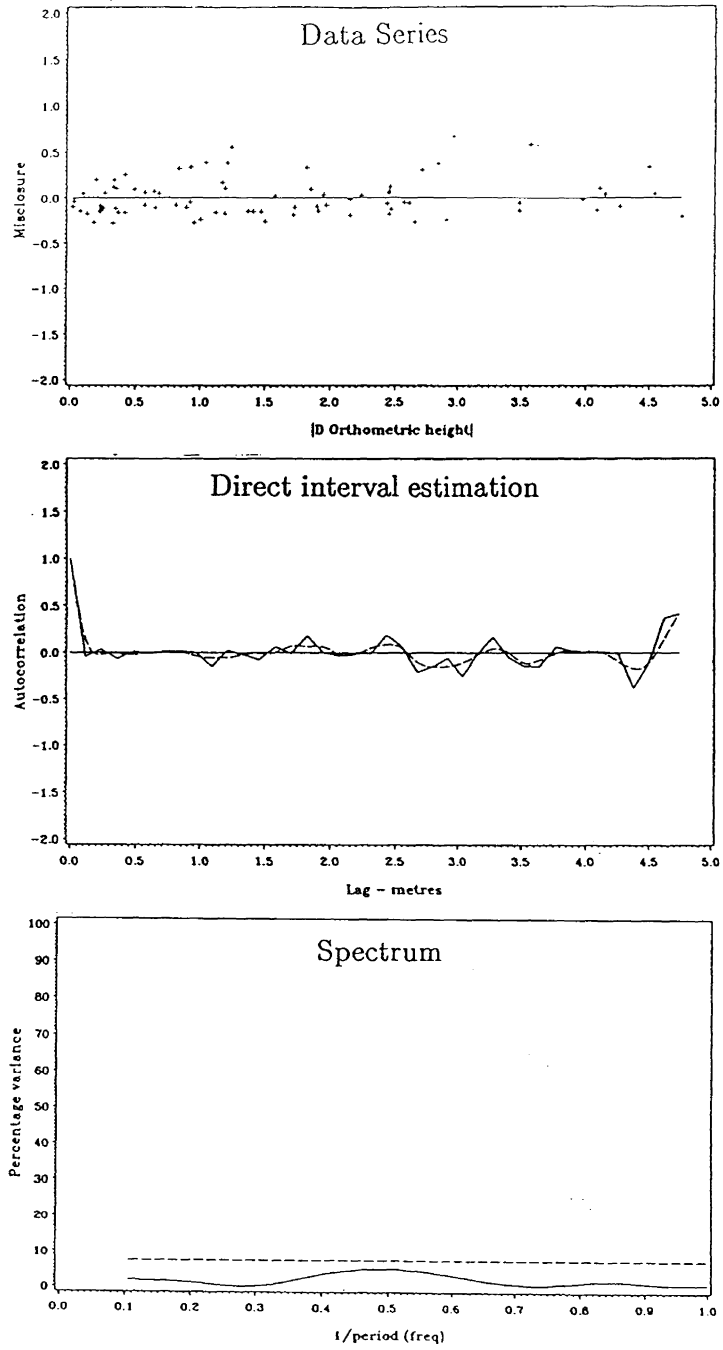


Figure 7.18: Analysis of the North West Territories UNB86 data series (ordered according to absolute change in orthometric height).



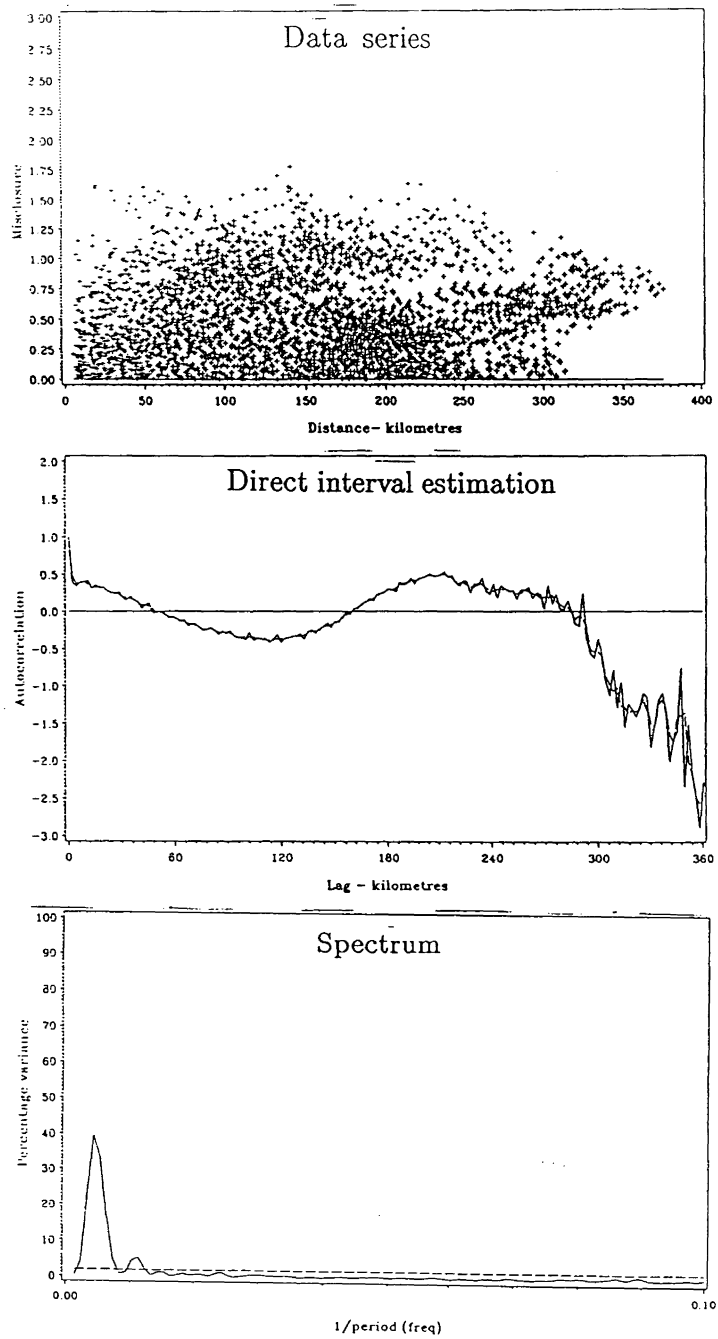


Figure 7.19: Analysis of the North West Territories UNB86 data series (ordered according to length of baseline).

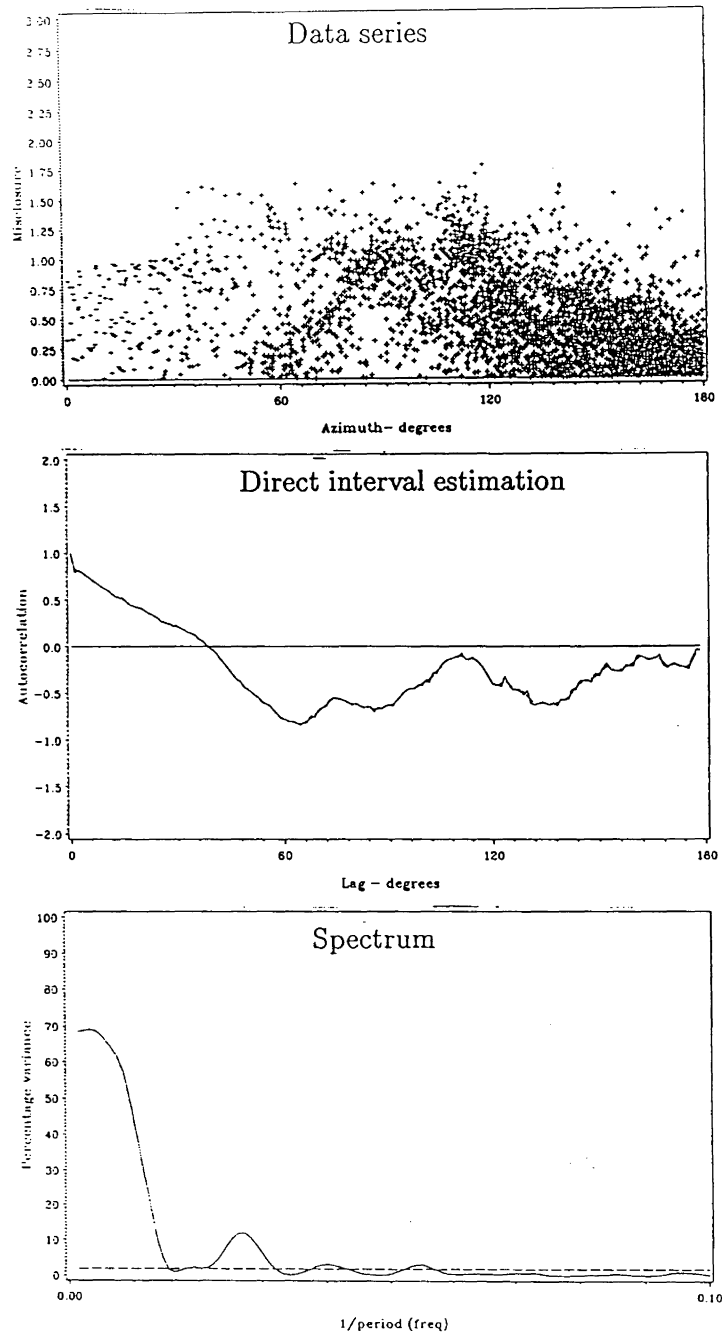


Figure 7.20: Analysis of the North West Territories UNB86 data series (ordered according to azimuth of the baseline).

<i>"UNB Dec. '86"</i> <i>NWT network</i>		
<i>Argument</i>	<i>Attribute</i>	<i>Analysis</i>
<i>latitude</i>	<u><i>Linear trend</i></u> <u><i>Autocorrelation</i></u> <i>character</i> <i>distance</i> <u><i>Spectrum</i></u> <i>peaks</i>	small-long period 3°  > 10° to 0.5°
<i>longitude</i>	<u><i>Linear trend</i></u> <u><i>Autocorrelation</i></u> <i>character</i> <i>distance</i> <u><i>Spectrum</i></u> <i>peaks</i>	± 2ppm  medium-long period 6°  > 10°, 1.7°, 0.7°
<i>orthometric height</i>	<u><i>Linear trend</i></u> <u><i>Autocorrelation</i></u> <i>character</i> <i>distance</i> <u><i>Spectrum</i></u> <i>peaks</i>	very small-wavy 140 metres  not significant
<i>azimuth</i>	<u><i>Linear trend</i></u> <u><i>Autocorrelation</i></u> <i>character</i> <i>distance</i> <u><i>Spectrum</i></u> <i>peaks</i>	large-long period 180°  36°, 24°
<i>baseline length</i>	<u><i>Linear trend</i></u> <u><i>Autocorrelation</i></u> <i>character</i> <i>distance</i> <u><i>Spectrum</i></u> <i>peaks</i>	±1ppm  large-long period 360 kilometres  222 km, 83 km

Table 7.8: Summary of the analyses of the North West Territories network using "UNB Dec. '86".

## 7.6.2 The Ontario Network

The series of 23 misclosures is ordered according to increasing latitude and is shown with its autocorrelation function and spectrum in Figure 7.21. There appears, from the plot of the series, to be evidence of a linear trend. The trend is, however, in the opposite direction to that encountered in the NWT (latitude) series. The two networks are separated by more than  $15^\circ$  of latitude so it is possible that an effect due to the geoidal model long wavelength influence could have reversed its sign. The autocorrelation function shows clear evidence of systematic effect and the spectrum has significant peaks at frequencies of 0.28 and approximately 0.8 which translate reciprocally to periods of  $3.6^\circ$  and  $1.2^\circ$ . Both these periods imply features that are defined by the terrestrial contribution to the geoidal solution. As mentioned earlier these results would have very large error bars and can only be taken as an indication due to the very limited size of the data series.

The data series, ordered according to increasing longitude, is shown in Figure 7.22. There is clear visual evidence of a linear trend and this was removed using the option in the LSSA program. It amounts to  $\pm 3$  parts per million (251 millimetres per  $1^\circ$ ). The residual series, with its autocorrelation function and spectrum appear in Figure 7.23. There is evidence of systematic effect in the residual series and the spectrum has significant peaks between frequencies of 0.3 and 0.6 which correspond to periods of between  $3.3^\circ$  and  $1.6^\circ$ . These periods correspond to the terrestrial contribution which is sensitive to features of smaller extent. The trend that was removed first could be due to the reference field, GEM9. It is also possible that some systematic error has been introduced into the GPS levelling by the procedures adopted for observation or processing of the data. The trend has the same direction of slope as that found in the NWT(longitude) series but has a greater magnitude. Not too much should be read into this because of the sparseness of the data and the uneven way in which they are distributed.

If the data series is ordered according to orthometric height as in Figure 7.24

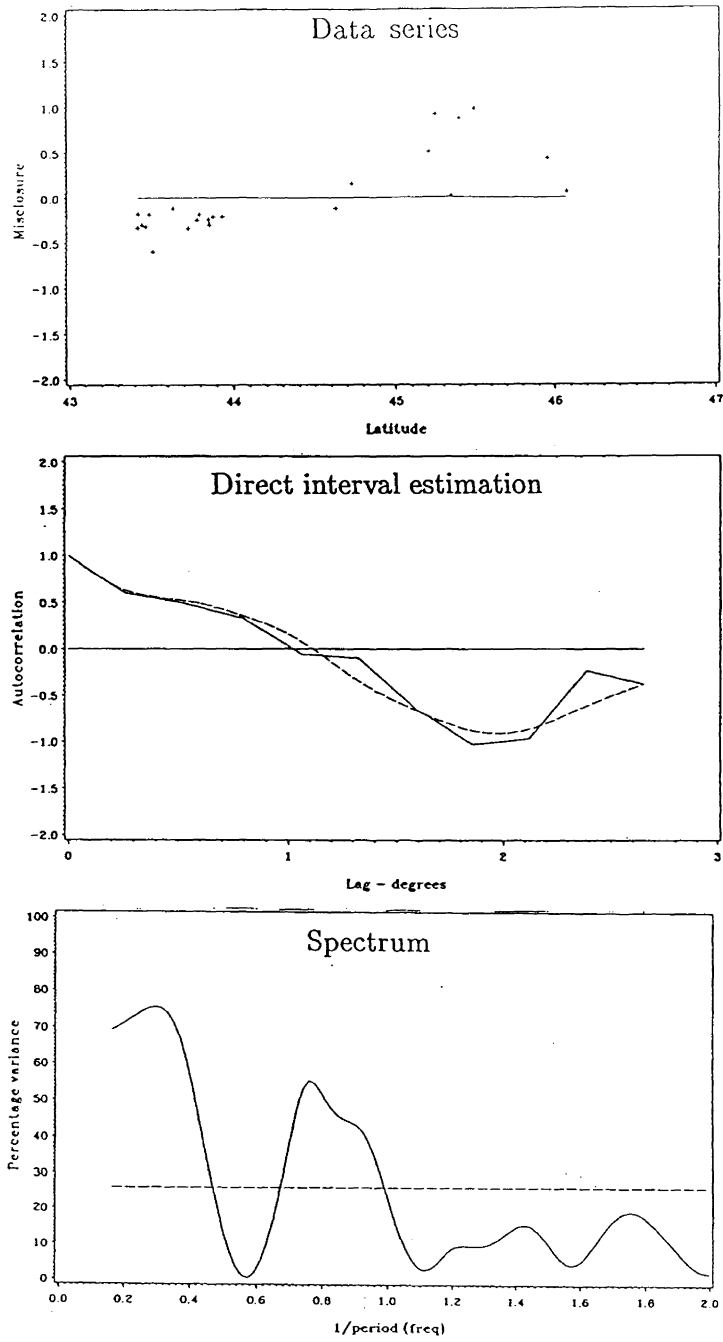


Figure 7.21: Analysis of the Ontario network UNB86 data series (ordered according to latitude).

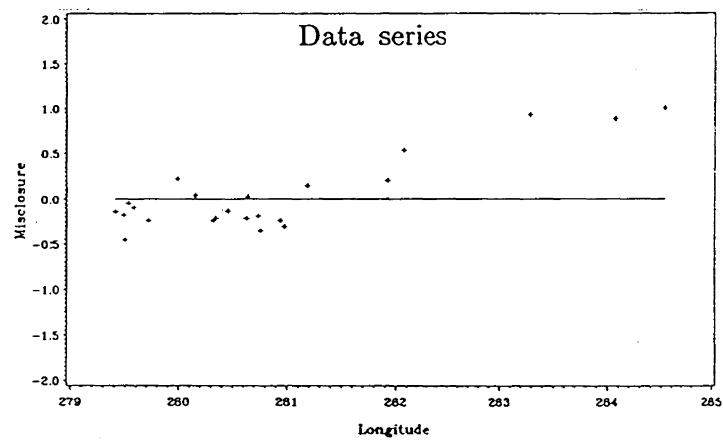


Figure 7.22: The Ontario network UNB86 data series (ordered according to longitude).

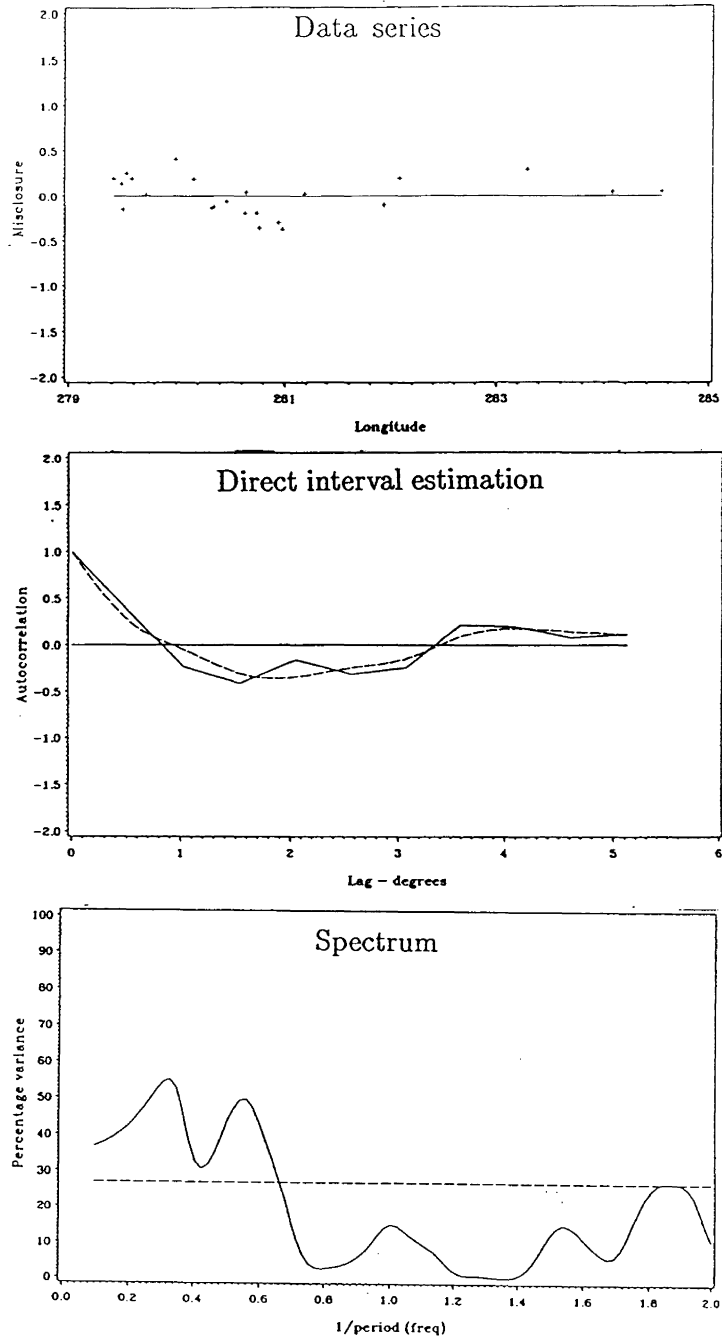


Figure 7.23: Analysis of the Ontario network UNB86 data series (ordered according to longitude).

then the corresponding autocorrelation function displays a periodic motion about the zero line. This is most likely due, again, to the size of the data and the indication is that there may be some systematic effect. The spectrum has significant peaks at frequencies of between 0.004 and 0.008 and at 0.014 or alternatively at periods of between 250 and 125 metres and at 71 metres. These are all harmonics of 500 metres.

In Figure 7.25 each length of the baselines that make up the Ontario network are used as the argument ordering the misclosures obtained by comparing “UNB Dec. ’86” undulation differences for each baseline with the differences obtained by comparing GPS and orthometric levelling. The same convention to ensure consistency is used i.e. using positive values. There is a clear relationship between the variance and the baseline length and so the series was normalised. The autocorrelation function shows some evidence of systematic effect. The spectrum has peaks at frequencies of 0.00255 (period 400 kilometres), 0.0055 (180 kilometres) and 0.0115 (87 kilometres). The latter values are approximate harmonics of the former. These values all fall within the influence of the terrestrial contribution.

In Figure 7.26 the baseline misclosures are ordered according to azimuth. There is some evidence of systematic effect as can be seen from the behaviour of the autocorrelation function about the zero line. The spectrum has a significant peak at 0.012 (period 83°) and at 0.030 (33°).

The results of these analyses are summarised in Table 7.9.

### **7.6.3 The Manitoba network**

This series of 11 misclosures is ordered according to latitude in Figure 7.27, according to longitude in Figure 7.28 and according to orthometric height in Figure 7.29.

The size of the sample here is very limited and therefore caution must be exercised in the analysis.

There appears to be some evidence of systematic error in all of the autocorrelation



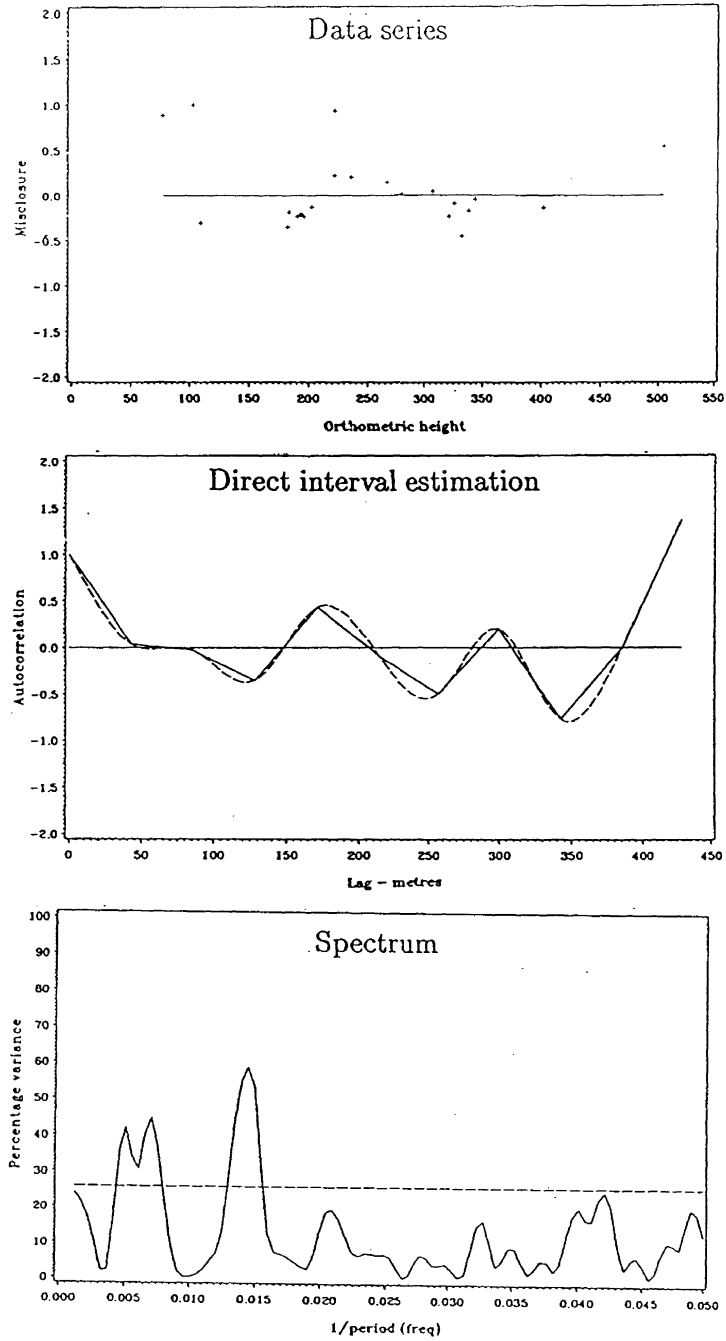


Figure 7.24: Analysis of the Ontario network UNB86 data series (ordered according to orthometric height).

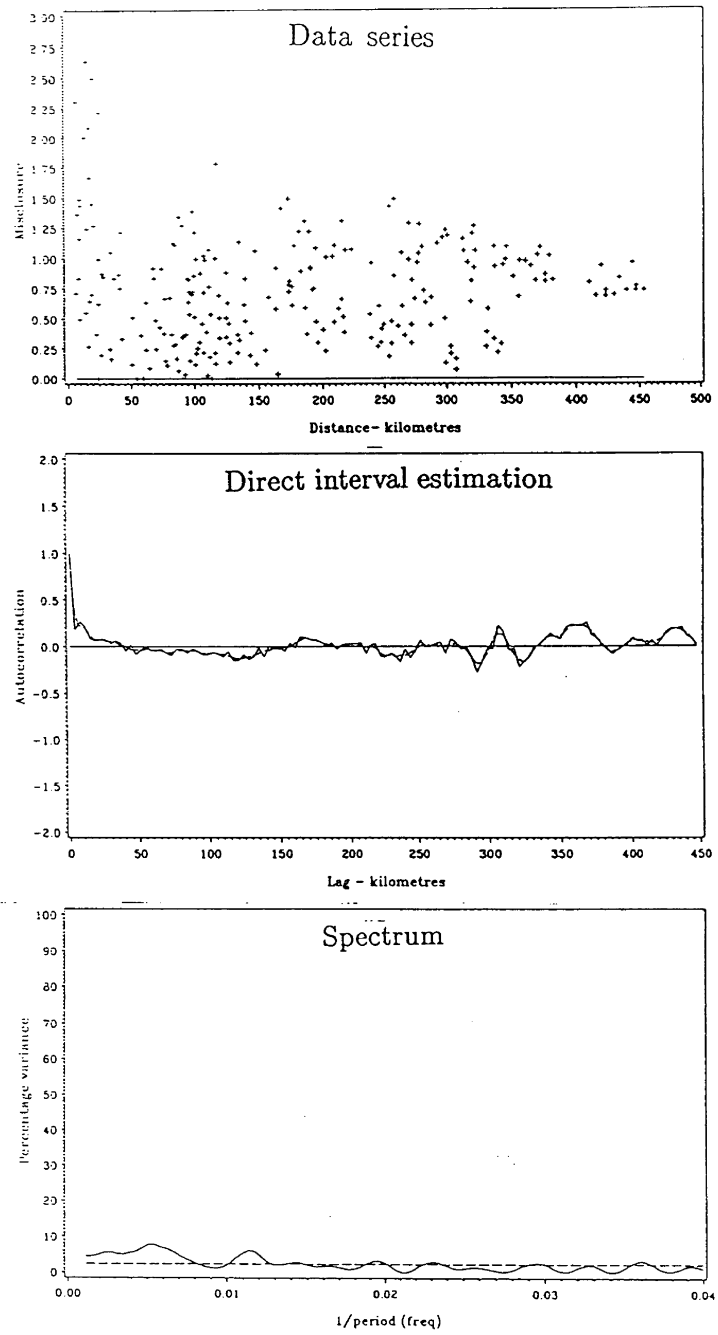


Figure 7.25: Analysis of the Ontario UNB86 data series (ordered according to baseline length).

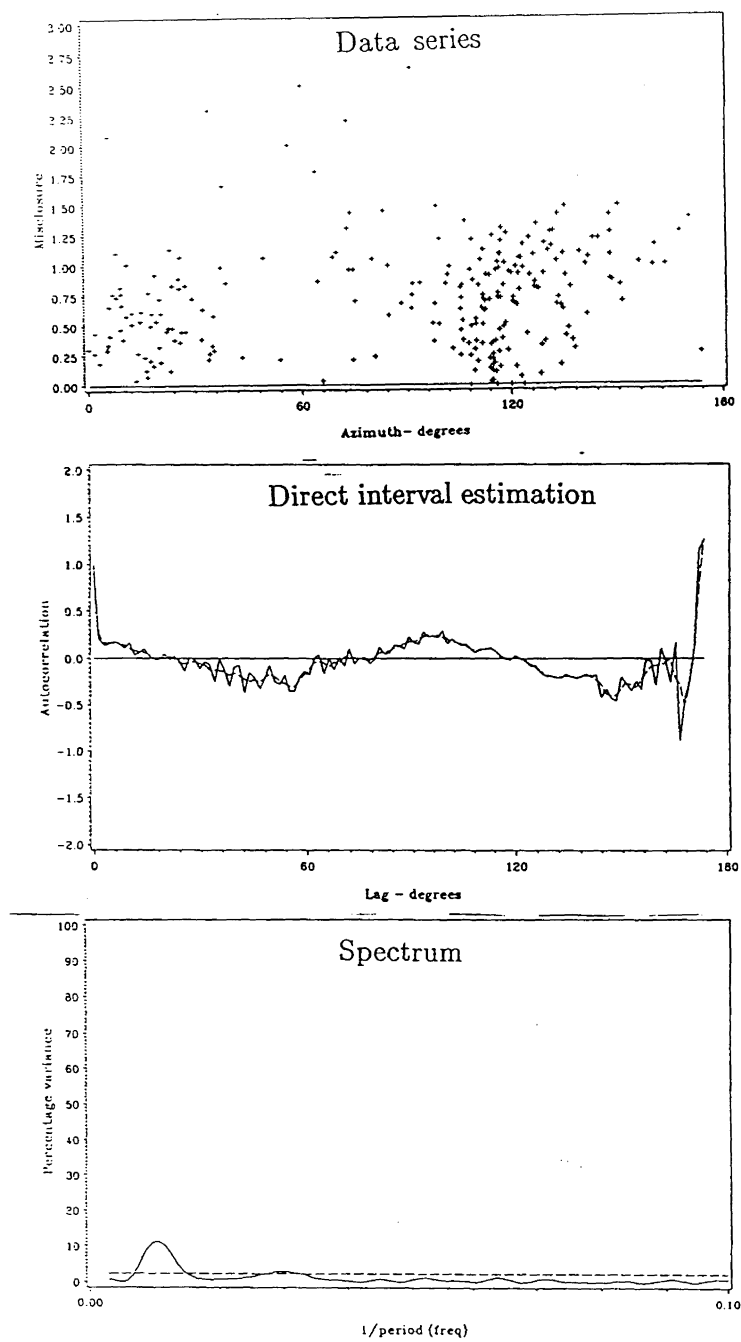


Figure 7.26: Analysis of the Ontario UNB86 data series (ordered according to azimuth).

<i>"UNB Dec. '86"</i> <i>Ontario network</i>		
<i>Argument</i>	<i>Attribute</i>	<i>Analysis</i>
<i>latitude</i>	<u><i>Linear trend</i></u> <u><i>Autocorrelation</i></u> <i>character</i> <i>distance</i> <u><i>Spectrum</i></u> <i>peaks</i>	large-long period 3°  3.6°, 1.2°
<i>longitude</i>	<u><i>Linear trend</i></u> <u><i>Autocorrelation</i></u> <i>character</i> <i>distance</i> <u><i>Spectrum</i></u> <i>peaks</i>	≅ 3 ppm  small-long period 5°  > 3.2° to 1.5°
<i>orthometric height</i>	<u><i>Linear trend</i></u> <u><i>Autocorrelation</i></u> <i>character</i> <i>distance</i> <u><i>Spectrum</i></u> <i>peaks</i>	medium-wavy 440 metres  250, 125, 71 metres
<i>azimuth</i>	<u><i>Linear trend</i></u> <u><i>Autocorrelation</i></u> <i>character</i> <i>distance</i> <u><i>Spectrum</i></u> <i>peaks</i>	small waves 180°  83°, 33°
<i>baseline length</i>	<u><i>Linear trend</i></u> <u><i>Autocorrelation</i></u> <i>character</i> <i>distance</i> <u><i>Spectrum</i></u> <i>peaks</i>	v.small waves 450 kilometres  400km, 180km, 87km

Table 7.9: Summary of the analyses of the Ontario network using "UNB Dec. '86".

functions especially in the case of latitude in Figure 7.27. The spectrum in Figure 7.27 shows no significant peaks. There is a peak at frequency 1.87 or reciprocally period  $0.5^\circ$  in Figure 7.28 and one at frequency 0.11 or period 9 metres in Figure 7.29.

The extreme sparseness of the data and its distribution, especially in Figure 7.29 prevent too much weight from being placed on these analyses, which are included for the sake of completeness.

In Figure 7.30 each of the baseline lengths that make up the Manitoba network is used as the argument to order the misclosures obtained by comparing the “UNB Dec. ’86 ” undulation differences for each baseline with the differences obtained from GPS/ orthometric levelling. The convention of taking positive values is used as for the other networks. In this case there is a less pronounced relationship between the variance and the length of the baseline but the series has nevertheless been normalised. There is little evidence of systematic effect and the autocorrelation function shows no significant peaks.

The baseline misclosures were then ordered according to azimuth and the analysis is shown in Figure 7.31. The data series shows a slight periodicity. The autocorrelation function has detected systematic effect and the spectrum is dominated by a low frequency peak at approximately  $180^\circ$ . There are no other significant peaks.

The results of these analyses are summarised in Table 7.10.

## **7.7 Analysis of the UNB ’90 geoid**

### **7.7.1 The North West Territories Network**

The series of misclosures, using increasing latitude as the argument, its autocorrelation function and spectrum are shown in Appendix III (cf. Figure III.1). The autocorrelation function gives some evidence of systematic effect. There appears to be slightly more than in the case of the “UNB Dec. ’86” geoid.

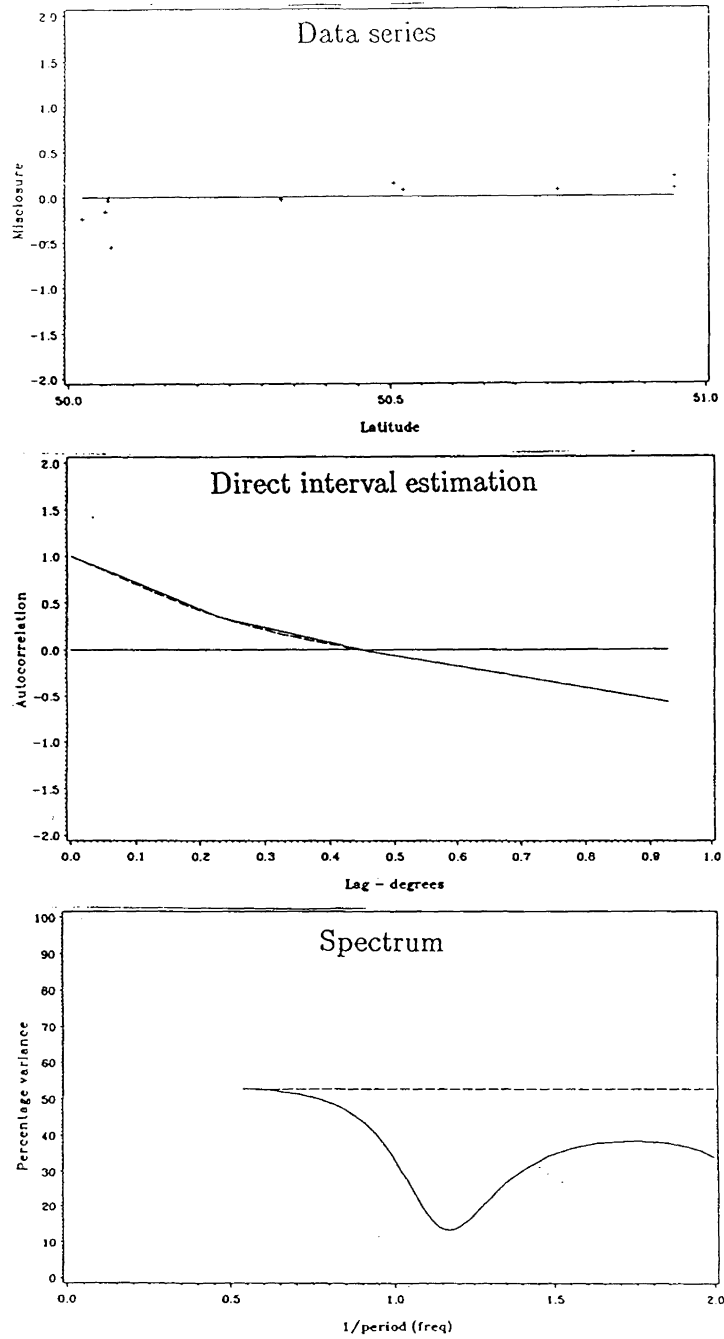


Figure 7.27: Analysis of the Manitoba UNB86 data series (ordered according to latitude).

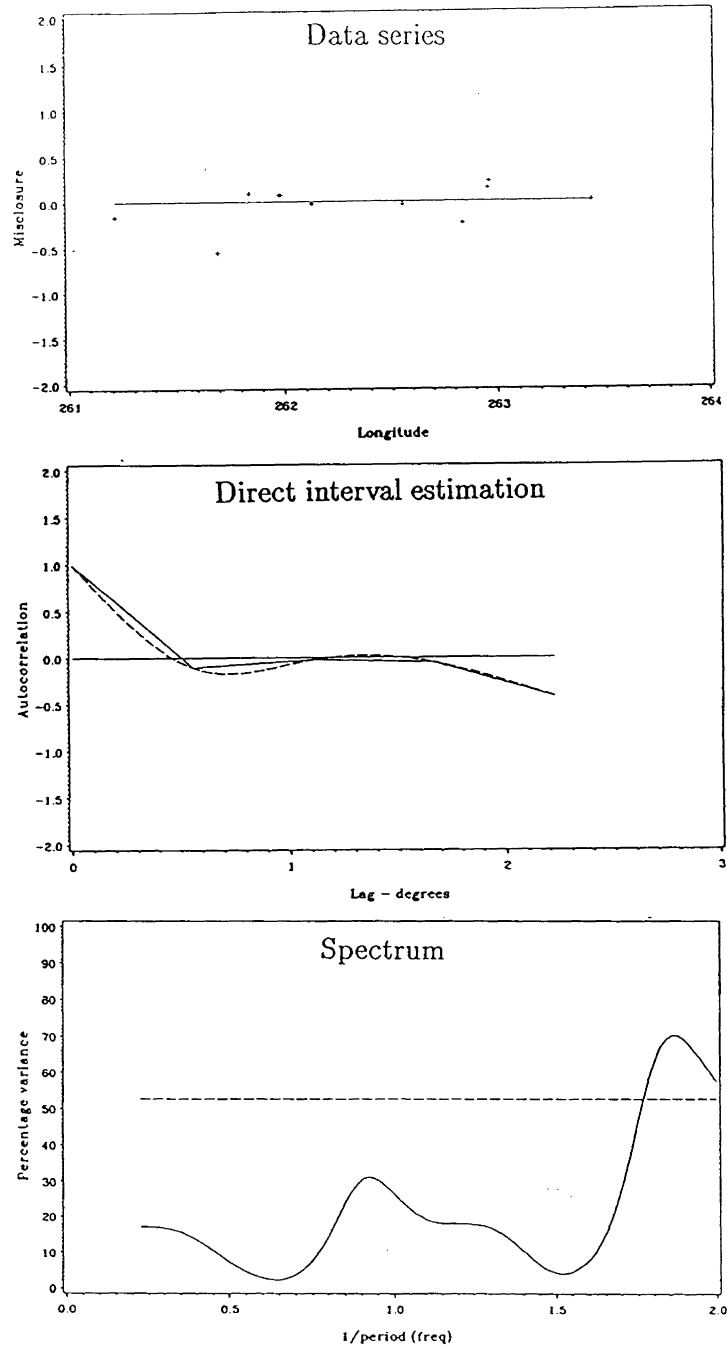


Figure 7.28: Analysis of the Manitoba UNB86 data series (ordered according to longitude).

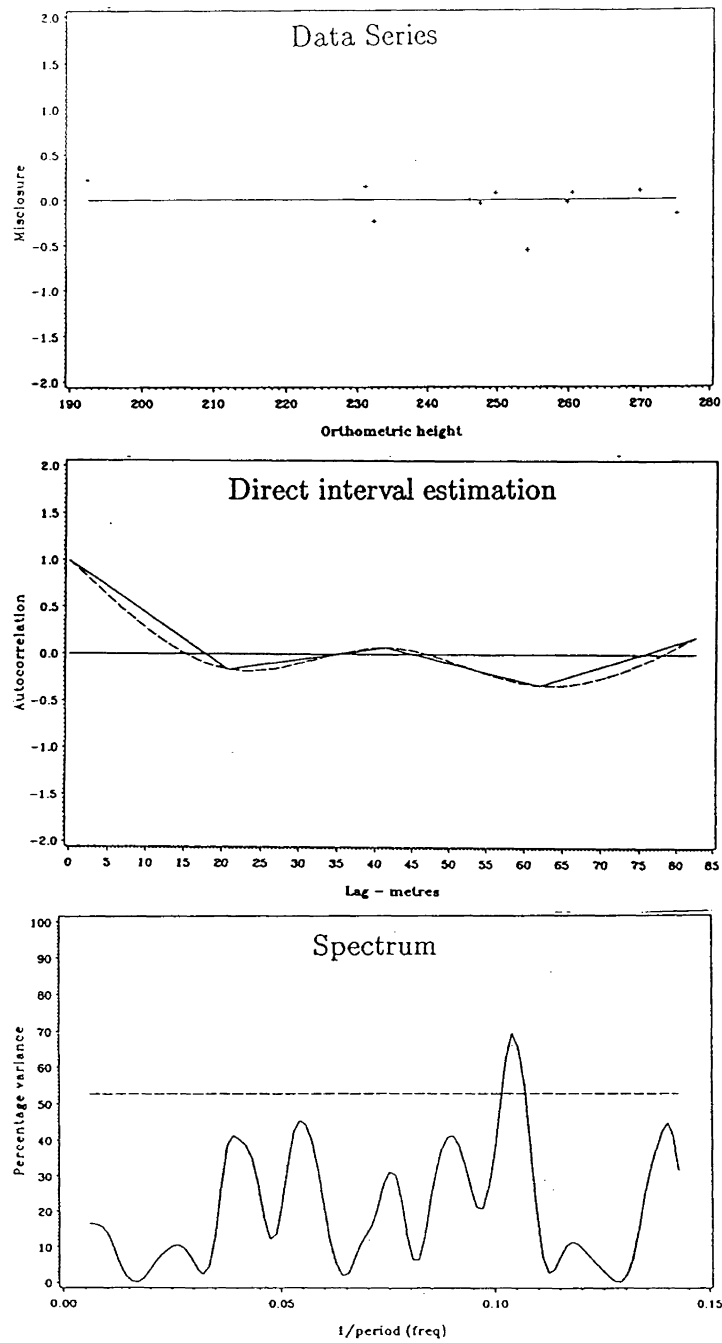


Figure 7.29: Analysis of the Manitoba UNB86 data series (ordered according to orthometric height).



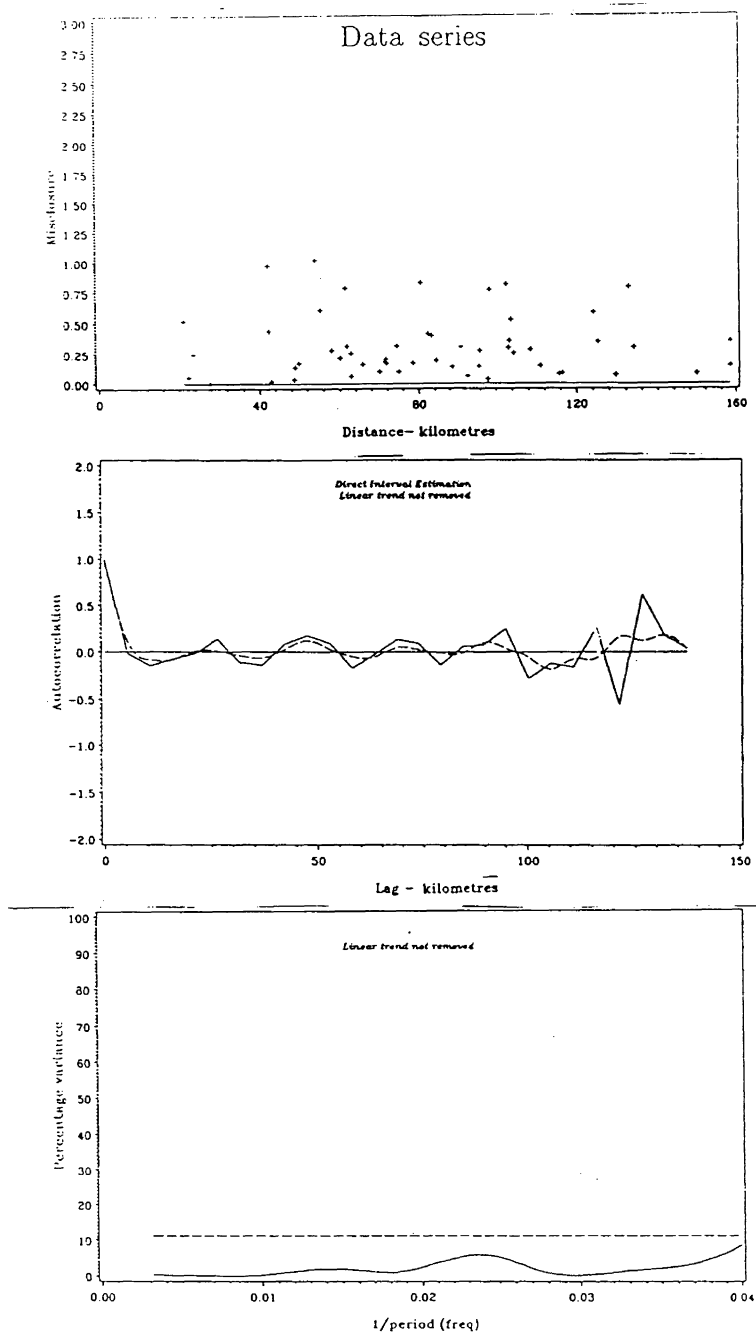


Figure 7.30: Analysis of the Manitoba UNB86 data series (ordered according to baseline length).

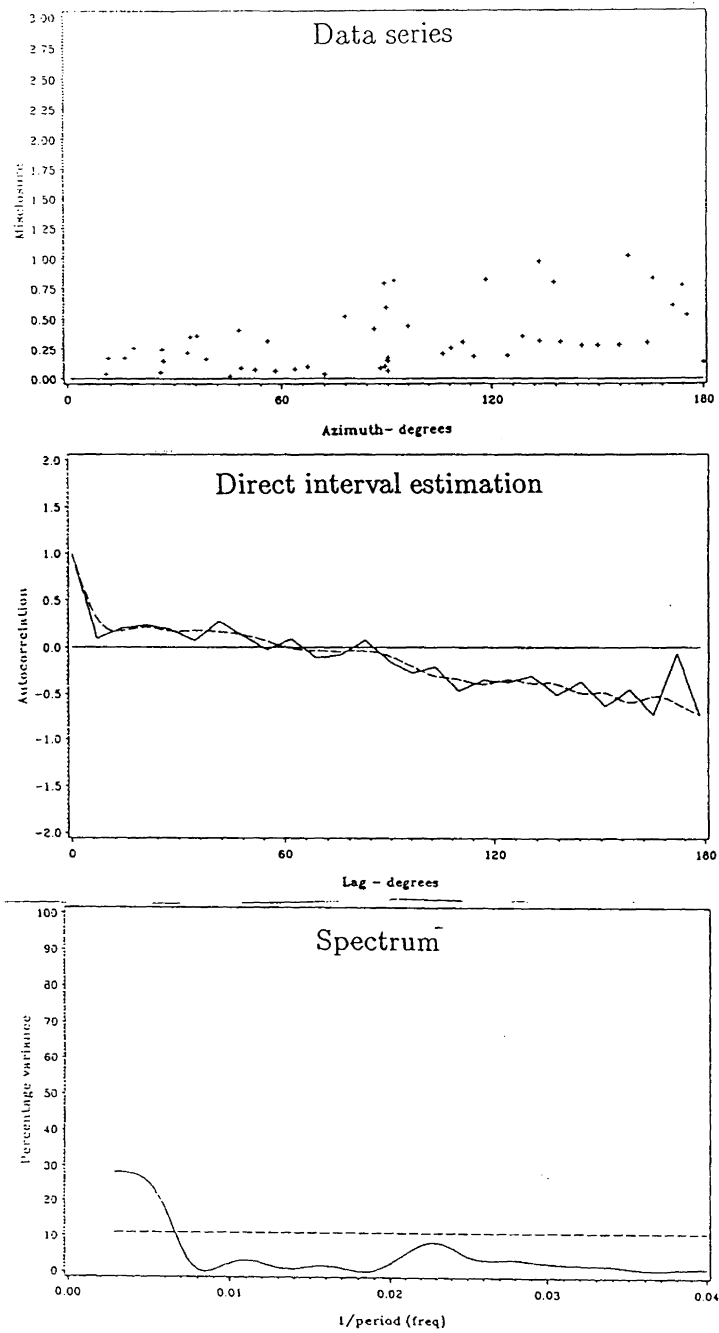


Figure 7.31: Analysis of the Manitoba UNB86 data series (ordered according to azimuth).

<i>"UNB Dec. '86"</i> <i>Manitoba network</i>		
<i>Argument</i>	<i>Attribute</i>	<i>Analysis</i>
<i>latitude</i>	<u><i>Linear trend</i></u> <u><i>Autocorrelation</i></u> <i>character</i> <i>distance</i> <u><i>Spectrum</i></u> <i>peaks</i>	medium-v.long period 0.9°  not significant
<i>longitude</i>	<u><i>Linear trend</i></u> <u><i>Autocorrelation</i></u> <i>character</i> <i>distance</i> <u><i>Spectrum</i></u> <i>peaks</i>	v.small-long period 2°  not significant
<i>orthometric height</i>	<u><i>Linear trend</i></u> <u><i>Autocorrelation</i></u> <i>character</i> <i>distance</i> <u><i>Spectrum</i></u> <i>peaks</i>	small-long period 80 metres  9 metres
<i>azimuth</i>	<u><i>Linear trend</i></u> <u><i>Autocorrelation</i></u> <i>character</i> <i>distance</i> <u><i>Spectrum</i></u> <i>peaks</i>	large-long period 180° > 143°
<i>baseline length</i>	<u><i>Linear trend</i></u> <u><i>Autocorrelation</i></u> <i>character</i> <i>distance</i> <u><i>Spectrum</i></u> <i>peaks</i>	v.small-wavy 140 km  not significant

Table 7.10: Summary of the analyses of the Manitoba network using "UNB Dec. '86".

The spectrum has significant frequencies almost continuously from 0.1 to 2.0 (that is periods greater than  $10^\circ$  to  $0.5^\circ$ ). The higher end of this range corresponds to periods that would be due to the satellite contribution and the lower end to the terrestrial gravimetric solution.

The series of misclosures shown in Figure III.2 are ordered according to increasing longitude. A linear trend is clearly visible and this may be removed using the option in the LSSA program. The linear trend was determined to be  $\pm 2$  part per million (126 millimetres per  $1^\circ$ ). This trend may result from the longer wavelength portion of the “UNB ‘90” which, because of the limited extent in longitude of the network, would alias as a linear trend.

The residual series, its autocorrelation and spectrum are shown in Figure III.3. There is evidence of residual systematic error. The spectrum yields a peak at frequency 0.10 and another at 0.59. These translate reciprocally to periods of greater than  $10^\circ$  and  $1.7^\circ$ . The former lies with the resolution of the GEM-T1 reference field while the latter is within the range of the terrestrial contribution to the regional geoidal model. The linear trend could be the result of a long periodic error in the satellite reference field, GEM-T1, or possibly to systematic error introduced into the GPS heights during the processing or observations. The comments made in Section 7.6.1 apply here also. The GEM-T1 reference field, although quoted to a higher accuracy than the GEM9 field (cf. see Figure 4.7), used some of the same satellite data in its derivation and so is not independent.

The results are summarized in Tables 7.11.

### 7.7.2 The Ontario and Manitoba networks

Similar analyses have been carried out on the “UNB ‘90” geoid using the GPS data collected during the Ontario and Manitoba campaigns. The data in these series are sparse and generally not very well distributed. The results are shown in Appendix III.

<i>"UNB '90"</i>		
<i>North West Territories network</i>		
<i>Argument</i>	<i>Attribute</i>	<i>Analysis</i>
<i>latitude</i>	<u><i>Linear trend</i></u>	small-long period 3°  > 10° to 0.5°
	<u><i>Autocorrelation</i></u>	
	<i>character</i>	
	<i>distance</i>	
	<u><i>Spectrum</i></u>	
<i>longitude</i>	<u><i>Linear trend</i></u>	≅ 2ppm  medium-long period 6°  > 10°, 1.7°, 0.7°
	<u><i>Autocorrelation</i></u>	
	<i>character</i>	
	<i>distance</i>	
	<u><i>Spectrum</i></u>	
	<i>peaks</i>	

Table 7.11: Summary of the analyses of the North West Territories network using "UNB '90".

The Ontario data series, ordered according to latitude, is shown in Figure III.4. There is some visual evidence of a linear trend that may suggest that the satellite reference field is contributing to the misclosures. The autocorrelation function shows clear evidence of systematic effect. The linear trend is apparent as a low frequency peak. There is a peak in the spectrum at frequency 0.4 and another at 0.8 which correspond to periods of 2.5° and 1.25°. The latter period is a harmonic of the former. The latter peaks are within the range of the terrestrial contribution to the geoidal model.

The Ontario data series, ordered according to longitude, is shown in Figure III.5. There is clear evidence of linear trend and this may be removed using the LSSA program. It amounts to approximately 3 parts per million (250 millimetres per 1°) and the residual series is in Figure III.6. The autocorrelation function gives evidence of systematic error in this residual series with peaks at frequencies 0.32 and 0.54 which correspond to periods of 3.1° and 1.9°, both of which are within the range of

the terrestrial contribution.

The Manitoba, ordered according to longitude, using “UNB '90” geoidal values shows some sign of autocorrelation (cf. Figure III.7). There are no significant peaks in the spectrum. The data series, ordered according to longitude, is shown in Figure ?? and shows some small evidence of autocorrelation and no larger significant peaks.

The results are summarized in Tables 7.12.

A comparison between the “UNB Dec. '86” and “UNB '90” analyses of the networks reveals the same degree or marginally less indication of systematic error in the case of the latter. The results of the spectral analyses are also similar.

<i>"UNB '90"</i>		
<i>Ontario network</i>		
<i>Argument</i>	<i>Attribute</i>	<i>Analysis</i>
<i>latitude</i>	<u><i>Linear trend</i></u>	large-long period 3°
	<u><i>Autocorrelation</i></u>	
<i>longitude</i>	<i>character</i>	2.5°, 1.2°
	<i>distance</i>	
<i>latitude</i>	<u><i>Spectrum</i></u>	≅ 3 ppm
	<u><i>peaks</i></u>	
<i>longitude</i>	<u><i>Linear trend</i></u>	small-long period 5°
	<u><i>Autocorrelation</i></u>	
<i>latitude</i>	<i>character</i>	> 3.2° to 1.5°
	<i>distance</i>	
<i>longitude</i>	<u><i>Spectrum</i></u>	
	<u><i>peaks</i></u>	
<i>Manitoba network</i>		
<i>Argument</i>	<i>Attribute</i>	<i>Analysis</i>
<i>latitude</i>	<u><i>Linear trend</i></u>	medium-v.long period 0.9°
	<u><i>Autocorrelation</i></u>	
<i>longitude</i>	<i>character</i>	not significant
	<i>distance</i>	
<i>latitude</i>	<u><i>Spectrum</i></u>	v.small-long period 2°
	<u><i>peaks</i></u>	
<i>longitude</i>	<u><i>Linear trend</i></u>	not significant
	<u><i>Autocorrelation</i></u>	
<i>latitude</i>	<i>character</i>	
	<i>distance</i>	
<i>longitude</i>	<u><i>Spectrum</i></u>	
	<u><i>peaks</i></u>	

Table 7.12: Summary of the analyses of the Ontario and Manitoba networks using "UNB '90".

# Chapter 8

## Conclusion

A combination of GPS and orthometric levelling has proved to be a valuable tool for the verification of regional gravimetric geoidal models such as “UNB Dec. ’86” and “UNB ’90”. This process of verification is susceptible to error. A combination of the autocorrelation function and least squares spectral analysis successfully detected the presence of systematic errors in simulated data and was subsequently used to detect the presence of systematic error in the data series constructed while verifying the regional geoidal models.

Each component of the measuring process has been considered and the following conclusions may be drawn.

Concerning the Canadian vertical network, it may be stated that:

1. The systems of heights used in Canada was historically not based on determinations of gravity and hence should, strictly speaking, not be termed orthometric.
2. Staff/ instrument settlement, staff graduation and temperature errors are among sources of systematic errors known to be present in the Canadian vertical network.
3. The heights in the Canadian system are referred to surfaces not coincident with the geoid due to incorrect assumptions made concerning especially sea surface



topography when they were adopted.

The main points concerning the Canadian geoidal solutions – “UNB Dec. ’86” and “UNB ’90” are:

1. These two comprehensive models are closely related, the latter making use of an updated gravity set and some streamlined computational procedures.
2. The former model made use of the less complete satellite derived GEM9 reference field while the later made use of the GEM-T1 field.

Accuracies of between 1 and 3 parts per million may be expected from relative GPS levelling:

1. Generally the most important error source is tropospheric refraction.
2. Other important errors and biases are geometry of the satellite configuration, orbit biases, ionospheric effect, antenna phase centre variations, multipath, antenna imaging and bias due to errors in fixed station co-ordinates.

It appears from the analysis of the normalised baseline misclosures for the three networks that “UNB Dec. ’86” generally yields considerably higher accuracy geoidal height differences than it leads one to believe from its own assessment of its accuracy. An analysis of the data has indicated that there is evidence of considerable systematic error. This is clearly the case in the North West Territories and the Ontario networks. This is especially the case in data series ordered according to longitude, latitude, azimuth and baseline length. The source of this dependence is in part the satellite reference fields where periods are longer than about  $9^\circ$  or the terrestrial gravity contribution where the periods are smaller. A systematic effect could be introduced by the GPS observing or processing procedure. There are also systematic errors in the levelling network.

Further insight could be obtained by ordering the data series according to other arguments, if this data was available, such as satellite elevation angle, number of

satellites visible, and various atmospheric condition parameters in order to isolate systematic errors in the GPS heights.

The combination of GPS and orthometric levelling is a useful tool for verifying geoidal models and will become more so as GPS coverage over Canada becomes more extensive.

All indications are, nevertheless, that “UNB Dec.’86” and “UNB ’90” are of a very high quality. This will continue to be confirmed as more GPS data becomes available.

# Bibliography

- [1] Angus-Leppan, P.V. (1982). "The frequency of gravity measurements for levelling reduction." *Australian Journal of Geodesy, Photogrammetry and Surveying*, 36, pp. 65 -82.
- [2] Bethea, R.M., B.S.Duran and T.L.Boullion (1985). *Statistical methods for engineers and scientists*. 2nd ed., Marcell Dekker, Inc., New York and Basel.
- [3] Beutler, G., D.Abell, I.Bauersima, W.Gurtner, G.Mader, M.Rothacher and T.Shildknecht (1987). "Evaluation of the 1984 Alaska GPS campaign with the bernese GPS software." *Journal of Geophysical Research*, 92(B2), pp. 1295 -1303.
- [4] Beutler, G., I.Bauersima, W.Gurtner, M.Rothacher, T.Shildknecht and A.Geiger (1987). "Atmospheric refraction and other important biases in GPS carrier phase observations." *Paper presented at XIX General Assembly of the IAGG*, Vancouver, Canada, 9 -22 August.
- [5] Beutler, G., I.Bauersima, S.Botton, W.Gurtner, M.Rothacher and T.Schildknecht (1989). "Accuracy and biases in the geodetic application of the global positioning system." *Manuscripta Geodaetica*, 14(1), pp. 28 -35.
- [6] Cannon, J.B. (1928). *Adjustment of the precise level net of Canada*. Geodetic Survey of Canada Publication No. 28, Ottawa.
- [7] Cannon, J.B. (1935). *Recent adjustments of the precise level net of Canada*. Geodetic Survey of Canada Publication No. 56, Ottawa.
- [8] Castle R.O. and M.R.Elliot (1982). "The sea slope problem revisited." *Journal of Geophysical Research*, 87(B8), pp. 6989 -7024.
- [9] Chamberlain, S., R.Eastwood and J.Maenpa (1986). "The WM101 GPS satellite surveying equipment." *Proceedings of the Fourth International Symposium on Satellite Positioning*. Austin, Texas, U.S.A., Vol 1, pp.439 -453.

- [10] Chang, R.G., N.Christou and H.Fashir (1986). "Software for geoid computations." Department of Surveying Engineering Technical Memorandum 10, University of New Brunswick, Fredericton, N.B., Canada.
- [11] Chrzanowski, A., Y.Q.Chen, R.Leeman and J.Leal (1988). "Integration of the Global Positioning System with geodetic levelling surveys in ground subsistence studies." *Proceedings of the 5th International (FIG) Symposium on Mining Surveying and Rock Deformation Measurements*, Eds. A.Chrzanowski and W.Wells, Fredericton, N.B., Canada, pp. 142 -155.
- [12] Clynych, J.R., D.S.Coco and M.P.Leach (1989). "GPS receiver comparison and interoperability." *Proceedings of the 5th International Geodetic Symposium on Satellite Positioning*, DMA and NGS, Las Cruces, U.S.A., March. Physical Science Laboratory, New Mexico State University, Las Cruces, U.S.A., pp 338 -347.
- [13] Colombo, O.L. (1986). "Ephemeris errors of GPS satellites." *Bulletin Geodesique*, 60, pp.64 -84.
- [14] Craymer, M.R. (1984). "Data series analysis and systematic effects in levelling." Technical Report No. 6, Survey Science, University of Toronto, Erindale Colledge, Mississauga, Ontario.
- [15] Delikaraoglou, D. (1989). "On principles, methods and recent advances in studies towards a GPS-based control system for geodesy and geodynamics." NASA Technical Memorandum 100716, Goddard Space Flight Center, Greenbelt, Maryland, U.S.A.
- [16] Denker, H. and H.G.Wentzel (1987). "Local geoid determinations and comparison with GPS results." *Bulletin Geodesique*, 61, pp. 349 -366.
- [17] Dixon, T.H. and S.K.Wolf (1990). "Some tests of wet tropospheric calibration for the Casa Uno global positioning system experiment." *Geophysical Research Letters*, 17(3), pp.203 -206.
- [18] Engelis, T. R.Rapp and C.C.Tsherning (1984). "The precise computation of geoid undulation differences with comparison to results obtained from the Global Positioning System." *Geophysical Research Letters*, 1(9), pp. 821 -824.
- [19] Engelis, T., R.H.Rapp and Y.Bock (1985). "Measuring orthometric height difference with GPS and gravity data." *Manuscripta Geodaetica*, 10, pp.187 -194.
- [20] Feltens, J. (1988). "Several aspects of solar radiation pressure." *Lecture notes in earth sciences: GPS- Techniques applied to geodesy and surveying*. Springer-Verlag, Berlin.

- [21] Gareau, R.M. (1986). *History of precise levelling in Canada and the North American vertical datum readjustment*. M.Sc.E. thesis, Department of Civil Engineering, Division of Surveying Engineering, University of Calgary, Calgary, Alberta, Canada.
- [22] Georgiadou, Y. and A.Kleusberg (1988a). "On the effect of ionospheric delay on geodetic relative GPS positioning." *Manuscripta Geodaetica*, 13(1), pp. 1 -8.
- [23] Georgiadou, Y. and A.Kleusberg (1988b). "On carrier signal multipath in relative GPS positioning." *Manuscripta Geodaetica*, 13(3), pp. 172 -179.
- [24] Gilliland, J.R. (1986). "Heights and GPS." *The Australian Surveyor*, 33(4), pp. 277 -283.
- [25] Gilliland, J.R. (1989). "A gravimetric geoid for Australia." *The Australian Surveyor*, 34(7), pp. 699 -706.
- [26] Heiskanen, W. and H.Moritz (1967). *Physical Geodesy*. Institute of Physical Geodesy, Technical University, Graz, Austria, Reprint 1987.
- [27] Heroux, P., and A.Kleusberg (1989). "GPS precise relative positioning and ionosphere in auroral regions." *Proceedings of the 5th International Geodetic Symposium on Satellite Positioning*, DMA and NGS, Las Cruces, U.S.A., March, Physical Science Laboratory, New Mexico State University, Las Cruces, U.S.A., pp. 475 -486.
- [28] Holloway, R.D. (1988). "The integration of GPS heights into the Australian Height Datum." School of Surveying Report Unisurv S33, University of New South Wales, Kensington, NSW, Australia.
- [29] Kearsley, A.H.W. (1986). "Data requirements for determining precise relative geoid heights from gravimetry." *Journal of Geophysical Research*, 91(B9), pp.9193 -9201.
- [30] Kearsley, A.H.W. (1988a). "The determination of the geoid ellipsoid separation for GPS levelling." *The Australian Surveyor*, 34(1), pp. 11 -18.
- [31] Kearsley, A.H.W. (1988b). "Tests on the recovery of precise geoid height differences from gravimetry." *Journal of Geophysical Research*, 93(B6), pp.6559 -6570.
- [32] King, R.W., E.G.Masters, C.Rizos, A.Stolz and J.Collins (1985). "Surveying with GPS." Monograph No. 9, School of Surveying, University of New South Wales, Kensington, NSW, Australia.
- [33] Kleusberg, A. (1986). "Ionospheric propagation effects in geodetic relative GPS positioning." *Manuscripta Geodaetica*, 11, pp.256 -261.

- [34] Kleusberg, A. (1990). Personal Communication. Professor, Department of Surveying Engineering, University of New Brunswick, Fredericton, Canada, January.
- [35] Kouba, J. (1987). "GPS capabilities and limitations for geodynamics." *EOS, Transactions of the AGU*, 68(16), p.286.
- [36] Lachapelle, G. and C.T.Whalen (1979). "Redefinition of North American Vertical Geodetic Networks." Presented to the joint meeting of IAG CRCM/REUN subcommissions held at The Hague, May 14 -18, 25 pages.
- [37] Leal, J. (1989). "Integration of GPS and levelling for subsidence monitoring studies at Costa Bolivar oil fields, Venezuela." Department of Surveying Engineering Technical Report No. 144, University of New Brunswick, Fredericton, N.B., Canada.
- [38] Lerch, F.J., S.M.Klosko, R.E.Laubscher and C.A.Wagner (1979). "Gravity model improvement using GEOS-3 (GEM 9 and 10)." *Journal of Geophysical Research*, 84(B8), pp. 3897 -3916.
- [39] Lerch, F.J., S.M.Klosko, C.A.Wagner and G.B.Patel (1985). "On the accuracy of recent Goddard gravity models." *Journal of Geophysical Research*, 90(B11), pp. 9312 -9334.
- [40] Lippincott, H.A. (1985). "Great Lakes vertical control." *Proceedings of the Third International Symposium on the North American Vertical Datum*, Ed. D.B.Zilkoski. IAG/ US Department of Commerce, Rockville, U.S.A., 21 -26 April. National Geodetic Information Center, NOAA, Rockville, MD, U.S.A., pp.21 -36.
- [41] Mainville, A. (1987). "Intercomparison of various geoid computational methods at GPS stations." Presented at the XIX General Assembly of the International Union of Geodesy and Geophysics, Vancouver, August, 17pp.
- [42] Mainville, A. and M.Veronneau (1989). "Orthometric heights using GPS." Presented at the CISM annual meeting, Halifax, Nova Scotia, June, 17pp.
- [43] Mertikas, S.P., D.Delikaraoglou and R.Santerre (1986). "Alert program for NAVSTAR Global Positioning System, Transit, Lageos and Starlette Satellites." Department of Surveying Engineering Technical Report No. 85, University of New Brunswick, Fredericton, N.B., Canada.
- [44] Marsh, J.G., F.J.Lerch, B.H.Putney, D.C.Christodoulidis, D.E.Smith, T.L.Fel-sentreger and B.V.Sanchez (1988). "A new gravitational model for the earth from satellite tracking data: GEM-T1." *Journal of Geophysical Research*, 93(B6), pp. 6169 -6215.

- [45] Merry, C.L. (1985). "Distortions in the South African levelling networks due to the influence of gravity." Presented to the Conference of Southern African Surveyors, Durban, South Africa, May.
- [46] Merry, C.L., and H.van Gysen (1987). "A regional geoid for southern Africa." 19th General Assembly, International Union of Geodesy and Geophysics, Vancouver, August.
- [47] Merry, C.L. (1988). *Introduction to the Global Positioning System*, Private Publication, Cape Town.
- [48] Mitchell, H.L. (1988). "GPS heighting in Australia: an introduction." *The Australian Surveyor*, 34(1), pp.5 -10.
- [49] Moritz, H. (1980). "Geodetic Reference System 1980." *Bulletin Geodesique*, 54, pp. 395 -405.
- [50] Penney, R.C. (1990). Personal Communication. Canada Centre for Surveying, Department of Energy, Mines and Resources, Canada, Ottawa, January.
- [51] Rapp, R.H. (1983). "The development of the January 1983 1×1 degree mean free-air anomaly data tape." Internal report of the Department of Geodetic Science and Surveying, Ohio State University, Columbus, Ohio, U.S.A.
- [52] Rapp R.H., and C.Wichiencharoen (1984). "A comparison of satellite doppler and gravimetric geoid undulations considering terrain corrected gravity data." *Journal of Geophysical Research*, 89, pp. 1105 -1111.
- [53] Rappeleye, H.S. (1948). *Manual of geodetic levelling*. Publication No. 239, U.S. Department of Commerce.
- [54] Santerre, R. (1989). *GPS satellite sky distribution: impact on the propagation of some important errors in precise relative positioning*. Ph.D. dissertation, Department of Surveying Engineering, University of New Brunswick, Fredericton, N.B., Canada.
- [55] Schwarz, K.P., and M.G.Sederis (1985). "Precise geoid heights and their use in GPS interferometry." Contract report 85-004, Geodetic Survey of Canada, Department of Energy, Mines and Resources, Canada.
- [56] Schwarz, K.P., M.G.Sideris and R.Forsberg (1987). "Orthometric heights without levelling." *Journal of Surveying Engineering*, 113(1), pp.28 -40.
- [57] Sideris, M.G., K.P.Schwarz and A.C.Rauhut (1988). "The geoid in northern British Columbia." Contract report 88-004, Geodetic Survey of Canada, Department of Energy, Mines and Resources, Canada.

- [58] Sideris, M.G., I.N.Tziavos and K.P.Schwarz (1989). "Computer software for terrain reductions using Molodensky's operator." Contract report 89-003, Canada Centre for Surveying, Department of Energy, Mines and Resources, Canada.
- [59] Tingley, M. (1990). Personal Communication. Professor, Department of Mathematics and Statistics, University of New Brunswick, Fredericton, Canada, March.
- [60] Tscherning, C.C., R.H.Rapp and C.Goad (1983). "A comparison of methods for computing gravimetric quantities from high degree spherical harmonic expansions." *Manuscripta Geodaetica*, 8, pp.249 -272.
- [61] Tralli, D.M., T.H.Dixon and S.Stephens (1988). "The effect of the wet tropospheric path delays on the estimation of geodetic baselines in the Gulf of California using the Global Positioning System." *Journal of Geophysical Research*, 93(B), pp. 6545 -6557.
- [62] Tranquilla, J. (1986). "Multipath and Imaging problems in GPS receiver antennas." *Proceedings of the Fourth International Geodetic Symposium on Satellite Positioning*, Defence Mapping Agency and National Geodetic Survey, Austin, U.S.A., 28 April -2 May, University of Texas, Austin, U.S.A., Vol. 1, pp.557 -571.
- [63] Tranquilla, J. (1988). "GPS antenna design characteristics for high precision applications." Paper presented at the GPS-88 Engineering Applications of GPS Satellite Surveying Technology Symposium, Nashville, Tennessee, U.S.A.
- [64] Vaníček, P. (1971). "Further development and properties of spectral analysis by least squares." *Astrophysics and Space Science*, 12, pp. 10 -73.
- [65] Vaníček, P. (1973). "Gravimetric satellite geodesy." Department of Surveying Engineering Lecture Notes No. 32, University of New Brunswick, Fredericton, Canada.
- [66] Vaníček, P., R.O.Castle and E.I.Balzacs (1980). "Geodetic levelling and its applications." *Review of Geophysics and Space Physics*, 18(2), pp. 505 -524.
- [67] Vaníček, P. and M.Craymer (1983). "Autocorrelation function in the search for systematic error in levelling." *Manuscripta Geodaetica*, 8, pp.321 -341.
- [68] Vaníček, P., G.H.Carrera, M.R.Craymer (1985). "Corrections for systematic errors in the Canadian levelling network." Department of Survey Science Technical Report No. 10, University of Toronto, Toronto, Ontario, Canada.
- [69] Vaníček, P., A.Kleusberg, R.G.Chang, H.Fashir, N.Christou, M.Hofman, T.Kling and T.Arsenault (1986). "An analytical solution for the geoid in Canada." Geodetic Survey of Canada, Contract Report 86-001, Department of Energy, Mines and Resources, Canada.



- [70] Vaníček, P. and J.Krakiwsky (1986). *Geodesy: The Concepts*. 2nd ed. North-Holland, Amsterdam, The Netherlands.
- [71] Vaníček, P. and A.Kleusberg (1987) "The Canadian geoid -Stokesian approach." *Manuscripta Geodaetica*, 12, pp.86 -98.
- [72] Vaníček, P., and L.E.Sjöberg (1989). "Kernel modification in generalized Stokes's technique for geoid determination." Presented at the Geoid Symposium of the International Association of Geodesy General Assembly, Edinburgh, Scotland, August.
- [73] Vaníček, P., C.Zhang and P.Ong (1990). "Draft final report on computation of a file of geoidal heights using Molodenskij's truncation method." Geodetic Survey of Canada, DSS Contract No. 23244-8-4564/01-SS, Canada.
- [74] Wells, D.E., P.Vaníček and S.Pagiatakis (1985). "Least squares spectral analysis revisited." Department of Surveying Engineering Technical Report No. 84, University of New Brunswick, Fredericton, N.B., Canada.
- [75] Wells, D.E. and J.Traquilla (1986). "GPS Users equipment: Status and trends." *Proceedings of Colloquium IV Land, Sea and Space - Today's Survey Challenge*, Alberta, Canada, pp.449 -463.
- [76] Wells, D.E. (ed.) (1986). *Guide to GPS positioning*. Canadian GPS Associates, Fredericton, N.B.
- [77] Wells, D.E., W.Lindlohr, B.Schaffrin, E.Grafarend (1987). "GPS design: undifferenced carrier beat phase observations and the fundamental differencing theorem." Department of Surveying Engineering Technical Report No. 116, University of New Brunswick, Fredericton, N.B., Canada.
- [78] Young, F.W. and J.Murakami (1989). "The North American Vertical Datum of 1988 (NAVD '88) internal status report prepared for CISM '88, Winnipeg, Manitoba, May 24 -27, 1988." *CISM Journal*, 43(4), pp. 387 -393.
- [79] Zilkoski, D.B. and L.D.Hothem (1989). "GPS satellite surveys and vertical control." *Journal of Surveying Engineering*, 115(2), pp.262 -281.

# Appendix I

## The Molodenskij truncation coefficients

$t_0$	-0.11317
$t_1$	-0.11305
$t_2$	-0.11281
$t_3$	-0.11245
$t_4$	-0.11198
$t_5$	-0.11139
$t_6$	-0.11068
$t_7$	-0.10987
$t_8$	-0.10895
$t_9$	-0.10793
$t_{10}$	-0.10680
$t_{11}$	-0.10558
$t_{12}$	-0.10427
$t_{13}$	-0.10287
$t_{14}$	-0.10139
$t_{15}$	-0.09984
$t_{16}$	-0.09821
$t_{17}$	-0.09652
$t_{18}$	-0.09477
$t_{19}$	-0.09297
$t_{20}$	-0.09112

Table I.1: The Molodenskij truncation coefficients.

## Appendix II

### The jackknife

The baseline data series are highly correlated. The mean and standard deviation quoted in the text reflect this property. In order to obtain an estimate of the uncorrelated values, a variation of the jackknife technique may be employed. One characteristic of the data series is that it is highly correlated between ends of the baseline and on closed curves. The sampling technique employed must reflect this property in order to give sensible answers.

It was decided to take samples of three baselines and the procedure adopted was:

1. Pick a point A.
2. Pick a second point B connected to A along a baseline such that B is not equal to A.
3. Pick a third point C connected to B such that C is not equal to A or B.
4. Pick a fourth point D connected to C (not equal to C) but which may equal A (closed curve).

From these three baselines may be obtained the measurement of interest,  $\tilde{X}$ , which can be loosely thought of as the average of the three observations with variance,  $O_p(\frac{1}{3})$ . This operation was repeated a large number of times (1000). If  $d_i$  is the

estimated standard deviation of all possible combinations then this may be scaled down using the formula:

$$\delta_i = \sqrt{\frac{3}{n}}d_i, \quad (\text{II.1})$$

where  $n$  is the number of samples making up the measurement (three in this case). The 68 % confidence interval for the expected or mean value,  $\mu$ , of  $\bar{X}$  (the original mean of the whole data set) is:

$$\mu - d_2\sqrt{\frac{3}{n}} < \bar{X} < \mu + d_1\sqrt{\frac{3}{n}} \quad (\text{II.2})$$

and so:

$$\bar{X} - d_1\sqrt{\frac{3}{n}} < \mu < \bar{X} + d_2\sqrt{\frac{3}{n}}. \quad (\text{II.3})$$

The procedure yielded a (scaled) standard deviation of  $\pm 0.306$ .

## Appendix III

### “UNB ’90” data series

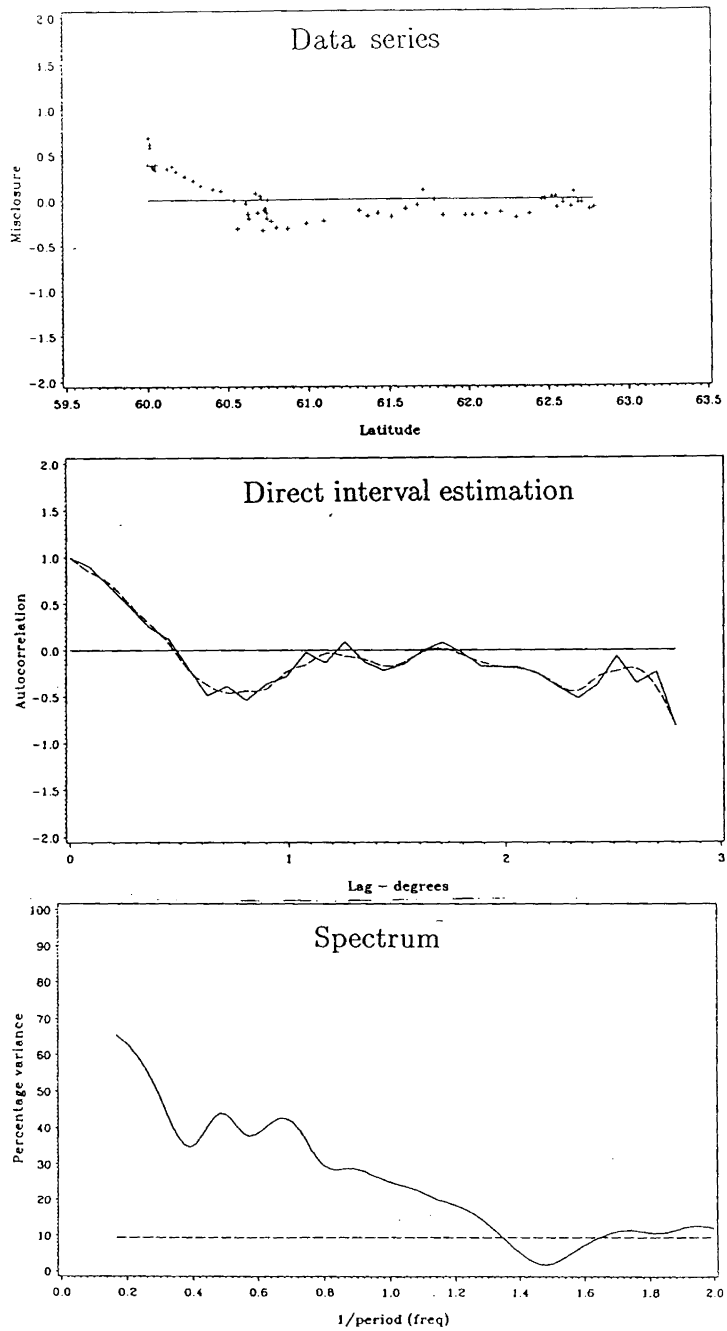


Figure III.1: Analysis of the North West Territories network UNB90 data series (ordered according to latitude).

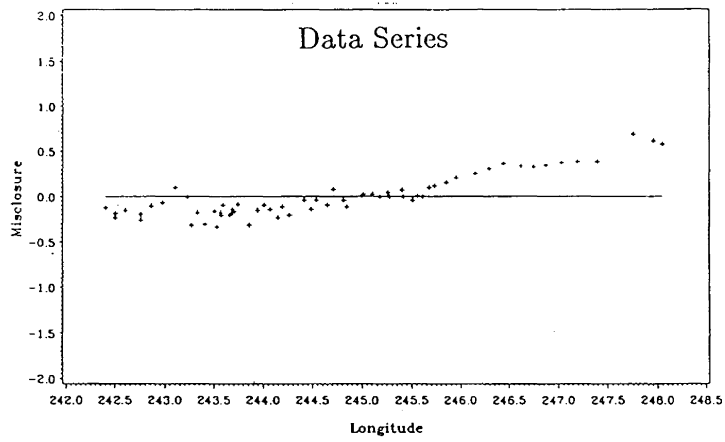


Figure III.2: The North West Territories network UNB90 data series (ordered according to longitude).



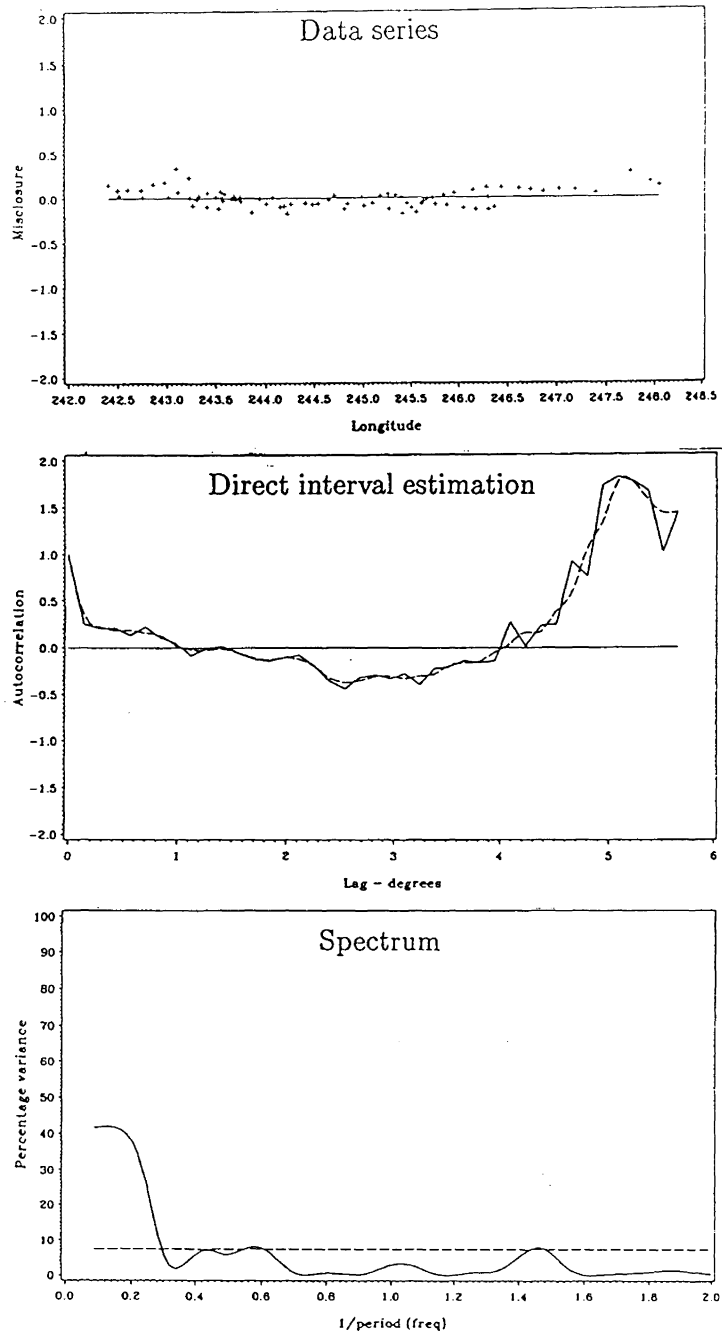


Figure III.3: Analysis of the NWT network UNB90 data series (ordered according to longitude).

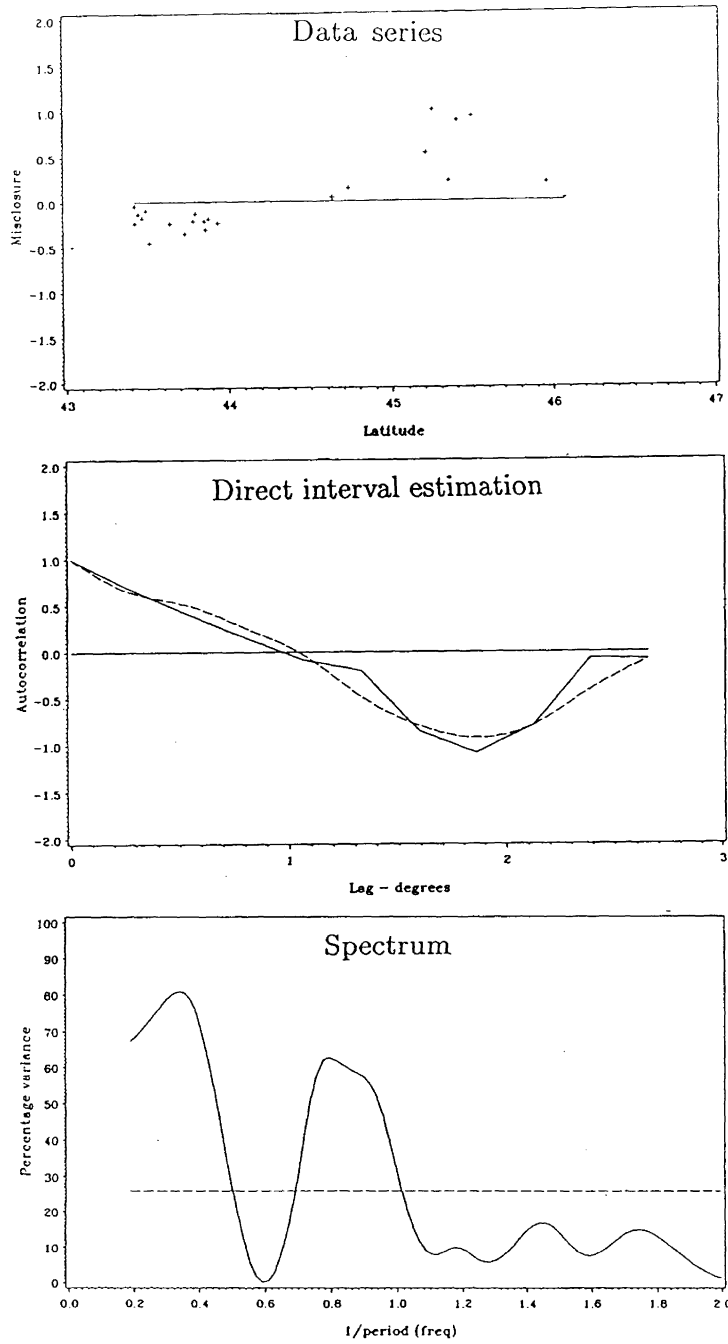


Figure III.4: Analysis of the Ontario network UNB90 data series (ordered according to latitude).

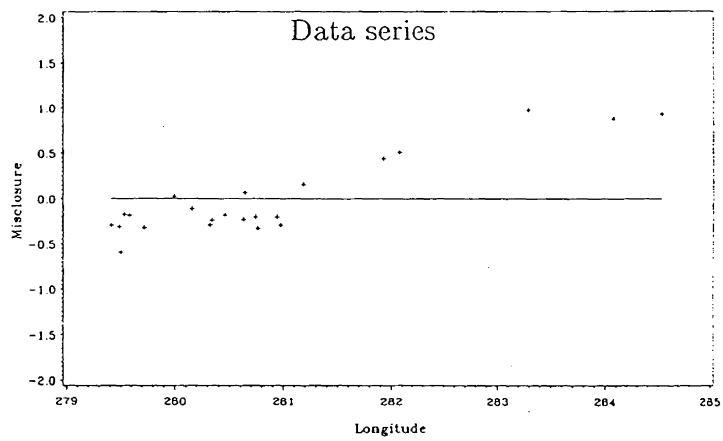


Figure III.5: The Ontario network UNB90 data series (ordered according to longitude).

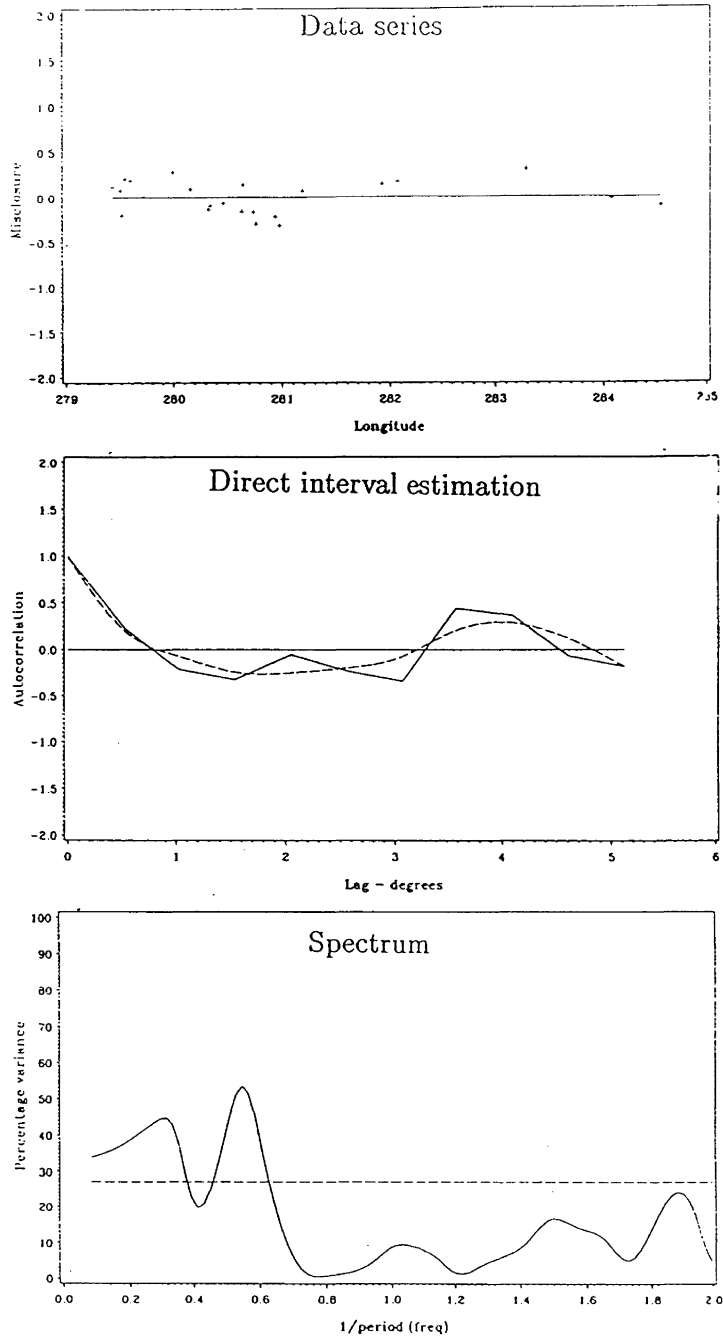


Figure III.6: Analysis of the Ontario network UNB90 data series (ordered according to longitude).

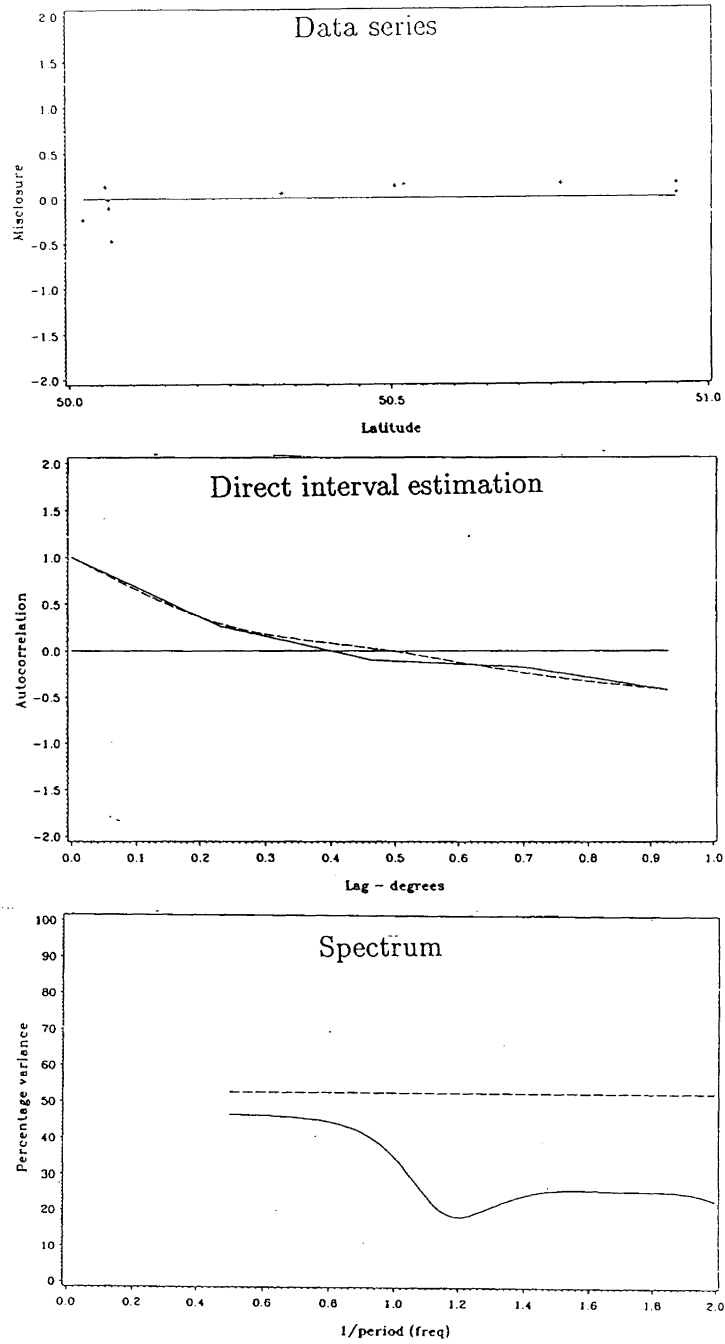


Figure III.7: Analysis of the Manitoba network UNB90 data series (ordered according to latitude).

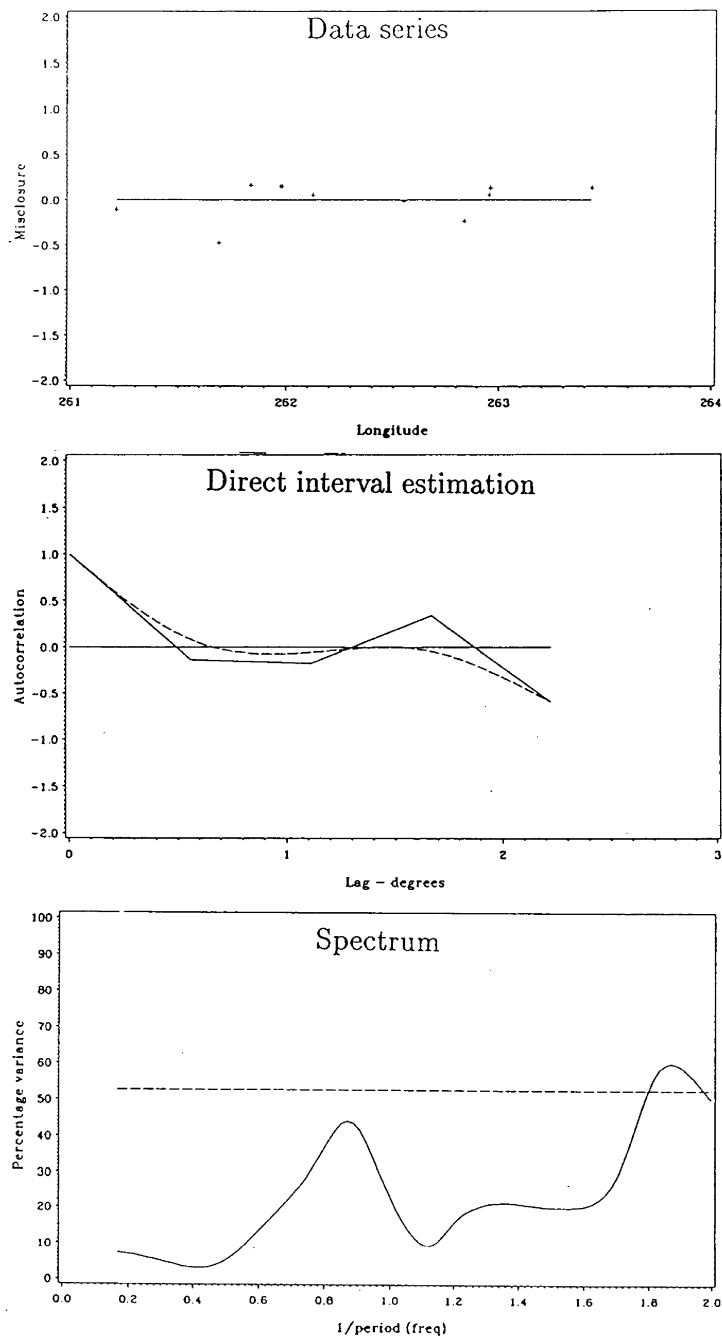


Figure III.8: Analysis of the Manitoba network UNB90 data series (ordered according to longitude).

VITA

Full name: Gregory Leonard Robinson

Place and date of birth: Durban, South Africa  
4 March 1956

Permanent address: 25 Rattray Place  
Sherwood  
Durban  
South Africa

Schools attended: St Henrys Colledge  
Marist Brothers  
Ridge Road  
Durban  
(1960 -1974)

Universities attended: University of Natal  
Durban  
South Africa  
B Sc (1975 -1978)

University of New Brunswick  
Fredericton, N.B.  
Canada  
M Sc E (1988 -1990)

Professional qualifications: Professional Land Surveyor  
South Africa